

Report No. **FAA-RD-80-45**  
**FAA-NA 80-1**

FC

**LEVEL II**

12

# THE LOW-LEVEL WIND SHEAR ALERT SYSTEM (LLWSAS)

R. Craig Goff

**NATIONAL AVIATION FACILITIES EXPERIMENTAL CENTER**  
**Atlantic City, New Jersey 08405**

ADA 087098



**FINAL REPORT**

**MAY 1980**

**DTIC ELECTE**  
JUL 25 1980  
S C

Document is available to the U.S. public through  
the National Technical Information Service,  
Springfield, Virginia 22161.

Prepared for

**U. S. DEPARTMENT OF TRANSPORTATION**  
**FEDERAL AVIATION ADMINISTRATION**  
Systems Research & Development Service  
Washington, D. C. 20590

DDC FILE COPY

80 7 24 026

NOTICE

The United States Government does not endorse products or manufacturers. Trade or manufacturer's names appear herein solely because they are considered essential to the object of this report.

1. Report No. <b>18</b> <b>19</b> FAA-RD-80-45	2. Government Accession No. AD-A087 098	3. Recipient's Catalog No.	
4. Title and Subtitle <b>6</b> THE LOW-LEVEL WIND SHEAR ALERT SYSTEM (LLWSAS)		5. Report Date <b>11</b> May 80	6. Performing Organization Code
7. Author(s) <b>10</b> R. Craig Goff	8. Performing Organization Report No. <b>14</b> FAA-NA-80-1		10. Work Unit No. (TRAIS) 154-451-150
9. Performing Organization Name and Address Federal Aviation Administration National Aviation Facilities Experimental Center Atlantic City, New Jersey 08405		11. Contract or Grant No.	
12. Sponsoring Agency Name and Address U.S. Department of Transportation Federal Aviation Administration Systems Research and Development Service Washington, D.C. 20590		13. Type of Report and Period Covered <b>9</b> Final <del>rept.</del> January 1977-March 1979 14. Sponsoring Agency Code	
15. Supplementary Notes <b>12</b> 131			
6. Abstract <p>The results of the Low-Level Wind Shear Alert System (LLWSAS) field test and evaluation are reported. The system is a computer controlled anemometer mesonet network used to detect near-surface wind discontinuities associated with strong thunderstorms and cold fronts—those that are potentially hazardous to low-flying aircraft. The test and evaluation was conducted at seven major airports in the United States.</p> <p>This report discusses the principal meteorological events that will trigger alarms, the system hardware and software, and characteristics of the system that are unique to each airport.</p> <p>Heavy emphasis is placed on the proper siting of anemometry which was found to be the most important factor influencing high quality system performance. The siting criteria enumerated should serve as a model for future installations. Deviations from the model will severely impact system performance.</p> <p>The origin and justification for the vector difference threshold is discussed as well as LLWSAS by-products: wind gust determination and special displays for Terminal Radar Approach Control Facility (TRACON) rooms. ←</p>			
17. Key Words Wind Shear Wind Hazards to Aviation Anemometry Radio Telemetry Weather (Meteorology)		18. Distribution Statement Document is available to the U.S. public through the National Technical Information Service, Springfield, Virginia 22151	
19. Security Classif. (of this report) Unclassified	20. Security Classif. (of this page) Unclassified	21. No. of Pages 130	22. Price

240550

116



TABLE OF CONTENTS

	Page
INTRODUCTION	1
Purpose and Background	1
DISCUSSION	1
Description of the Meteorological Problem: Origin of LLWSAS	1
The Nature of Meteorological Phenomena Producing Wind Shear	5
LLWSAS Hardware	17
LLWSAS Software	46
Anemometer Siting Criteria	64
LLWSAS Data Collection and Analysis	88
Airport Sensor Configurations, Special Siting Factors, and Qualitative Test Results	96
SUMMARY	115
CONCLUSIONS	116
REFERENCES	119

Accession For	
NTIS GSA&I	<input checked="" type="checkbox"/>
NSC TAB	<input type="checkbox"/>
Unannounced Justification	<input type="checkbox"/>
By _____	
Distribution/	
Availability Codes	
Dist	Avail and/or special
A	

## LIST OF ILLUSTRATIONS

Figure		Page
1	Typical Thunderstorm Cross-Section (Schematic)	6
2	Surveillance Weather Radar Representation of a Squall Line Thunderstorm	7
3	Squall Line Thunderstorm Outflow (Schematic)	8
4	Gust Front in a Supercell Thunderstorm (Schematic)	10
5	Satellite View of Tropical Thunderstorms over the Florida Peninsula	11
6	Two Varieties of Desert or High Plains Type Thunderstorms	13
7	Vertical Cross Sections of Two Types of Cold Fronts	16
8	Low-Level Wind Shear Alert System: Relationship of Units	19
9	Structural Damage to Frangible Tower	21
10	Wind Vector Transmitter used in LLWSAS	22
11	Environmental Electronics Box—Closed	23
12	Environmental Electronics Box—Open	24
13	Remote Station Power and Signal Distribution Diagram	25
14	Averager Functional Block Diagram	27
15	Peak Detector Printed Wire Assembly (PWA) Functional Block Diagram	27
16	Remote Station Controller Printed Wire Assembly (PWA) Functional Block Diagram	28
17	Analog-to-Digital Converter and Multiplexer Functional Block Diagram	29
18	Modem Functional Block Diagram	30
19	VHF Radio Link Functional Block Diagram	30
20	Central Station Controller Functional Block Diagram (Excluding Modem)	32

LIST OF ILLUSTRATIONS (CONTINUED)

Figure		Page
21	Wind Shear Indicator (Old Type)	34
22	Wind Shear Indicator Assembly Display Unit Front Panel	35
23	Wind Shear Indicator in Place in Atlanta Tower	36
24	Wind Shear Indicator (New Type)	38
25	Wind Shear Indicator Front Panel (New Type)	39
26	Central Station Rack Power Distribution Diagram	41
27	Hypothetical Peak Wind Analog Signal with Exaggerated Bleed-Off Between Peaks	43
28	TRACON Display	47
29	LLWSAS Program Flow Diagram	51
30	Master-Controller-Ready Subroutine Flow Diagram	52
31	Master-Controller-Busy Subroutine Flow Diagram	53
32	Initiate-CRT-Data-Terminal Subroutine Flow Diagram	53
33	BLFRTD Fortran Data Processing Flow Diagram (2 sheets)	54
34	Vector Component Pair (u, v) and Corresponding Scaled Peak Voltages on Each Leg	57
35	Diagnostic CRT Display Format	61
36	Relationship Between Direction Difference and Vector Difference in Proposed Algorithm Change for Programs 6B and 7B	63
37	Airflow in a Ridge and Valley Terrain Configuration	66
38	Streamline Pattern When Air Flows Down an Incline	68
39	Streamline Pattern When Air Flows Up an Incline	68
40	Contours of Equal Amplification Factor Over Various Escarpment Slopes	69

LIST OF ILLUSTRATIONS (CONTINUED)

Figure		Page
41	Sensor Locations and Heights Relative to Tree Lines and Buildings	70
42	Area of Influence Created by Obstructions Upwind from a Sensor	71
43	Streamlines in an Airflow Transition from Forest to Open Terrain	71
44	Distance of Critical Anemometer from Decision Height Projection on Surface (Feet)	75
45	Distribution of Frontal Widths (50 Cases)	76
46	Relationship Between Frontal Width and Vector Shear (50 Cases)	81
47	Alarm Miss Rate Versus Critical Remote-to-Centerfield Station Spacing	84
48	Application of System Performance Criteria in Selecting Anemometer Sites at a Hypothetical Airport	86
49	Distributions of Vector Differences for Houston, Texas, October 10, 1977	93
50	Distribution of Wind Direction for Tampa, Florida, July 1977	95
51	Objectively Analyzed Wind Direction and Speed Data for a Thunderstorm Gust Front Passage at Tampa, Florida, June 29, 1977	97
52	Objectively Analyzed Wind Direction and Speed Data for a Seabreeze Front at Kennedy Airport, New York, May 19, 1978	98
53	Airport Runway Map with Anemometer Locations, Tampa International Airport, Florida	99
54	Airport Runway Map with Anemometer Locations, Hartsfield Airport, Atlanta, Georgia	102
55	Airport Runway Map with Anemometer Locations, Houston Intercontinental Airport, Texas	105

LIST OF ILLUSTRATIONS (CONTINUED)

Figure		Page
56	Airport Runway Map with Anemometer Locations, Will Rogers Airport, Oklahoma City, Oklahoma	107
57	Complex Airflow at Denver Stapleton Airport, March 7, 1979	110
58	Airport Runway Map with Anemometer Locations, Denver Stapleton Airport, Colorado	111
59	Airport Runway Map with Anemometer Locations, J. F. Kennedy International Airport, New York	112

## LIST OF TABLES

Table		Page
1	Principal Types of Wind Shear in Their Component Finite Difference Forms	2
2	Thunderstorm Types Observed (X) at Each of the Seven LLWSAS Airports	15
3	Centerfield Wind Readouts for NAFEC LLWSAS, December 17, 1978	44
4	Parameter Polling Sequence	48
5	LLWSAS Software Program Versions	56
6	List of Parameters	58
7	Sensors Repositioned During the Course of the LLWSAS Test	65
8	Delay Factors Inherent in LLWSAS	74
9	Frontal Characteristics (Data from Goff, 1976)	78
10	Frontal Characteristics (Data from Goff, et al., 1977)	79
11	Frontal Characteristics (Unpublished Cases)	80
12	Critical Sensors for the Seven-Airport LLWSAS Network	83
13	Remote-to-Centerfield Sensor Spacing in the Seven-Airport LLWSAS (NMI)	83
14	Variation of Vector Differences During a Thunderstorm Passage at Tampa, Florida, July 13, 1977	90
15	Bivariate Distribution of Wind Speed and Direction for Tampa, Florida, July 3, 1977	92

## INTRODUCTION

### PURPOSE AND BACKGROUND.

The National Transportation Safety Board (NTSB) in 1974 cited weather as the dominant contributing factor in 36 percent of all general aviation accidents. In 1975, nearly 45 percent of all air traffic delays greater than 30 minutes were caused by thunderstorms and wind factors (Bromley, 1977, reference 1). Since 1974, there have been at least six major carrier accidents worldwide caused in part by low-level wind shears. These accidents have resulted in over 200 fatalities.

Weather, then, and specifically wind shear in the terminal zone, is a significant factor in aircraft operations. In certain weather conditions, aircraft may experience a large, unexpected headwind loss at a time that is most critical--when the aircraft is close to the ground on approach or departure. Loss of headwind results in a loss of aerodynamic lift which will result in a loss of altitude if unchecked.

Normally, airports have only one wind sensing device located approximately at centerfield. This sensor is incapable of detecting critical winds in the approach and departure corridors. Thus, if a wind change zone is propagating toward the airport, it cannot be detected until it reaches the center of the airfield.

In 1976 the Federal Aviation Administration (FAA) began to formulate a new concept to detect these critical winds around the airport periphery. This was the Low-Level Wind Shear Alert System (LLWSAS). The concept is simple. Locate additional wind sensing devices around the airport, relay the data to a computer, detect wind shifts before they move onto the airfield, and relay this information to pilots through the local air traffic controller.

The project was begun as an operational test in 1977 at six airports in Tampa, Houston, Atlanta, Oklahoma City, Denver, and New York. A seventh airport (Boston) was added in 1978. Tangible results have already been evident. Sixty more LLWSAS's are to be installed by 1982.

This report describes LLWSAS--its hardware, software, siting of anemometry, meteorological considerations, and results of the 18-month test.

## DISCUSSION

### DESCRIPTION OF THE METEOROLOGICAL PROBLEM: THE ORIGIN OF LLWSAS.

The term "wind shear," the difference in wind between two points in space, is relatively new in the vernacular of pilots and air traffic controllers. The term is not new, however, to meteorologists. Further, wind shear is a property of the atmosphere that is almost always present. Even when the atmosphere

is so still that motions cannot be detected by conventional sensors, there is still some motion (ever so slight), thus, there is still wind shear. To express the change of any atmospheric parameter (wind, temperature, pressure, density, moisture) over a unit of space, the rectangular coordinate system may be used with positive x pointing north, y pointing east, and z pointing up. Of the five atmospheric variables mentioned above, all are scalars except the wind, which is a vector with wind blowing toward the east representing the positive u component, north the positive v component, and wind moving up having a positive w component.

In formal meteorological treatises, wind shear is subdivided into the nine possible combinations of the u, v, and w wind components and x, y, and z space. Therefore, if we wish to express the value of the change of the east-west wind in the east-west direction, we do this by writing

$$\frac{u_2 - u_1}{x_2 - x_1} \quad (1)$$

where the subscripts refer to locations in space. Expression (1) is one of the nine possible wind shear components. Thus,  $u_1$  is the value of u at the  $x_1$  position, and  $u_2$  is the value of u at the  $x_2$  position.

The LLWSAS, which is described in this report, will detect four of the nine possible wind shear components, all related to the change of the horizontal wind (u, v) in horizontal space (x, y). This type of wind shear is called horizontal wind shear. It is believed to be the most hazardous (unflyable) of wind shear types under certain conditions. (It is assumed that aircraft will remain well clear of thunderstorm centers where other wind shear types are of extreme magnitude and very possibly, unflyable.)

Other types of wind shear are vertical wind shear (the change of the horizontal wind in vertical space), and the shearing of the upward and downward wind (w) in three-dimensional space. Vertical shear accounts for two of the nine shear components and shearing of the vertical wind accounts for three components. Using the symbol  $\Delta$  to represent differences, expression (1) can be equated to  $\Delta u/\Delta x$ . We then can describe the nine components of wind shear as shown in table 1.

TABLE 1. PRINCIPAL TYPES OF WIND SHEAR IN THEIR COMPONENT FINITE DIFFERENCE FORMS

Horizontal Wind Shear	$\Delta u/\Delta x, \Delta u/\Delta y, \Delta v/\Delta x, \Delta v/\Delta y$
Vertical Wind Shear	$\Delta u/\Delta z, \Delta v/\Delta z$
Shearing of the Vertical Wind	$\Delta w/\Delta x, \Delta w/\Delta y, \Delta w/\Delta z$

Now that the types of wind shear have been defined, an explanation of atmospheric scales is necessary. Scale relates to the distance over which the variables may change. Meteorologists often subdivide atmospheric scales into three broad categories: the small or microscale, the middle or mesoscale, and the large or synoptic scale. Small-scale variations in the wind produce a bumpiness or a chop for aircraft. The wind variations have widths of 10's or 100's of feet with respect to the ground. Under most circumstances, this small-scale change (called turbulence), while occasionally severe, is not hazardous unless the aircraft is in or near a thunderstorm (in which case, the turbulence may be severe enough to result in structural damage). Large-scale wind variations are those fluctuations having widths of 100's to 1,000's of miles. They are so broad, aircraft have no difficulty traversing them.

Middle or mesoscale wind variations produce the major wind hazards for aircraft. They are typically 1 to 10 miles wide. It is the mesoscale wind fluctuation about 1 mile wide that causes the most problem. This scale wind fluctuation is found in the warm front, the cold front, the thunderstorm gust front, and inversion perturbations.

Although wind shear magnitudes are generally inversely proportional to the shear scale, aircraft do not respond fully to the small-scale shear. They do respond fully to middle-scale shear, and for this reason, the latter are the most important. When encountered, they may produce a highly unstable moving platform depending on the magnitude of the shear. Of the four meteorological events mentioned above, thunderstorm gust fronts produce the strongest horizontal wind shears followed by cold fronts. The strongest cold fronts do have hazardous horizontal shears, but the frequency of such shears occurring in any one cold front case is low compared to the thunderstorm gust front. Warm fronts and inversions produce mostly vertical shear. However, strong vertical shears are flyable shears if the pilot is informed of their presence. It is the surprise element that causes the problem for pilots in the vertical wind shear situation. This will be discussed more fully later.

Although meteorologists have known about the association of strong shears with certain meteorological events for many years, most knowledge was based on visual observations rather than quantitative information. It has not been until recently that precise atmospheric measurements have been made in many weather events that cause problems for pilots.

In 1949, following the development of the powerful tool of weather radar, a comprehensive study by Byers and Brahan (reference 2) was published which significantly advanced the knowledge of thunderstorm behavior for aviation interests. In subsequent years, there occurred simultaneous technological developments involving the improvements in weather radar and the advent of the jet age.

In the 1960's, a wealth of knowledge on the thunderstorm character was gleaned by comparing data from an instrumented aircraft with reflectivity data from a surveillance radar (Lee, reference 3). From this work, specific guidelines

were established governing flight near thunderstorms. Whereas the Byers and Braham study investigated the atmosphere below 20,000 feet, the Lee studies extended the investigation up to 50,000 feet.

There ensued a fairly quiet period in terms of new meteorological information from the late 1960's to the mid-1970's. During this interval, however, the jet age had fully developed. Aircraft numbers had increased substantially and encounters with hazardous weather events increased proportionally. In 1975 and 1976, there occurred three major aircraft accidents caused by aircraft encounters with strong shears close to the ground. At the time of the accidents, the FAA was investigating the use of the Acoustic Doppler Radar for detection of wake vortices. The radar was considered for detection of low-level wind shear, but its immediate use as an operational tool was not possible.

At about this time, two studies were published (Charba, 1974, reference 4; Goff, 1975, reference 5) describing the thunderstorm outflow, considered one of the most significant wind shear hazards. Additional studies investigating the weather conditions at the time of the disastrous air carrier accidents (Caracena, 1976, reference 6; Fujita and Caracena, 1977, reference 7) added to knowledge of the atmosphere's behavior. Frost, et al., 1979 (reference 8) and McCarthy, et al., 1979 (reference 9) have discussed aircraft response characteristics in thunderstorm outflows.

A search for a readily operational means to sense low-level wind shear led the FAA to consider the surface anemometer concept. This system has inherent limitations; namely, its inability to detect wind shear in three dimensions. It is only capable of horizontal shear detection in two dimensions in a plane near the ground. However, the studies by Charba and Goff indicated that horizontal shear was a principal hazard in thunderstorm outflows and that detection of horizontal shear implied the existence of other shear types (vertical shear and shear of the vertical wind). The Goff study also revealed that wind flows near the ground were fairly uniform up to at least 300 to 500 feet in all thunderstorm outflow and cold front cases, implying that events observed near the ground would also be encountered up to 300- to 500-foot levels and often much higher. Since the anemometer network concept had been used by meteorologists as a research tool for many years, it appeared to be easily adaptable to operational status in the FAA. Thus, in late 1976, planning work on LLWSAS began.

LLWSAS is an anemometer mesonetwork designed to detect wind changes associated with thunderstorm gust fronts and cold fronts. Average reference-to-remote station spacing is about 1.5 nautical miles (nmi). Recall that this distance is within the scale posing the greatest hazard to aircraft.

LLWSAS is designed similarly to the Portable Automated Mesonetwork (PAM) of the National Center for Atmospheric Research (NCAR) in Boulder, Colorado (Cotton and George, 1978, reference 10), except LLWSAS employs fewer stations,

senses only the wind, and is not portable. It is similar in that it is computerized and uses solid-state electronics with radio as a data transmission medium. It is deemed quite adequate in operational detection of most hazardous shear until highly sophisticated remote sensing devices (e.g., the microwave Doppler) are available.

#### THE NATURE OF METEOROLOGICAL PHENOMENA PRODUCING WIND SHEAR.

The LLWSAS was designed to detect large wind differences between anemometer pairs in a quasi-horizontal plane near the ground. Atmospheric phenomena that exhibit large wind differences over this horizontal distance scale (mesoscale) are the thunderstorm (its gust front and internal wind flow pattern), the strong cold front, and the seabreeze front. However, since the LLWSAS cannot distinguish between small- and middle-scale wind fluctuations, the system also alarms when strong near-surface winds are accompanied by turbulence, a small-scale event. Alarms created by turbulence are intermittent and irregular causing some annoyance to air traffic controllers. However, turbulence-generated alarms are real atmospheric hazards that should not be ignored.

The LLWSAS also triggers alarms if a remote site anemometer output is biased by local obstructions (see section on Anemometer Siting Criteria). These "false" alarms look to the user much like turbulence alarms, but with experience controllers can recognize the differences. Hopefully, adequate siting standards will minimize the problem in future systems.

THUNDERSTORMS. The LLWSAS was designed primarily to warn pilots of hazardous winds caused by the thunderstorm gust front. The project was given considerable priority following three disastrous air carrier accidents at New York (Kennedy), Denver (Stapleton), and Philadelphia in 1975 and 1976. The thunderstorm gust front is the leading edge of a shallow (500 to 3,000 feet thick) layer of cold air flowing from the thunderstorm base.

The horizontal width of the wind change zone in the front averages about 1.1 miles (see Anemometer Siting Criteria). Across this expanse which moves along in advance of the thunderstorm, the wind often changes dramatically producing vector changes of up to 100 knots in magnitude. Typically, vector change magnitudes are in the 20- to 40-knot range. Figure 1 shows a classical thunderstorm, gust front, and outflow.

To generalize about the thunderstorm that produces the outflow and leading-edge gust front is difficult since there are variations from region to region within the United States and the world. Thunderstorms can be classified into four broad and sometimes overlapping categories: squall lines, supercell thunderstorms, tropical thunderstorms, and high plains or desert thunderstorms. Each type has its own unique outflow structure.

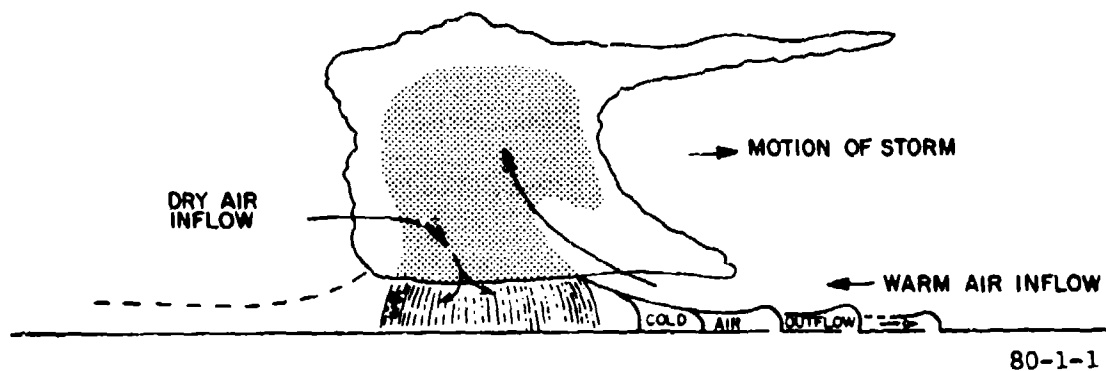


FIGURE 1. TYPICAL THUNDERSTORM CROSS-SECTION (SCHEMATIC)

Squall Lines. Squall lines are clusters of thunderstorms forming along a line. Figure 2 is a surveillance radar representation (contoured) of a typical squall line. Line formations of thunderstorms are common in locations affected by a low-level atmospheric discontinuity like a cold front, warm front, or dry line (the discontinuity of moisture often evident near the western borders of Oklahoma, Kansas, and/or Nebraska in the spring and summer). Squall lines usually are from 50 miles to several hundred miles long. They can be composed of broken cells (open spaces between cells), or they can be a solid wall of storms forming a barrier to all air traffic en route or operating in the terminal area. Naturally, the long, solid squall line is the most hazardous to aircraft since it sweeps over a wide area. During its lifetime, it will ultimately affect aircraft operations in many locations. The lifetime of a squall line may range from a few hours to a day or more but is typically 6 to 8 hours. Squall lines move west to east, northwest to southeast, or north to south, depending on their orientation and the upper atmospheric flow. Lines are almost exclusively confined to the area east to the Rocky Mountains in the United States. They are common in the Southern Prairie States in the spring and fall, in the Northern Plains States and Eastern United States in summer, and in the Florida Peninsula in the winter. Squall lines typically move about 15 to 25 knots after maturity.

The outflow that spills from the base of the thunderstorm line moves, in part, in advance of the precipitation zone (figure 3). A large volume of air is left in the wake of the storm. It is the leading edge of the cold air outflow (the gust front) ahead of the squall line that produces potentially hazardous shears. The gust front is often a dry wind discontinuity.

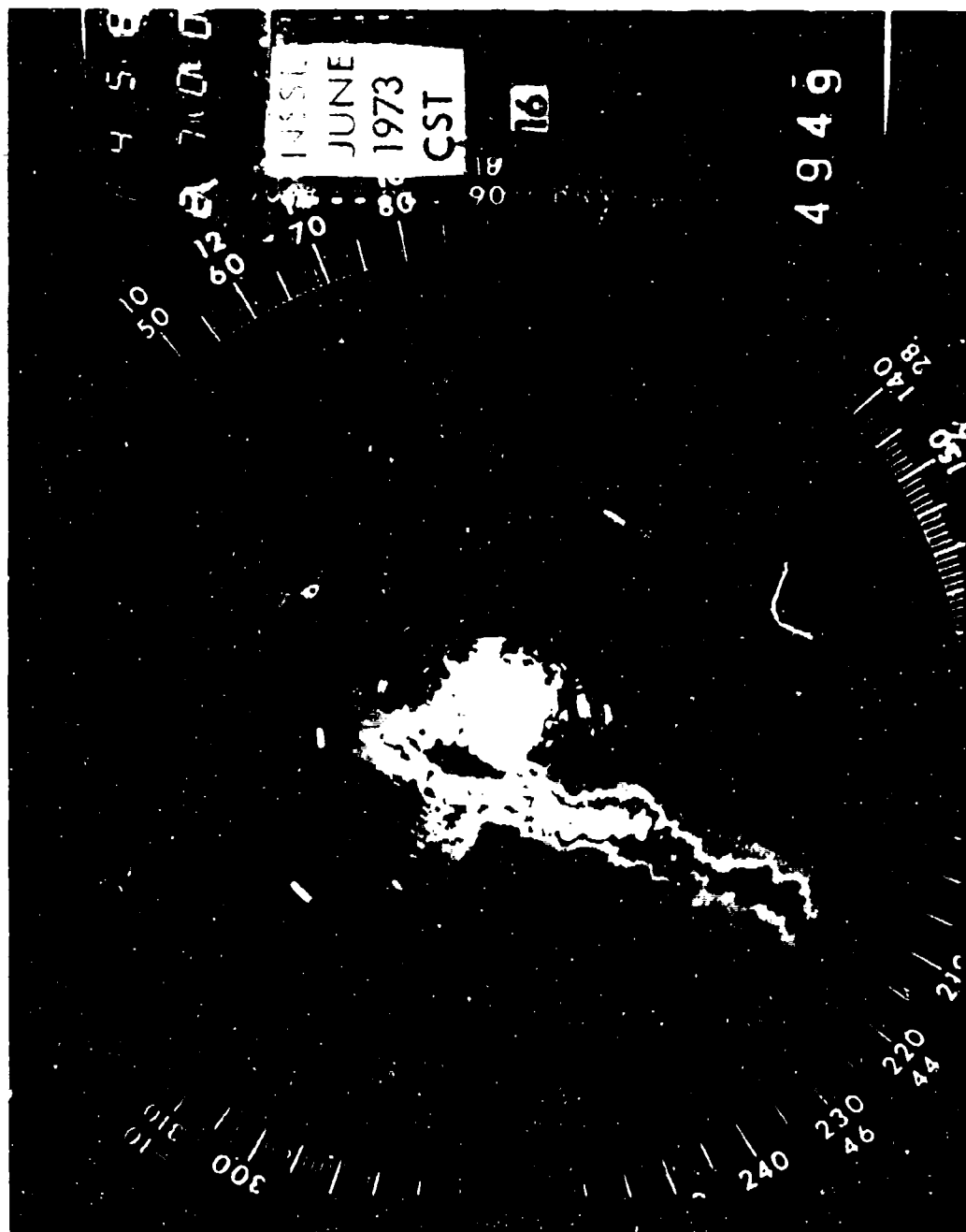


FIGURE 2. SURVEILLANCE WEATHER RADAR REPRESENTATION OF A SQUALL LINE THUNDERSTORM

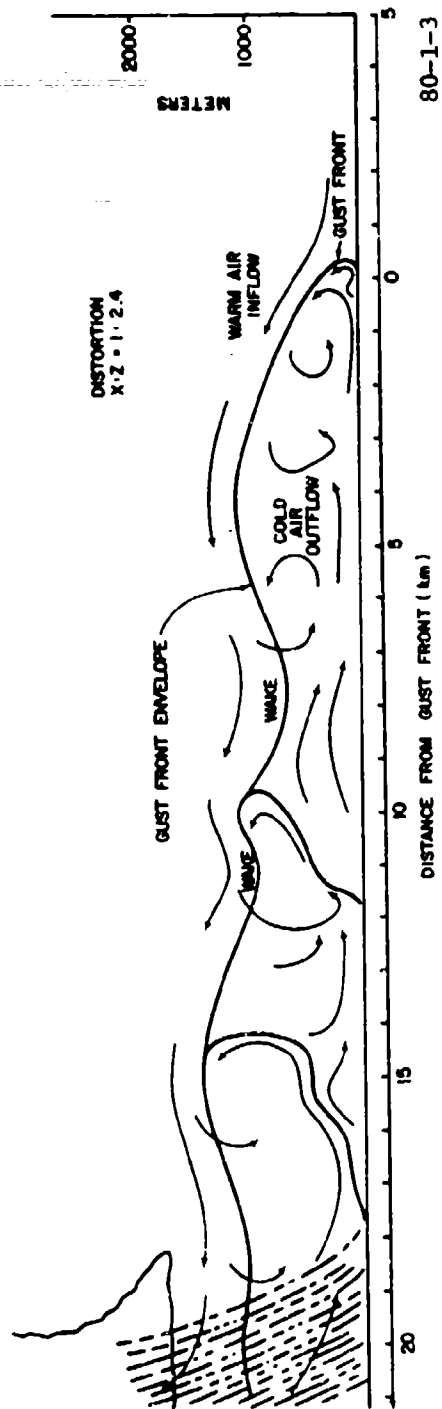


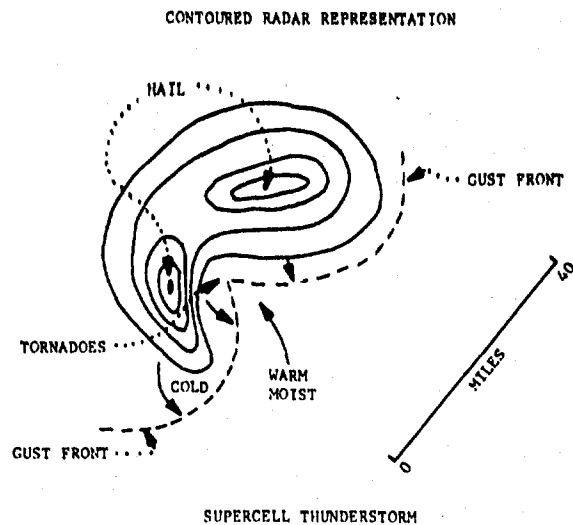
FIGURE 3. SQUALL LINE THUNDERSTORM OUTFLOW (SCHEMATIC)

This wind change zone may be as much as 15 miles ahead of the precipitation; therefore, it is not readily detectable by radar. Aircraft on approach to an airfield in which a gust front lies between the outer and middle markers and is moving toward the airport will penetrate the outflow top and experience a headwind-to-tailwind transition. If the pilot decides to continue his approach and if the gust front has not passed the outer LLWSAS anemometer, the aircraft will pass through the gust front and experience a tailwind-to-headwind transition coupled with a strong updraft. Within the outflow, the pilot can expect updrafts, downdrafts, severe turbulence, and secondary windshifts.

If a pilot planning departure heeds wind shear warnings issued from the outer ring of LLWSAS anemometers, there never should be a gust front penetration in the squall line thunderstorm case. However, if the gust front, but not the main body of the thunderstorm, has passed the airfield and the warnings have ceased, the pilot may elect to depart heading into the outflow airmass; i.e., toward the convective cells. This is dangerous in two ways. First, upon rising through the top of the outflow, the pilot will encounter a headwind-to-tailwind transition. If the transition is made too close to the ground, power changes to compensate for a loss of altitude may be inadequate. Second, the pilot faces the risk of a possible thunderstorm penetration with the ultimate consequence of encountering extreme turbulence. Clearly, any contact with the outflow airmass on approach or departure is not recommended.

Supercell Thunderstorms. The supercell thunderstorm is a massive, single-cell thunderstorm with which the tornado is usually associated. As such, this type of thunderstorm is confined to the Prairie States and the Southeastern United States. It is only rarely observed east of the Appalachian Mountains and almost never west of the Rocky Mountains. Although the supercell thunderstorm occurs as a single cell, several cells may line up in a broken (squall) line configuration. Individual cells typically move southwest to northeast. They move rapidly, sometimes at speeds of up to 55 knots. It suffices to say, the whole storm entity, including the outflow, is extremely dangerous for aircraft penetration. Fortunately, the size and speed of this type storm imply only a short span effect on any airport, and operations are interrupted only a short while to allow passage of the cell.

The gust front in the supercell storm rings the leading edge of the precipitation. The speed of the storm insures that the gust front will remain close to the precipitation line. The gust front, however, traces the classical hook echo radar shape of the storm with a wedge toward the storm's circulation center (figure 4). This wedge is usually on the storm's southeast side. From the apex of the wedge toward the trailing southwest portion of the storm, the gust front and outflow are particularly strong and will be extremely hazardous for aircraft penetration. The scenario discussed in the Squall Lines subsection for approach or departure operations should never be attempted in the supercell thunderstorm case.



80-1-4

FIGURE 4. GUST FRONT IN A SUPERCCELL THUNDERSTORM (SCHEMATIC)

Tropical (Airmass) Thunderstorms. Tropical thunderstorms are relatively weak compared to the first two described but are much more numerous in certain parts of the United States. This type of thunderstorm develops as a result of strong surface heating in summer months. It is confined to those regions where there are both strong heating of the near-surface air and ample quantities of low-level moisture. These conditions are prevalent in the Florida Peninsula, along the gulf coast, and along the Eastern United States coast. For example, of the 90 or so thunderstorms observed at Tampa annually (highest frequency in the United States), 80 to 90 percent are the tropical type. Tropical thunderstorms are almost exclusively a late afternoon phenomenon in these areas. Since thunderstorms are steered in large part by the upper atmospheric flow which is usually weak or light in midlatitudes in summer months, tropical storms may exhibit little apparent movement. A cell may grow to maturity, then dissipate over one spot on the earth's surface. The lifetime of a tropical cell is typically 1 hour. Tropical storms forming near large water bodies may be enhanced in severity by the common seabreeze discontinuity which is described later in this section. Extra pilot and controller caution should be exercised in those areas. Figure 5 shows a satellite's view of tropical type thunderstorms forming over the Florida Peninsula on a typical summer day.

Because of the cellular nature of tropical storms and their slow movement, outflows tend to form a circle around the precipitation. Outflows and gust fronts are not strong compared to those in squall lines and supercell storms because the upper atmosphere is usually moist. This inhibits the evaporative

1831 06AU77 13A-H 03391 17361 MA27N82W-1



FIGURE 5. SATELLITE VIEW OF TROPICAL THUNDERSTORMS OVER THE FLORIDA PENINSULA

cooling mechanism responsible for strong downdrafts. They may, however, approach severe limits. The storm's frequency is such that possible encounters with the rare severe tropical thunderstorm will be just as frequent as the less numerous but more typically severe squall line.

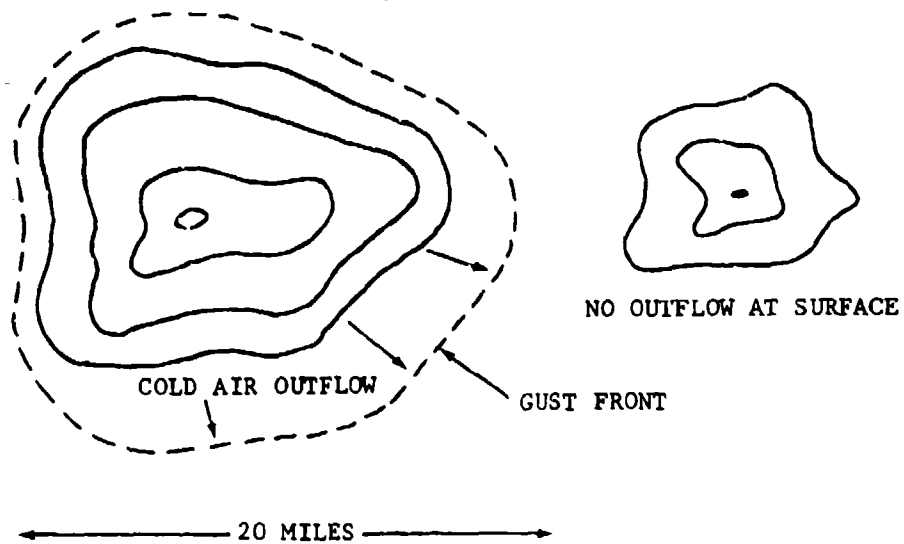
Gust fronts do not move far in advance of the precipitation in the tropical storm and, therefore, do not form an extensive shallow layer of cold air as in the squall line. Although horizontal shears across the front are not strong, up and downdrafts and turbulence are common, internal to the outflow.

High Plains or Desert Thunderstorms. These thunderstorms resemble tropical thunderstorms when viewed on weather radar. They are about the same size and have about the same lifetime. There are important differences however. As the name implies, desert thunderstorms form in regions where the atmosphere is dry at low levels. These conditions occur west of 90° west longitude to the west coast mountain ranges. Included in this area is not only the true desert of the Southwestern United States, but also a north-south band about 300 to 500 miles wide east of the Rocky Mountains which is not normally thought of as a desert. Large airports in the desert region are Denver, Salt Lake City, Las Vegas, Phoenix, Tucson, and Albuquerque. Since any thunderstorm needs moisture (water vapor) in large quantities to sustain itself, the moisture supply for desert thunderstorms comes from layers well above the surface. Thunderstorms that form with a dry lower atmosphere and a moist upper atmosphere often have a circulation confined to the upper atmosphere. Other than the visible cloud and the rain falling under it and evaporating before reaching the surface, there is often no disturbance of the airflow near the ground and no rainfall reaching the ground. This is one aspect of these types of storms. Another possibility is to have such copious rain falling beneath the cloud base that it cannot all evaporate in the dry atmosphere below before it reaches the ground. If by chance rainfall does reach the ground in the desert thunderstorm, it may bring with it a tremendous downdraft resulting in a strong outflow. Whereas, tropical storm downdrafts are due primarily to precipitation drag, downdrafts internal to desert storms are due to precipitation drag plus the more important effect of atmospheric instability in the desert regime. Figure 6 shows the above-described two varieties of desert type thunderstorms.

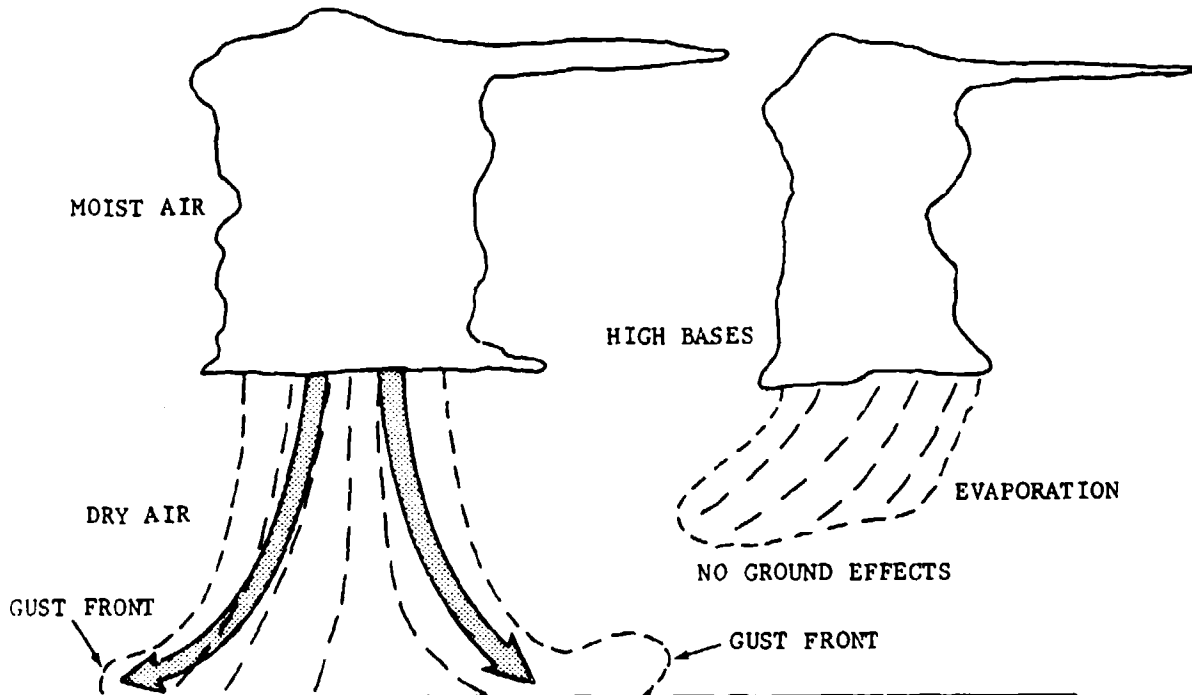
In the Denver Stapleton Continental accident in August 1975, the aircraft on departure started rollout with a light tailwind and encountered a 20-knot headwind after passing through the gust front. Shortly after takeoff, the wind changed to a tailwind calculated to be between 60 to 90 knots or a wind shear of roughly 80 to 110 knots per mile (NTSB-AAR-76-14, reference 11). If one compares the situation of the desert thunderstorm where no rain reaches the surface with the case where rain and a downdraft reach the surface, it is obvious that there is a large variation from storm to storm with this type of convection.

Desert thunderstorms are roughly circular. Their movement is slow. If there is a surface outflow, it rings the storm as in the tropical thunderstorm, but the gust front may move further ahead of the precipitation as it has considerable momentum. Pilots can expect these outflows to be highly turbulent with large updrafts and downdrafts.

PLAN VIEW  
(RADAR CONTOURS)



VERTICAL CROSS SECTION



80-1-6

FIGURE 6. TWO VARIETIES OF DESERT OR HIGH PLAINS TYPE THUNDERSTORMS

The four principal types of United States thunderstorms have been described in their classical form. It is important to note that not only may two thunderstorm types occur together but also that two thunderstorm types may be disjoined and be in existence simultaneously in proximity to one another. In addition, any given locale may experience type variations from season to season. Regarding the joining together of two types, the only combination possibility is the supercell and squall line. Others are not observed. On a given day, however, a squall line may coexist with but be disjoined from either a supercell or airmass type thunderstorm. Other coexisting but disjoined possibilities are rarely observed. Table 2 shows the thunderstorm types observed at each of the seven LLWSAS airports.

Occasionally, thunderstorms are embedded in a large-scale general rain or overcast associated with frontal convection. In this case, low-level flow features of the thunderstorms are masked by the flow of the larger-scale pattern. The danger is not reduced, but visual awareness of the hazard may be imperceptible because the pilot is flying instrument flight rules (IFR) in light rain or clouds before penetrating the hazard zones of the thunderstorm and is using as guidance an onboard radar whose signal may be attenuated by moisture on the radome. The CSB report of the Southern Airways accident of April 4, 1977 (reference 12), can be reviewed as an example of the scenario described.

What emerges to the nonmeteorologist reader at this point may be an indiscriminate picture of thunderstorm behavior and its low-level characteristics. If this is the case, then the objective in presenting this description has been accomplished; i.e., the thunderstorm is a highly complex and variable atmospheric phenomenon defying a simple generalized description.

COLD FRONTS. Cold fronts are zones of delineation between warm and cold airmasses. Whereas, the surface frontal zone or wind shift band is on the order of miles or tens of miles wide, the length of the frontal zone may be 1,000 miles or more. The wind shift band is, then, in the middle scale of atmospheric phenomenon or that scale that influences aircraft the most in terms of wind shear. The whole extent of the frontal line and the weather feature producing it is a large-scale phenomenon. Cold fronts are a midlatitude cold season phenomenon.

About half of all the cold fronts are weak in terms of horizontal shear even when there is a strong temperature contrast across the front. In these cases, the wind change boundary is quite wide compared with the very narrow wind shift zone of typical gust fronts. For example, if the cold front wind change transition zone is 50 miles wide and the wind change is a uniform 25 knots across the boundary, this amounts to a wind shear of 0.5 knots per mile (or roughly 1.2 knots per minute for an aircraft on approach); a shear easily handled by any aircraft. It is when the cold front wind change zone becomes very narrow that the problem arises. This describes a strong cold front that is usually rapidly moving. Strong cold fronts may have shear values that approach the values usually observed in gust fronts. This occurs about 6 to 12 times a year at airports at midlatitudes, especially those with a large fetch of flat terrain in the direction of the approaching front. The rough

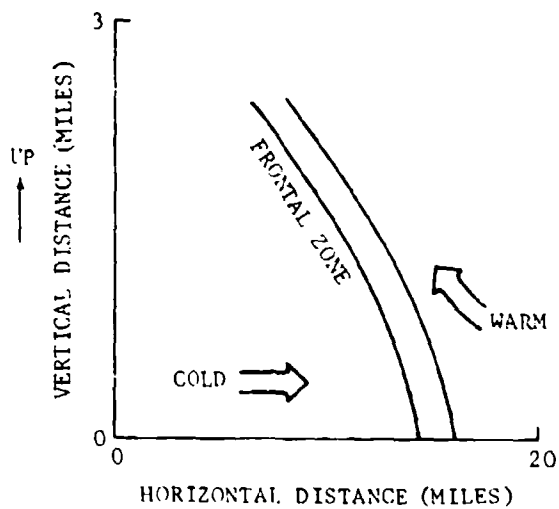
TABLE 2. THUNDERSTORM TYPES OBSERVED (X) AT EACH OF THE SEVEN LLWSAS AIRPORTS

<u>Airport</u>	<u>Season</u>	<u>Squall Line</u>	<u>Supercell</u>	<u>Tropical</u>	<u>Desert</u>	<u>Supercell-Squall Line Combination</u>
Tampa	Spring	XR		X		
	Summer			X		
	Fall	XR		X		XR
	Winter	X		X		
Atlanta	Spring	X	X			X
	Summer	X		X		
	Fall	X				
	Winter					
Oklahoma City	Spring	X	X			X
	Summer			X		
	Fall	X	XR			
	Winter					
Houston	Spring	X	X	X		X
	Summer	XR		X		
	Fall	X		X		
	Winter	X				
Denver	Spring	XR				
	Summer	X	XR		X	
	Fall	XR				
	Winter					
New York City	Spring					
	Summer	X	XR	X		XR
	Fall					
	Winter					
Boston	Spring					
	Summer	X	XR	X		XR
	Fall					
	Winter					

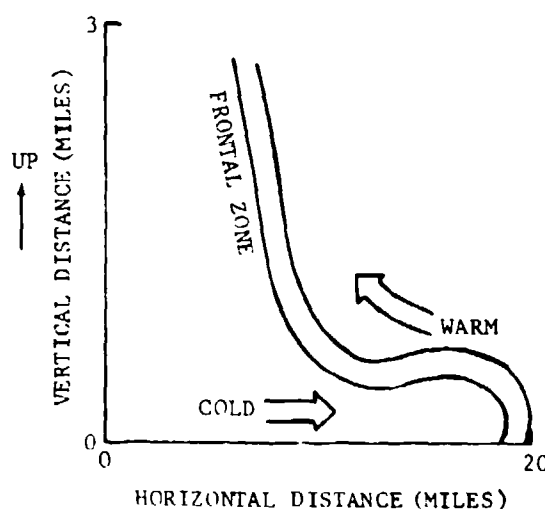
R = Rare or Infrequent

terrain of the Rocky Mountains and the Appalachian Mountains tends to break-up the flow structure of fronts and makes them more diffuse and weaker in terms of horizontal shear. The highest frequency of strong cold fronts in the United States is in the Midwest from Oklahoma north to the Canadian border and from the east slope of the Rocky Mountains to Ohio. (Table 11, Frontal Characteristics, shows data from some strong cold fronts in Oklahoma.)

The cold air mass behind a cold front may be as thick as the outflow from a thunderstorm, but typically, it is 1 to 3 miles thick compared with the 500- to 3,000-foot thickness of thunderstorm outflows. The cold front has strongest horizontal shears near the ground. Aloft (above 3,000 feet), the cold front becomes quite diffuse and wide, and horizontal shears are correspondingly weak. Occasionally though in the Southern Plains, strong surface fronts outrun the cold air aloft as shown in figure 7. In this case, the cold air following the front is relatively thin, like the thunderstorm outflow.



TYPICAL FRONTAL CONFIGURATION



SURFACE FRONT OUTFRUNNING FRONT ALOFT

80-1-7

FIGURE 7. VERTICAL CROSS SECTIONS OF TWO TYPES OF COLD FRONTS

SEABREEZE FRONTS. The seabreeze front is a phenomenon commonly found in areas where a landmass is adjacent to a large water body. In order for the seabreeze to be well developed, the general weather pattern should be characterized by fair weather and a light offshore airflow in the morning. The fair weather will allow ample heating of the ground and the air near the ground in the forenoon hours. The light offshore wind will be a precondition for a wind shift to an onshore breeze after the seabreeze develops. Another condition for a significant seabreeze is to have the water temperature and the air above it cold, relative to the temperature of the air over the heated landmass. It is the juxtaposed warm and cold air over land and water, respectively, that causes the seabreeze front. The warm air rises and the cold air replaces the rising warm air by moving inland. Seabreeze fronts tend to move inland in daylight hours and recede toward the shore or dissipate after nightfall.

The seabreeze front moves slowly, typically 5 knots, but the frontal width is narrow. The shears associated with the front are never large but may exceed the preset vector difference threshold of the LLWSAS if weather criteria necessary for strong seabreeze development are favorable. Such is frequently the case at New York Kennedy and Boston Logan airports in the late spring or early summer. Seabreeze fronts are not strong at Tampa because the water temperature is warm. Because Houston is so far from the gulf coastline, seabreeze fronts have lost much of their strength before reaching the airport. Lake breezes scenarios may be expected at future LLWSAS sites near the Great Lakes.

OTHER WEATHER PHENOMENA. Two other weather phenomena produce low-level vertical wind shear but only insignificant amounts of horizontal wind shear. These are the warm front and the low-level jet, the latter prevalent in the Midwest at night. Since the LLWSAS cannot measure winds in a vertical plane, vertical shears cannot be calculated. Vertical shears are believed to be flyable shears, but their danger lies in the surprise element. Vertical shears not expected by pilots may cause an unstable platform at a critical point in an approach or departure (Iberian Airlines, Logan Airport accident—NTSB report, reference 13). Unexpected low-level atmospheric wind flows divert pilot attention when it is needed most for other important functions on approach or takeoff. Since LLWSAS cannot detect vertical shears, atmospheric phenomena producing such shears will not be fully described.

#### LLWSAS HARDWARE.

Portions of the text and many of the diagrams in this section have been extracted from the contractor's instruction book (Sangano Weston Instruction Book, LLWSAS, Contract No. DOT-FA78WA-4244).

The LLWSAS utilizes state-of-the-art, solid-state electronics and a minicomputer to collect and process the data from up to six wind sensors. Data are output on three types of displays. Although system simplicity is desired, LLWSAS is relatively sophisticated. Figure 8 illustrates the LLWSAS equipment which at the six sensor sites consists of:

1. Wind Sensor (Anemometer)
2. Radio Antenna
3. Remote Station Data Box
4. Remote Controller Printed Wire Assembly (PWA)
5. Peak Wind/Averager/Multiplexer PWA
6. Analog to Digital (A/D) Converter PWA
7. Modulator-Demodulator (modem) PWA
8. Very High Frequency-Frequency Modulation (VHF-FM) Transceiver PWA
9. Direct Current (d.c.) Power Supply and Regulator
10. 12-volt d.c. Battery

and at the master station consists of:

1. Cathode-Ray Tube (CRT) Diagnostic Display with Keyboard
2. Radio Antenna
3. Central Station Rack
4. Paper Tape Reader
5. VHF-FM Transceiver PWA
6. Master Controller PWA
7. Modem PWA
8. Central Processing Unit (CPU) Microcomputer and CPU Memory Backup
9. Direct Current Power Supply and Regulator with Blower Assembly
10. Uninterruptible Power Supply (UPS)
11. Tower Cab Wind Shear Displays with Power Supplies
12. Terminal Radar Approach Control (TRACON) Displays with Power Supplies

During the course of the LLWSAS test, a floppy disk was also interfaced to the central processing unit. A line printer was used occasionally in series with the 20-milliampere (mA) current loop line to the tower cab displays.

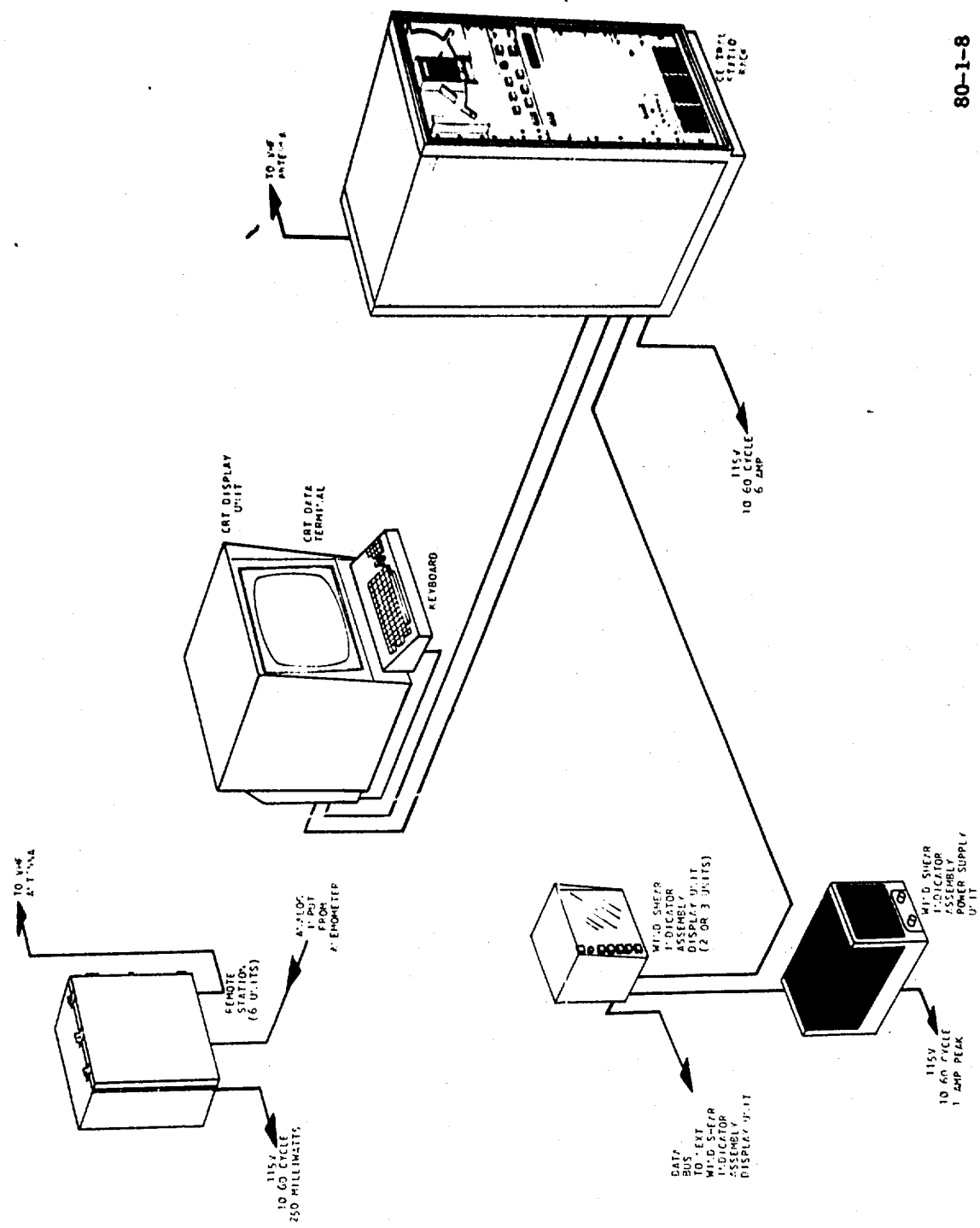


FIGURE 8. LOW-LEVEL WIND SHEAR ALERT SYSTEM: RELATIONSHIP OF UNITS

80-1-8

**REMOTE STATIONS.** Three types of masts were used to support LLWSAS anemometer sensors during the test. The recommended and most commonly used type was the wooden utility pole with climbing steps. At certain locations, where frangibility standards were required, a three-legged, thin wall aluminum tubing mast was used. This type of tower is not climbable, and a lift device is necessary for in situ sensor calibrations. Although one such 8-foot, lightweight tower installed on a pier at Kennedy airport proved adequate because of its short height, the 20-foot version installed at two other Kennedy locations, three Atlanta locations, and three Tampa locations proved troublesome as evidenced by the structural damage shown in figure 9. Sensor wind loading and torque action during high winds caused the aluminum tubing sections to loosen, resulting in tower collapse. A heavier duty, three-legged tower with steel rod legs and welded steel crossmembers on a frangible base plate was used successfully at one Kennedy location and all six Boston locations. This type is climbable and deemed adequate for LLWSAS sensors. One site each at Atlanta and Tampa uses a 2-inch pipe mast affixed to a runway transmissometer platform. All of the remaining airport LLWSAS sensor mounts are utility poles.

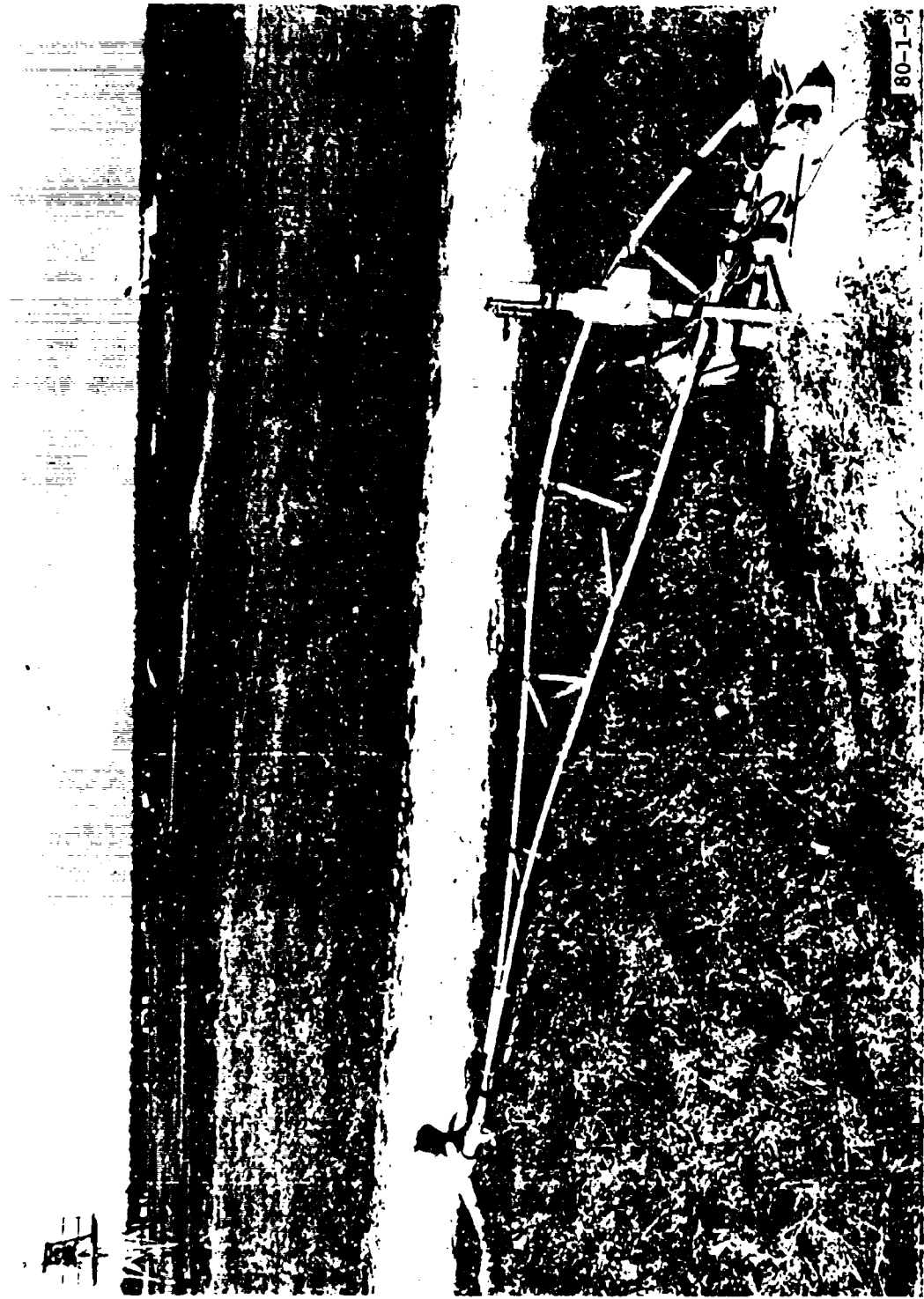
Since LLWSAS uses FM radio for communication, an antenna at each remote site is necessary. Antennae are easily mounted on utility poles and heavy duty metal towers, but use of the lightweight tower for the sensor requires the installation of a separate support for the antenna (and electronics box). This is another disadvantage of these types of masts.

FM antennae used in the LLWSAS are of two types: a quasi-directional dipole and directional yagi. Yagi antennae are used at Boston exclusively. Dipoles are used at other sites. Both give adequate performance.

The wind sensor employed in LLWSAS at each field station measures wind speed and direction in one unit (figure 10). The speed transducer feeds its signal to a sine/cosine potentiometer which produces u- and v-component voltages proportional to the east-west and north-south wind components.

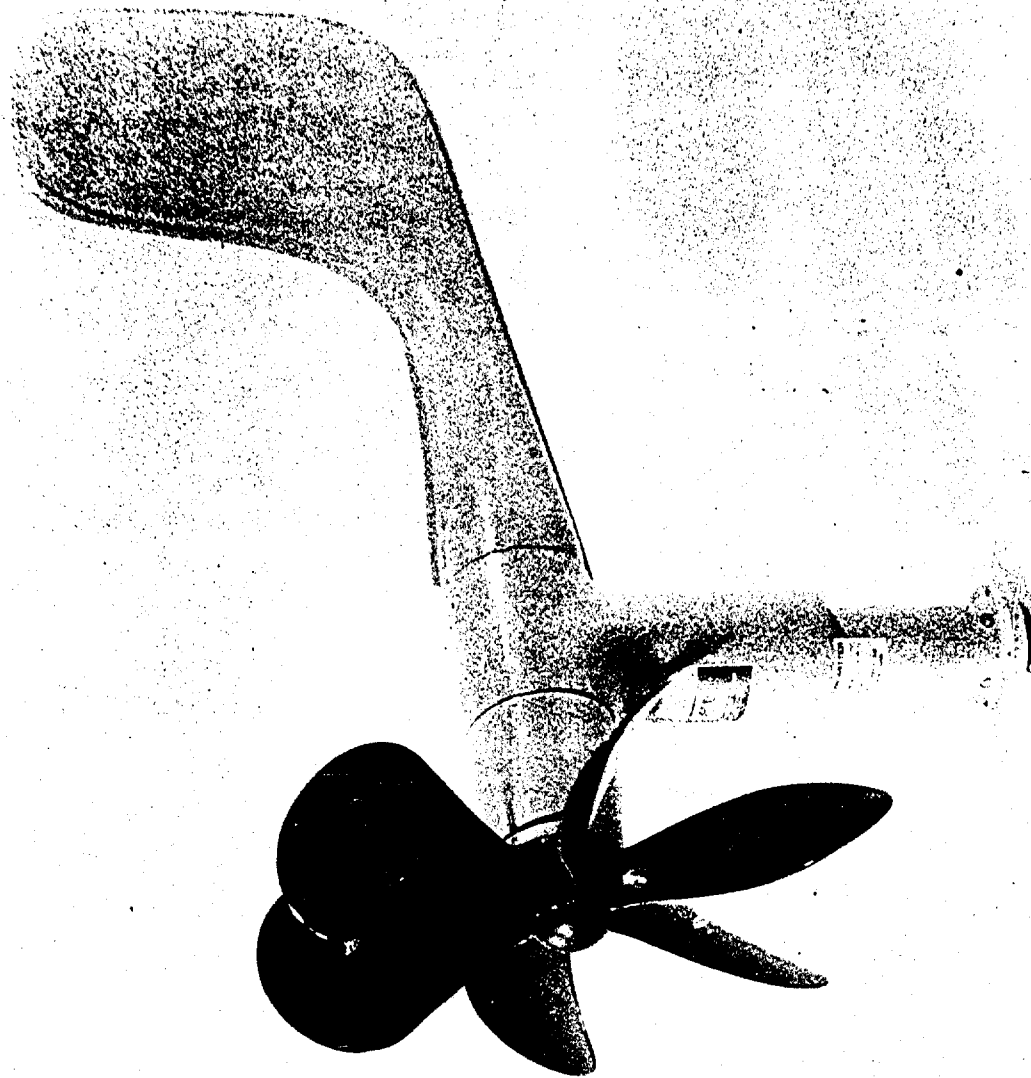
At the centerfield station only, one branch of the speed transducer signal bypasses the sine/cosine potentiometer and together with the u- and v-component analog voltages from the potentiometer (second branch) is fed to the electronics box. At the five remote stations, only the u- and v-component analog voltages are fed to the electronics box.

The electronics box (figure 11) is a watertight metal frame containing five printed circuit boards (LLWSAS remote station hardware, items 4 through 8), connecting mother board (data bus), battery, and power supply (figure 12). Incoming analog signals are fed through a plug to the averager board at remote sites or the peak wind detector board at the centerfield site (figure 13).



80-1-9

FIGURE 9. STRUCTURAL DAMAGE TO FRANGIBLE TOWER



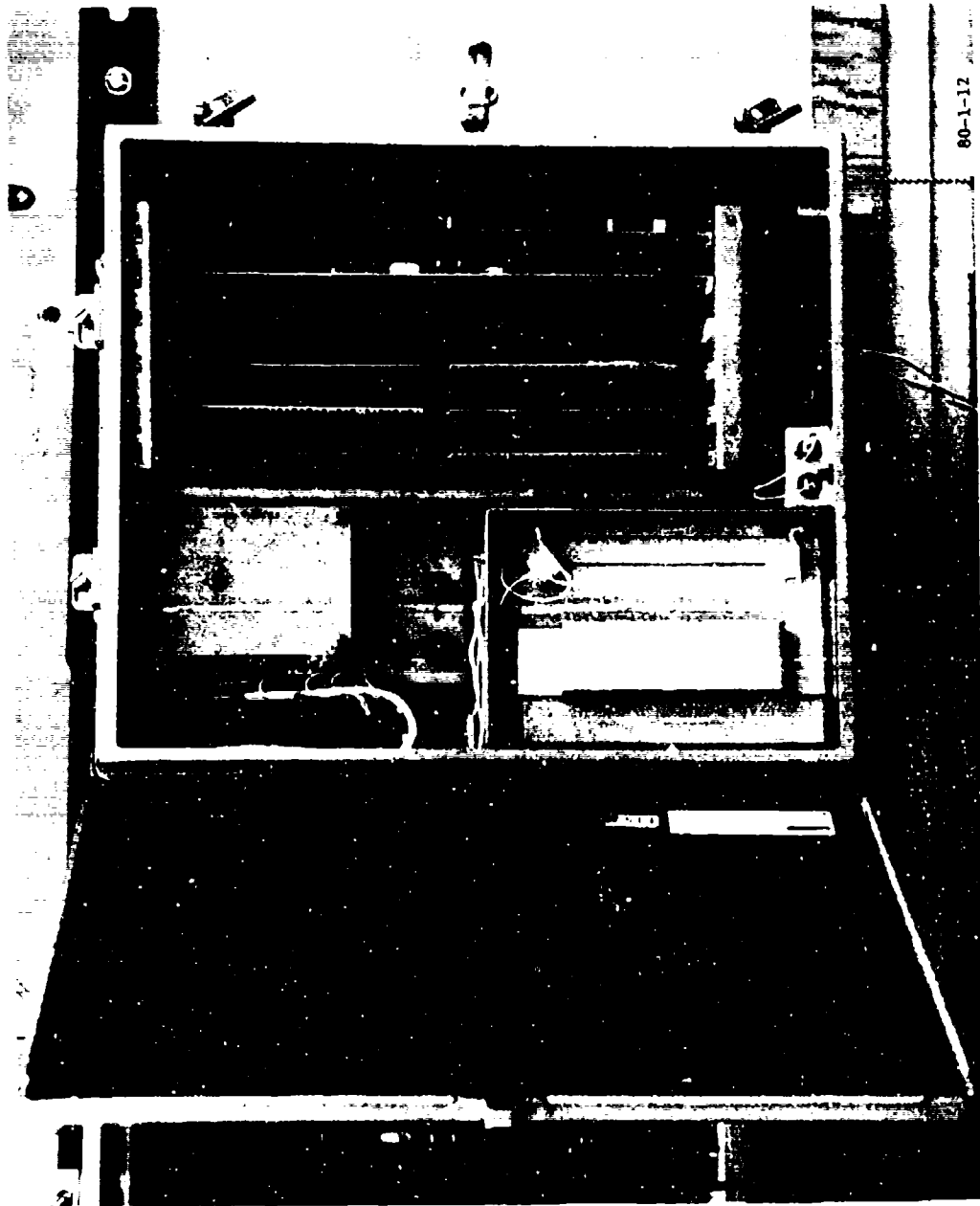
80-1-10

1 2 3 4 5 6 7 8 9 10 11 12 13 14  
FEDERAL AVIATION ADMINISTRATION

FIGURE 10. WIND VECTOR TRANSMITTER USED IN LLWSAS



FIGURE 11. ENVIRONMENTAL ELECTRONICS BOX—CLOSED



80-1-12

FIGURE 12. ENVIRONMENTAL ELECTRONICS BOX—OPEN

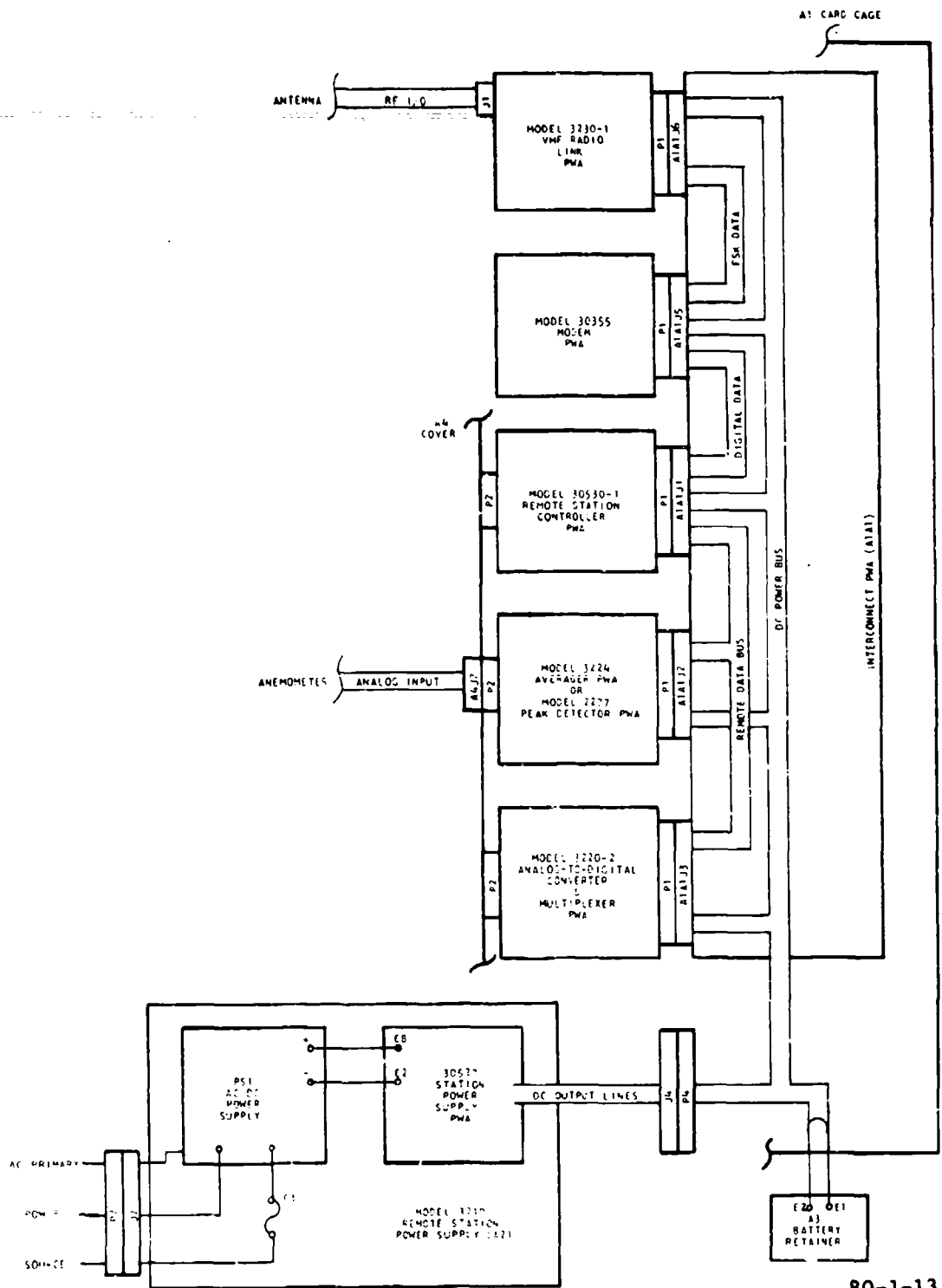


FIGURE 13. REMOTE STATION POWER AND SIGNAL DISTRIBUTION DIAGRAM

80-1-13

In the most updated version of LLWSAS, the averager and peak wind circuitry are built onto the same board. The board is labelled "peak detector." As received from the factory, the board will operate as an averager card with no reconfiguring. When this board is used at the centerfield site as a peak detector, however, the averager function must be deactivated. When the board is used as an averager, the peak detector function is bypassed because it conditions the signal on channel three (peak wind) which is not available at remote sites.

Two other standard functions are performed on the peak wind/averager cards: scaling and time multiplexing. The scaling function changes the raw input voltage to a fixed  $\pm 5$ -volt. After the signal leaves the averager/peak wind-detector board, all signals use the same circuitry. Functional diagrams of the averager and peak detector boards are shown in figures 14 and 15, respectively.

The remote controller and analog-to-digital (A/D) converter cards are linked via the data bus. The controller card (figure 16) intercepts the serial incoming interrogation message from the master station, performs a serial-to-parallel conversion, determines if the incoming message has the correct station code, and if it does, commands the A/D converter to accept analog signals from the averager/peak detector and to send a burst of digital data back to the controller. The A/D converter (figure 17) digitizes the two (remote stations) or three (centerfield stations) analog signals inbound from the averager/peak detector multiplexer, and relays the digitized data stream upon command to the controller. The controller converts from parallel to serial data stream.

The serial digital data stream is sent from the remote controller to the remote modem. The modem (figure 18) converts the outgoing signal from a bilevel digital data stream to a frequency shift keying (FSK) signal for the radio transmitter. The modem also receives the incoming parallel signal from the master controller via the remote transceiver and performs the FSK-to-bilevel digital data conversion for the remote controller.

The radio is a VHF transceiver (figure 19) and is connected to an FM antenna. The radio has transmit and receive crystals. Several frequencies are used throughout the LLWSAS network: 162.375, 165.250, 165.350, 165.7625, and 169.375 megahertz (MHz), but only two per airport. All remote station transmitters will eventually be changed to the 169.375 MHz frequency because of possible interference with the National Oceanographic and Atmospheric Administration (NOAA) voice transmitted weather radio. NOAA uses the 162.4 MHz frequency and is listened to by private individuals often owning inexpensive, broadband radios. The steady "beeping" of the LLWSAS transmitters is overpowering if the listener is close to the LLWSAS airport. LLWSAS interference with NOAA Weather Radio has been reported at Atlanta, Oklahoma City, Houston, and NAFEC.

The LLWSAS radio transmitter outputs 8 watts of power capable of communications within 10 to 15 miles if an omnidirectional antenna is used. By and large, remote stations use a quasi-directional dipole antenna configuration or yagi antenna, but the master station antenna is omnidirectional.

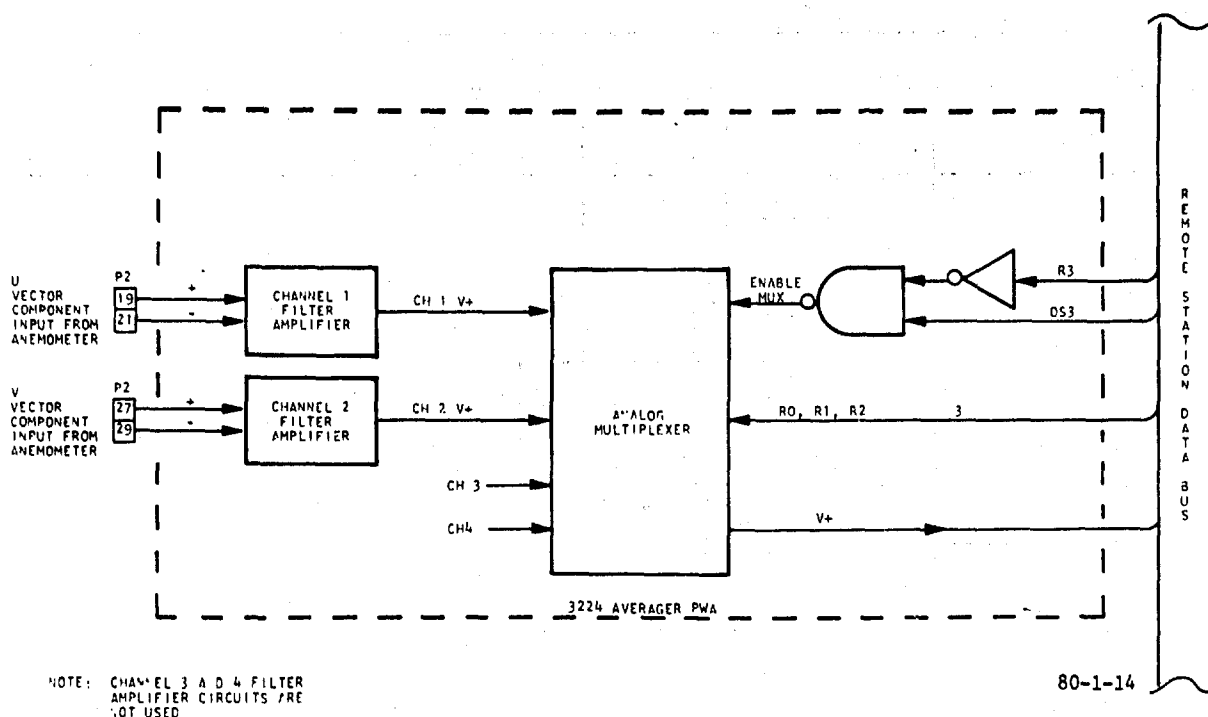


FIGURE 14. AVERAGER FUNCTIONAL BLOCK DIAGRAM

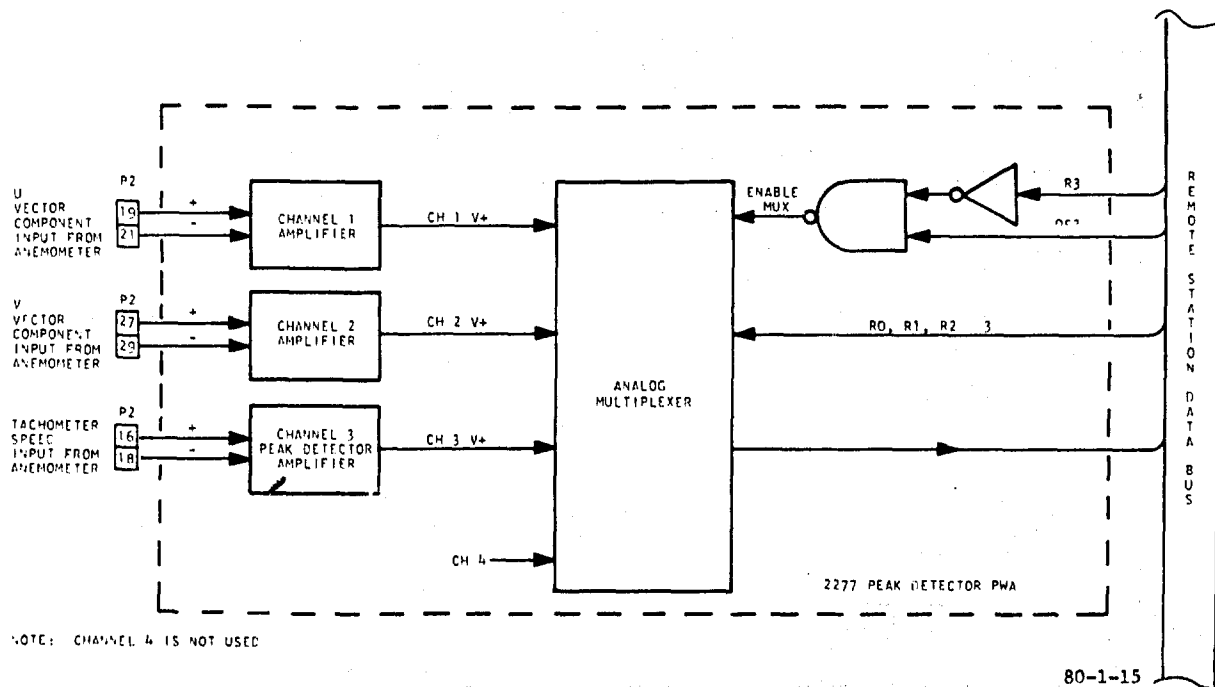
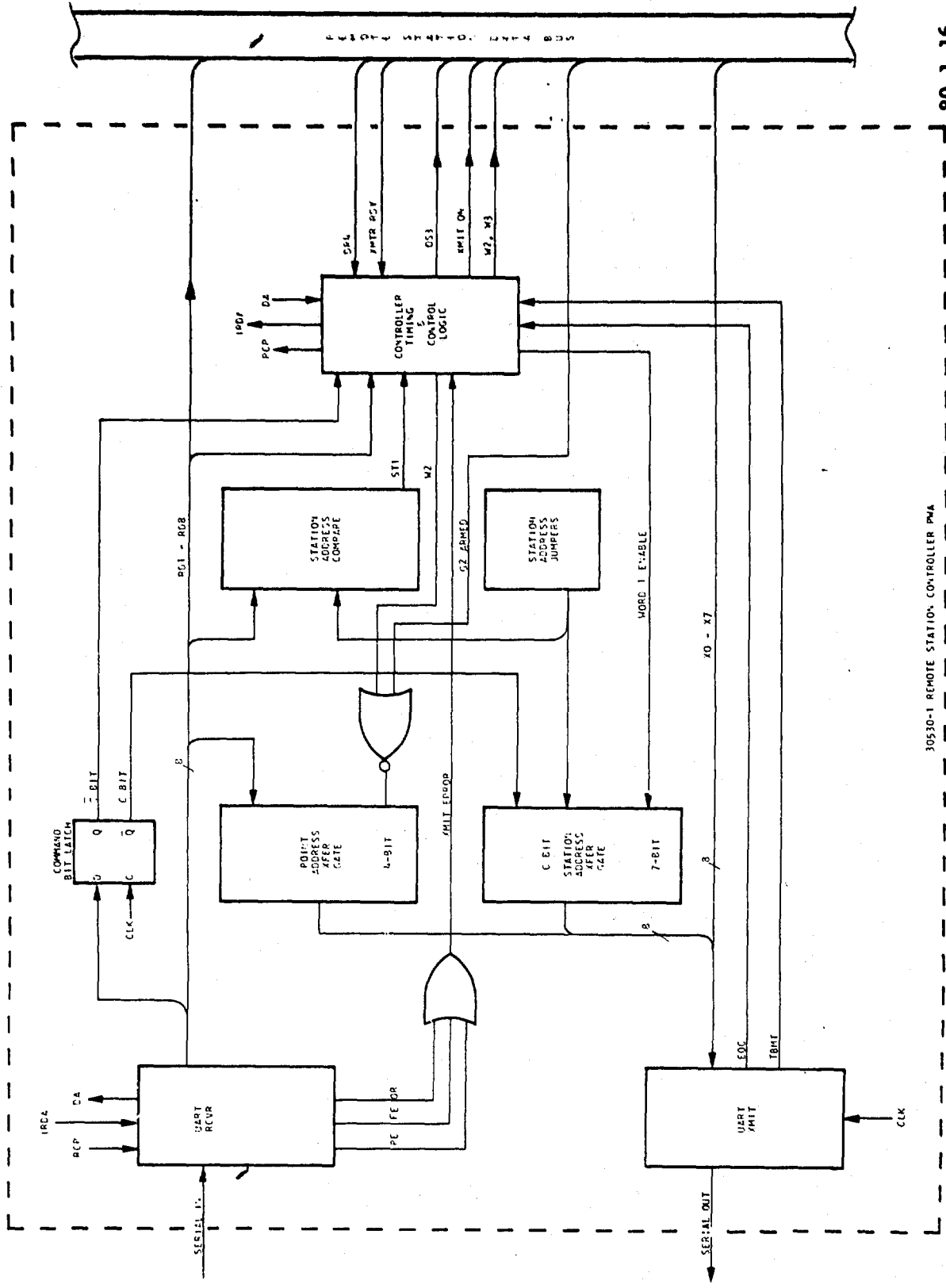


FIGURE 15. PEAK DETECTOR PRINTED WIRE ASSEMBLY (PWA) FUNCTIONAL BLOCK DIAGRAM



30530-1 REMOTE STATION CONTROLLER PWA

80-1-16

FIGURE 16. REMOTE STATION CONTROLLER PRINTED WIRE ASSEMBLY (PWA) FUNCTIONAL BLOCK DIAGRAM

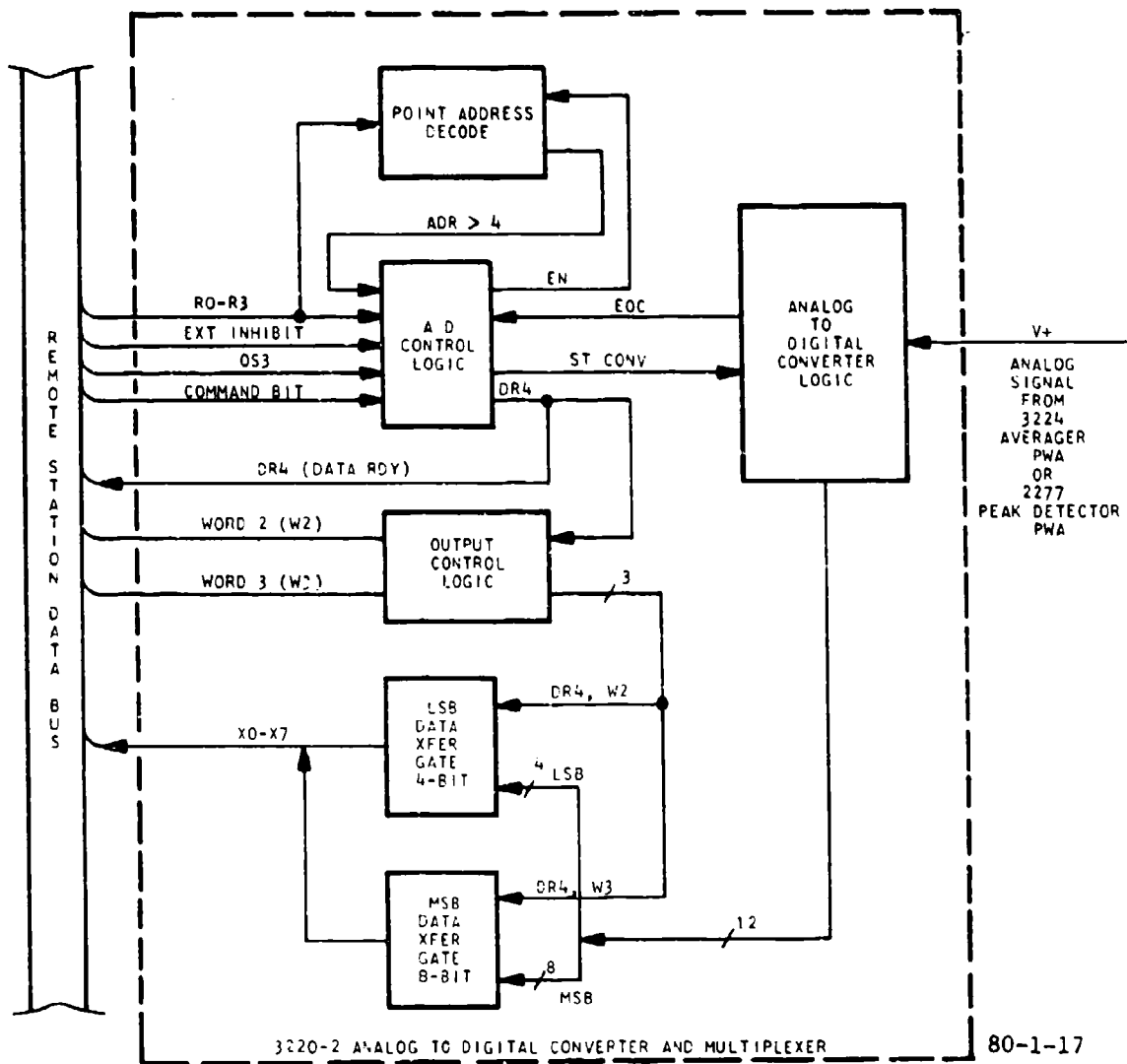


FIGURE 17. ANALOG-TO-DIGITAL CONVERTER AND MULTIPLEXER FUNCTIONAL BLOCK DIAGRAM

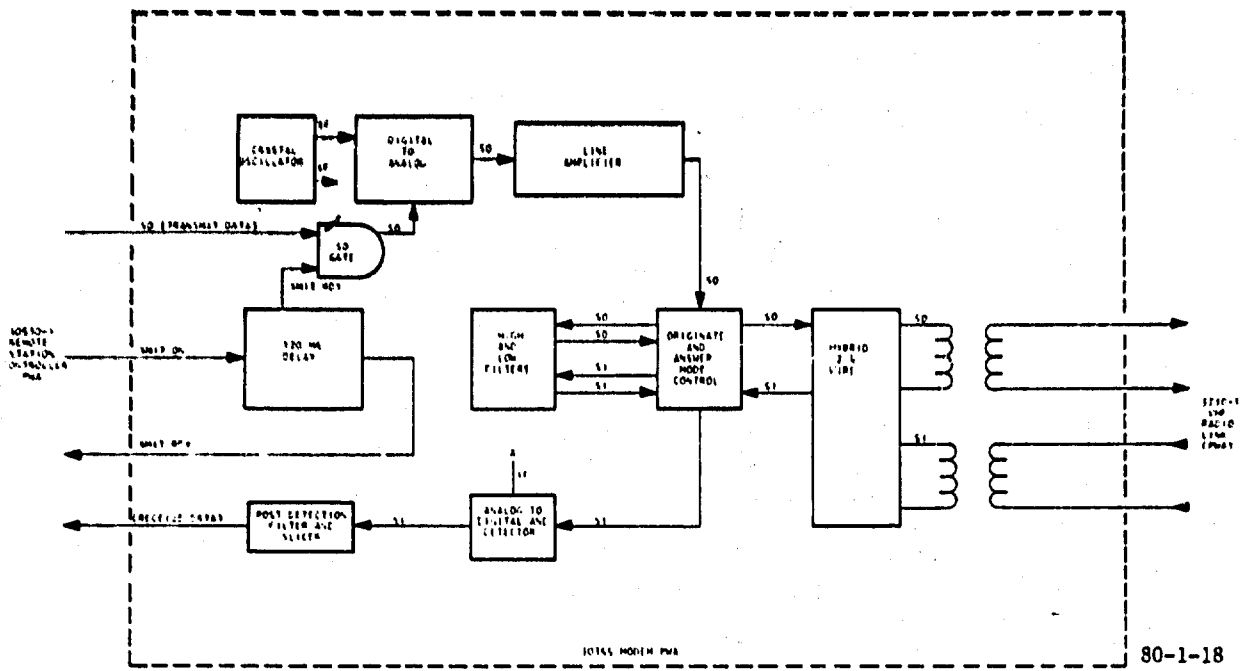


FIGURE 18. MODEM FUNCTIONAL BLOCK DIAGRAM

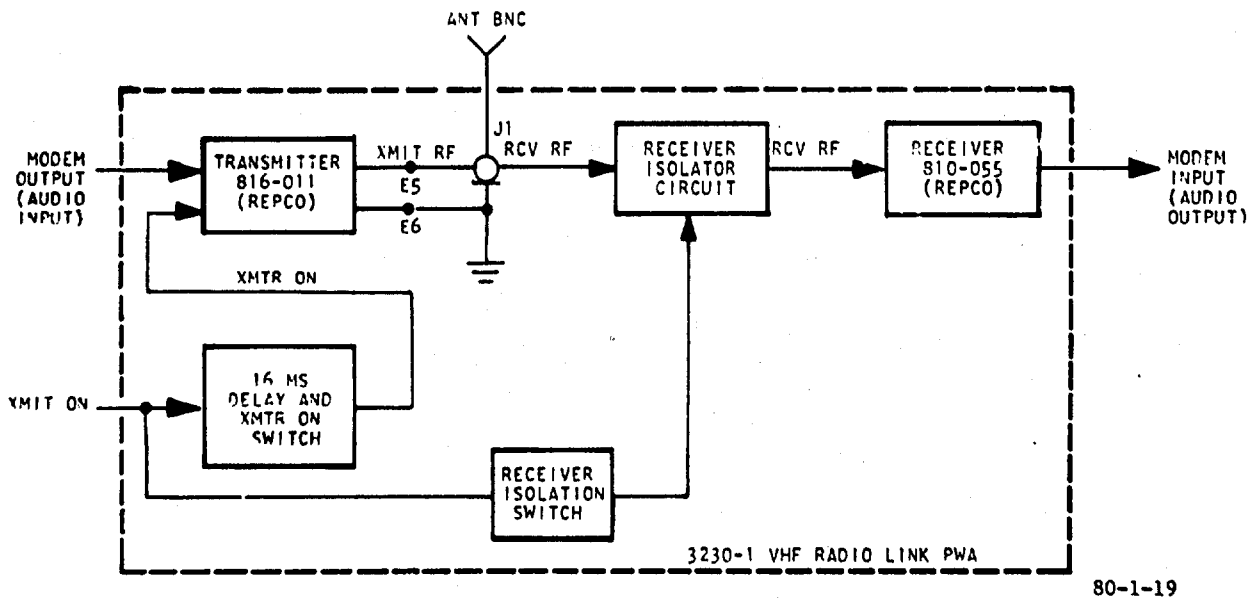


FIGURE 19. VHF RADIO LINK FUNCTIONAL BLOCK DIAGRAM

The radio requires 2 amps of current when transmitting. Data scanning rates are constrained in part by the power-up time of the radio. Each stream of data transmitted to the master station from the remote station requires 540 milliseconds (ms). Two data blocks are transmitted from each remote (u- and v-components) and three blocks from the centerfield station (u- and v-components plus peak wind).

Each sensor site electronics box is equipped with a power supply and backup battery. Although each facility will operate from d.c. power supplied by a 12-volt battery, a.c. is necessary to initiate operation. The site normally operates from a 115-volt a.c. source. If by chance a.c. power is lost, the sensor site will automatically switch to the backup d.c. power source. The battery should maintain enough charge to provide electronics operation for several hours. Thereafter, communications will be lost unless a.c. power is restored.

MASTER STATION. If all remote stations are operational, data will be transmitted to the master station once every 7 seconds (the scan rate is constrained principally by the power-up time of radio transceivers). At the master station, the first three components are nearly identical to those at each remote station: antenna, radio transceiver, and modem. Their functions have been described. The master station modem is part of the system master controller. As the name implies, the controller is the electronic regulator and coordinator of all incoming and outgoing signals to and from the master station. Its functional diagram is shown in figure 20. The unit controls the recurring transmit and receive phases of each system interrogation cycle. During the transmit phase of an interrogation cycle, the controller formats and regulates the transmission of messages. The controller checks returned messages for parity (even) and addresses echoing (the bit-for-bit comparison of outgoing and incoming station and data point addresses). The controller initiates the interrogation cycle when a NEW DATA READY signal is received from the CPU. Within the controller is a universal asynchronous receiver/transmitter (UART) which gates all data, address, and command bits into appropriate registers for parallel gating to the transmitter shift register (TSR). The TSR performs the parallel-to-serial signal conversion. Upon a strobing command from the master station modem, this serial data stream is sent from the UART to the modem. When a data stream is received from the remote station via the master radio and modem, it appears as a serial-in signal to the UART receiver, then is parallel gated to the UART receiver holding register.

After appropriate framing, parity, and address checks, the UART sends a parallel stream of wind data to the CPU. The software functions of the CPU are described in detail in the LLWSAS Software section. Hardware-wise, the CPU is configured with 16,000 (K) words by 16-bit semiconductor read/write memory, an extended arithmetic chip (allowing extended manipulation of fixed-point numbers and direct operations on single precision 32-bit words), serial line interfaces for the cathode-ray tube (CRT) terminal and cab displays, a parallel line interface for the controller, and a paper tape reader interface.

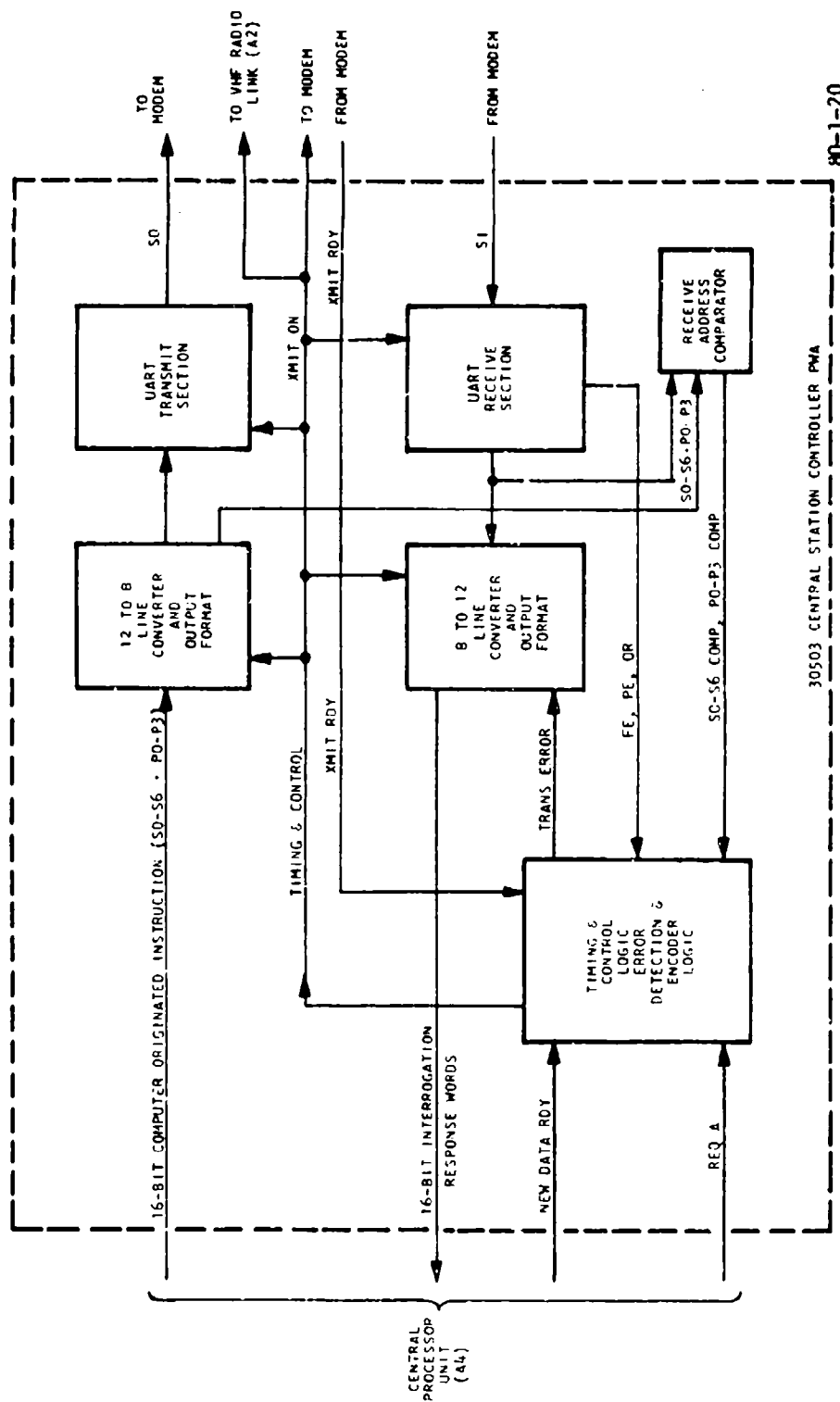


FIGURE 20. CENTRAL STATION CONTROLLER FUNCTIONAL BLOCK DIAGRAM (EXCLUDING MODEM)

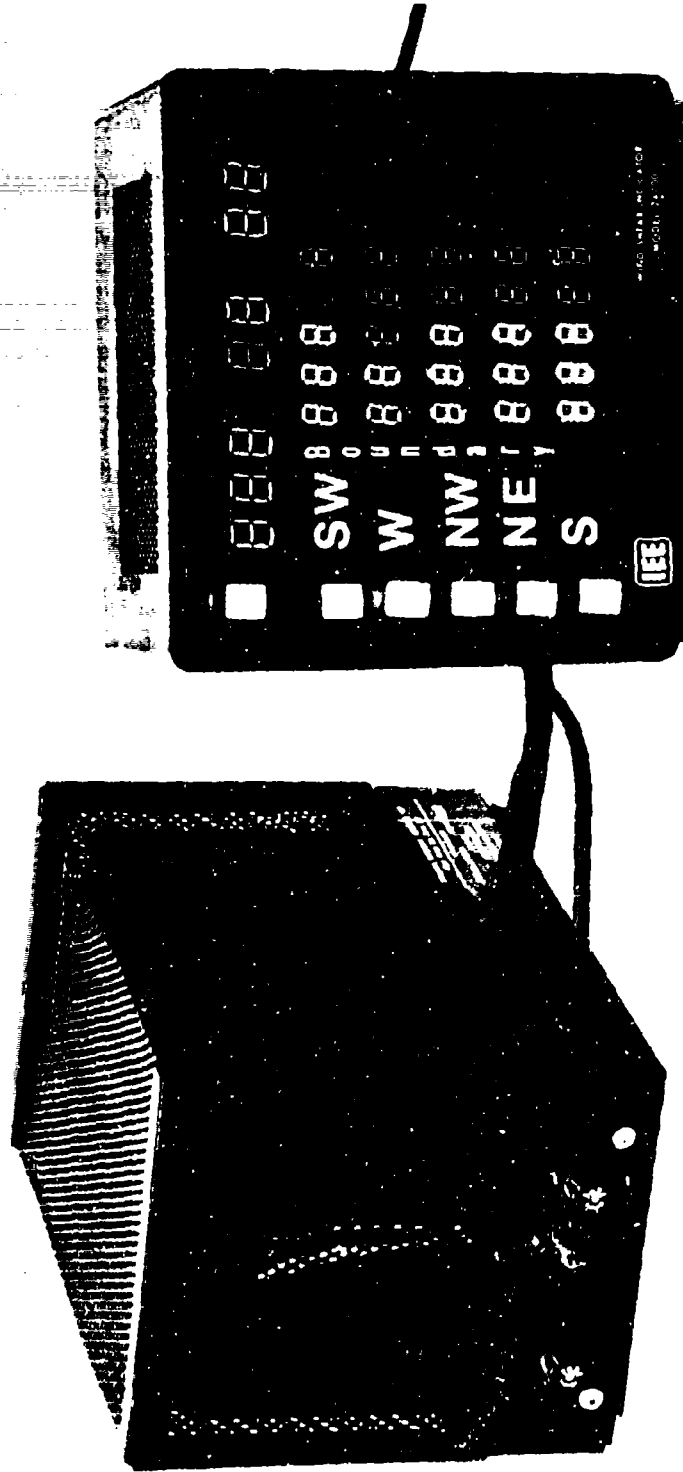
In addition to the CPU main frame and interfaces, the processing unit is equipped with a memory backup unit and an uninterruptible power supply (UPS). The memory backup unit retains system memory for 30 minutes in the event of primary power failure. To prevent unwanted transients in the event of a switchover to the backup battery, the unit contains a secondary power supply which replaces the main power supply if a switchover occurs. The memory backup unit also contains an a.c./d.c. converter, two d.c./d.c. converters, and battery charger. The a.c./d.c. converter accepts the 115-volt primary line voltage (from the UPS) and produces a 17-volt d.c. output for the d.c./d.c. converter. One module of the d.c./d.c. converter accepts the nominal 17-volt d.c. output of the a.c./d.c. converter and produces a regulated +5-volt d.c. output for the CPU. The battery charger unit also accepts the 17-volt output of the a.c./d.c. converter and outputs +14-volt d.c. to the second module of the d.c./d.c. converter. This module is responsible for maintaining a constant +12-volt d.c. charge to the battery.

The UPS unit was retrofit to all seven LLWSAS airports in the summer of 1978. This action was necessary, particularly at Denver which has an acute problem with frequent large amplitude transients on their 115-volt a.c. lines. These transients were of such a nature that the memory backup unit was incapable of filtering them and a fluctuating d.c. voltage was output to the CPU. This resulted in frequent system failures. The UPS unit not only provides a regulated 115 volts to the a.c./d.c. converter of the memory backup unit, but it also provides an additional 10 minutes of backup power to the LLWSAS master station in the event of a complete primary power failure. The unit contains a battery and a d.c./a.c. converter. At airports with clean primary power, the UPS unit is not necessary. For standardization, however, it has been included as an integral part of the master station electronics gear.

The main software program is loaded into the CPU via the paper tape reader (PTR). Assuming program reloading is not performed frequently, the PTR is usually a nonfunctioning part of the system and is turned off. This will ensure high reliability of this unit.

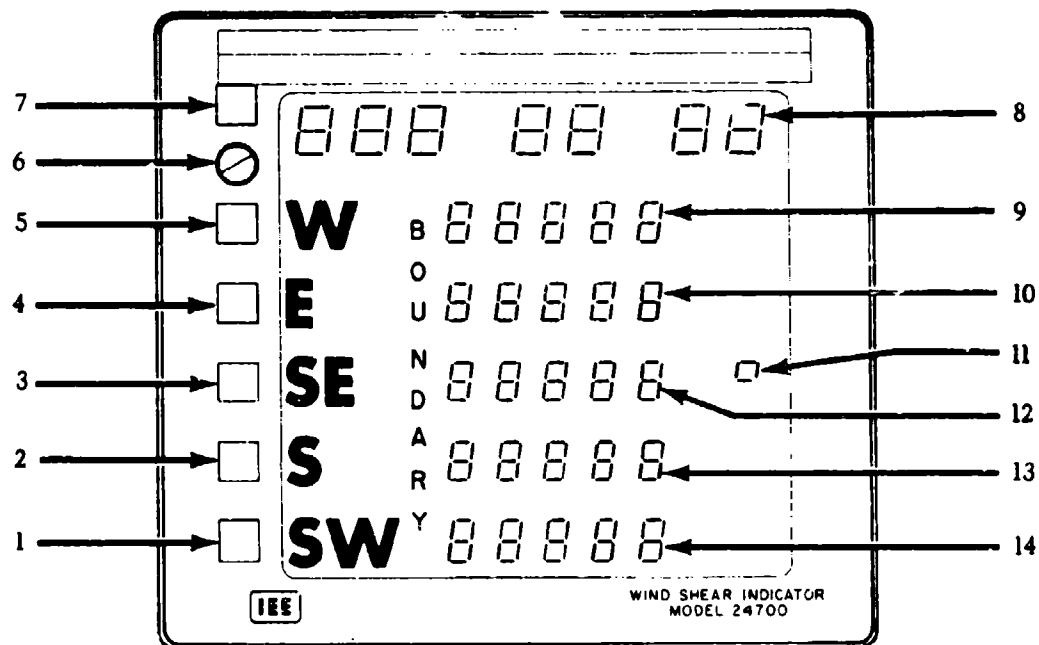
To load the paper tape and to perform certain maintenance functions, LLWSAS requires input commands from a keyboard connected to a CRT. Keyboard commands are simple for routine functions.

The CRT used at all LLWSAS test airports, except Boston, is a seven-color "smart" CRT. Boston is equipped with a black and white CRT. The color CRT was initially used as the tower cab display. Although CRT's are not suitable for the ambient light conditions of the tower and the LLWSAS color CRT is very large for the restricted space of the cab, a suitable off-the-shelf cab display was not available during the initial design phase of LLWSAS. In the summer of 1977, a more appropriate incandescent filament-type cab display replaced the CRT. The CRT was subsequently reformatted and used as a diagnostic display in the equipment room. The present CRT format is discussed further under LLWSAS Software. Figure 21 shows the cab indicator, figure 22 describes the indicator's data functions and front panel controls, and figure 23 is a representative cab installation (Atlanta). Dial-type wind indicators are also shown in the photograph.



80-1-21

FIGURE 21. WIND SHEAR INDICATOR (OLD TYPE)



- |   |   |
|---|---|
| 1. Boundary row (No. 6) blanking switch   | 9. No. 2 boundary indicator row (left-most three indicators display wind direction, right-most two indicators display wind speed) |
| 2. Boundary row (No. 5) blanking switch   | 10. No. 3 boundary indicator row (indicators same as No. 2 boundary indicator row)  |
| 3. Boundary row (No. 4) blanking switch   | 11. System failure indicator  |
| 4. Boundary row (No. 3) blanking switch   | 12. No. 4 boundary indicator row (indicators same as No. 2 boundary indicator row)  |
| 5. Boundary row (No. 2) blanking switch   | 13. No. 5 boundary indicator row (indicators same as No. 2 boundary indicator row)  |
| 6. Brightness control   | 14. No. 6 boundary indicator row (indicators same as No. 2 boundary indicator row)  |
| 7. Indicator test switch  |   |
| 8. CFA indicator row (left-most three indicators display wind direction, two middle indicators display wind speed, two right-most indicators display wind gust) |   |

80-1-22

FIGURE 22. WIND SHEAR INDICATOR ASSEMBLY DISPLAY UNIT FRONT PANEL

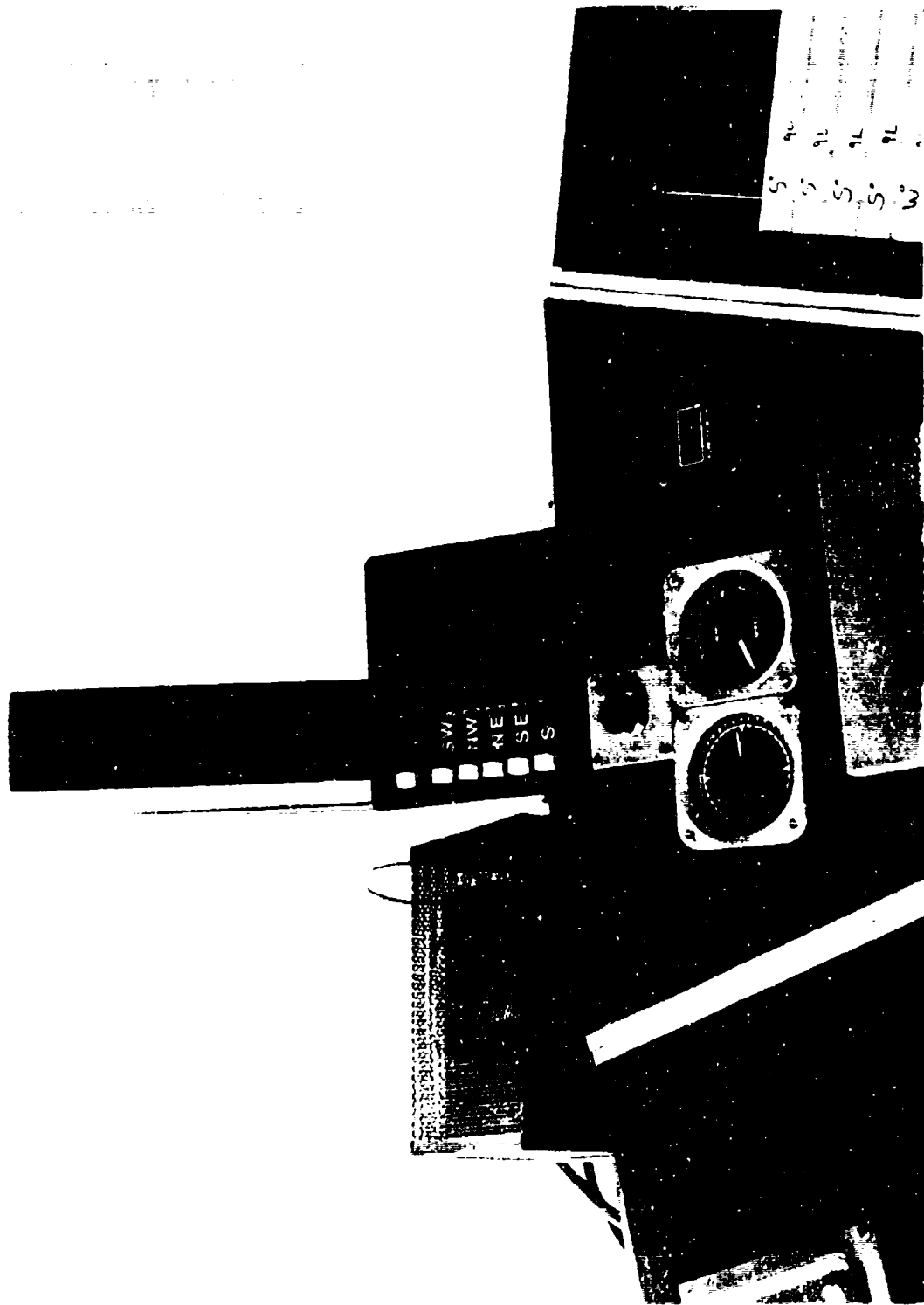


FIGURE 23. WIND SHEAR INDICATOR IN PLACE IN ATLANTA TOWER

The incandescent cab display (otherwise known as the wind shear indicator) is a six-row array of seven-segment indicators which displays the wind direction, speed, and gusts (the latter from the centerfield station only) input from the CPU. The logic circuitry accepts bit serial, character serial input at a 300-baud rate sent from the CPU along a 20-mA current loop. Each indicator is equipped with a power supply in a separate housing.

Two redesign features were added to the cab indicator after initial installation.

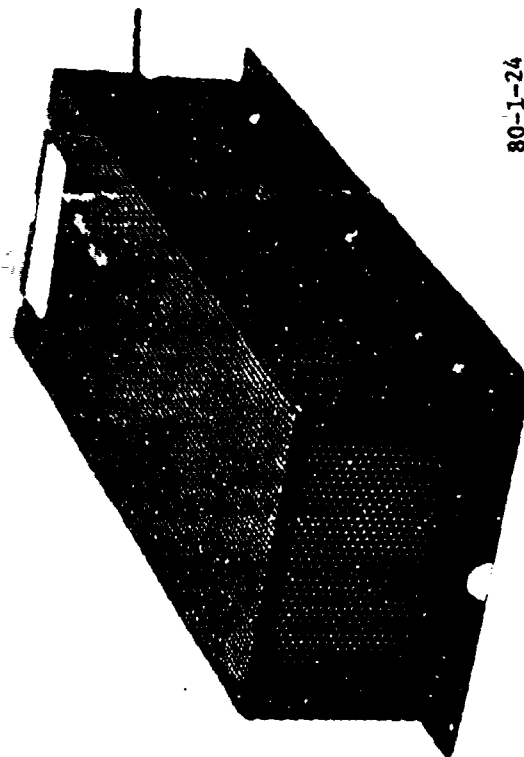
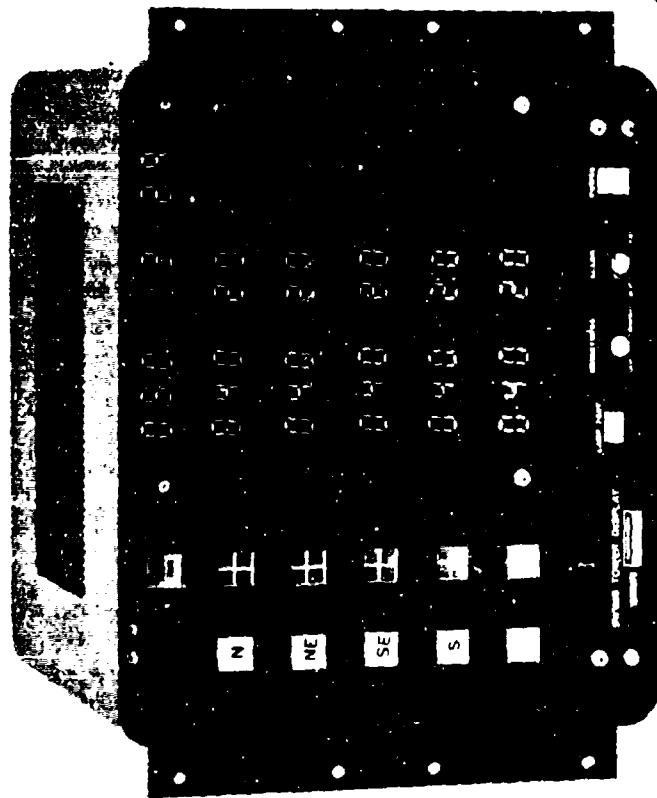
1. A control for intensity of the audible alarm.
2. A one-shot (time-out) device to light a red bulb in the event data was not refreshed in 45 seconds.

Item 2 was deemed necessary because air traffic controllers were unable to determine when a CPU failure or halt occurred. In the case of a failure or halt, the last good wind information from the CPU would be "frozen" on the indicator and might not be quickly recognized as old data. Incidents occurred during the test when controllers did not recognize the CPU halt condition for several hours.

When the Boston LLWSAS was planned, the tower cab display (figure 24) was redesigned. The major change was the adoption of the printed circuit board concept rather than the wire wrap concept of the original wind shear indicator. This change facilitates maintenance. The display's power supply is a separate unit. All manual controls (including those retrofit to the original indicator) are accessible from the front of the display (figure 25). The indicator also has extra display features to allow integration of future systems such as the Vortex Advisory System (VAS) or the Runway Use Program. The controller board of the wind shear indicator is interchangeable with a like board in the TRACON wind indicator (see section on LLWSAS Hardware, TRACON Display).

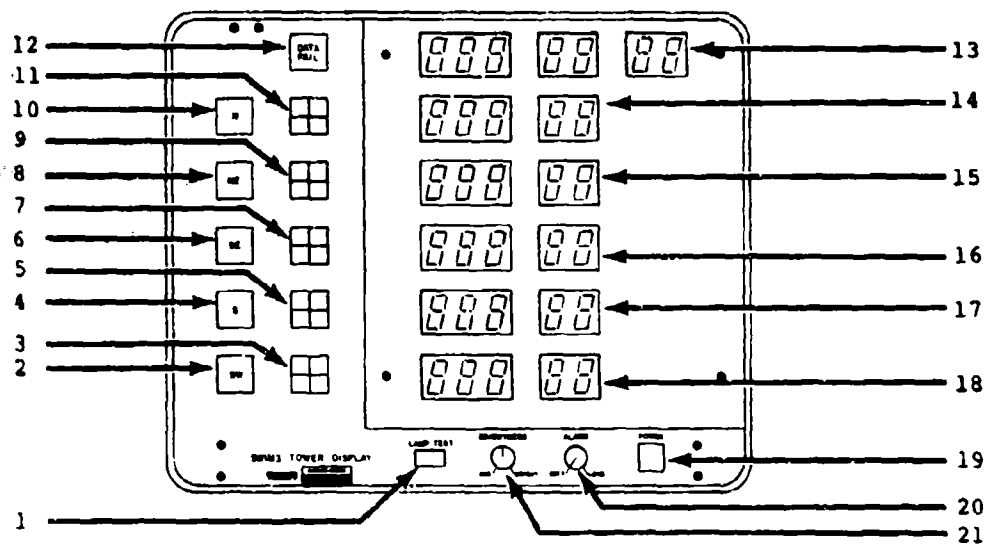
Three other pieces of auxiliary gear interfaced to the CPU were used during the LLWSAS test. This equipment was used exclusively for the LLWSAS data collection effort and includes a floppy disk, line printer, and telephone interface for the airport-to-NAFEC data transmission. None of this equipment is included in the operational version of LLWSAS.

The floppy disk unit is a dual floppy capable of recording up to 40 hours of LLWSAS wind information on a single disk. System software limited data recording to 24 hours per single disk. The floppy disk was used heavily in the fall of 1977 and spring of 1978 for data collection. Diskettes were mailed to NAFEC and the data analyzed using the NAFEC General Purpose Computer and NAFEC-generated data processing programs described later under LLWSAS Data Collection and Analysis. The floppy disks were disconnected at the end of the LLWSAS test in early 1979.



80-1-24

FIGURE 24. WIND SHEAR INDICATOR (NEW TYPE)



- |  |  |
|--|--|
| 1. LAMP Test switch                        | 12. DATA FAIL indicator  |
| 2. Boundary row (No. 6) blanking switch    | 13. CFA indicator row (left-most three indicators display wind direction, two middle indicators display wind speed, two right-most indicators display wind gust) |
| 3. Boundary row (No. 6) status indicators  | 14. Boundary indicator row No. 2 (left-most three indicator display wind direction, two middle indicators display wind speed)                                    |
| 4. Boundary row (No. 5) blanking switch    | 15. Boundary indicator No. 3 (indicators same as row 2)  |
| 5. Boundary row (No. 5) status indicators  | 16. Boundary indicator No. 4 (indicators same as row 2)  |
| 6. Boundary row (No. 4) blanking switch    | 17. Boundary indicator No. 5 (indicators same as row 2)  |
| 7. Boundary row (No. 4) status indicators  | 18. Boundary indicator No. 6 (indicators same as row 2)  |
| 8. Boundary row (No. 3) blanking switch    | 19. POWER switch   |
| 9. Boundary row (No. 3) status indicators  | 20. ALARM control  |
| 10. Boundary row (No. 2) blanking switch   | 21. BRIGHTNESS control   |
| 11. Boundary row (No. 2) status indicators |  |

80-1-25

FIGURE 25. WIND SHEAR INDICATOR FRONT PANEL (NEW TYPE)

Since the turnaround time for data collected on the floppy for conversion to analysable form was unacceptably long, a hand-carry line printer was procured and used for a real-time check of the LLWSAS data. The purpose of the line printer was not to collect long strings of data but rather to make a permanent record of short data bursts for adequate siting verification and sensor read-out comparisons. The line printer is daisy-chained in the 20-mA current loop of the wind shear indicator run and is connected to this loop via a port at the rear of the master station rack. The line printer and appropriate port is recommended for data checks in future systems prior to full commissioning.

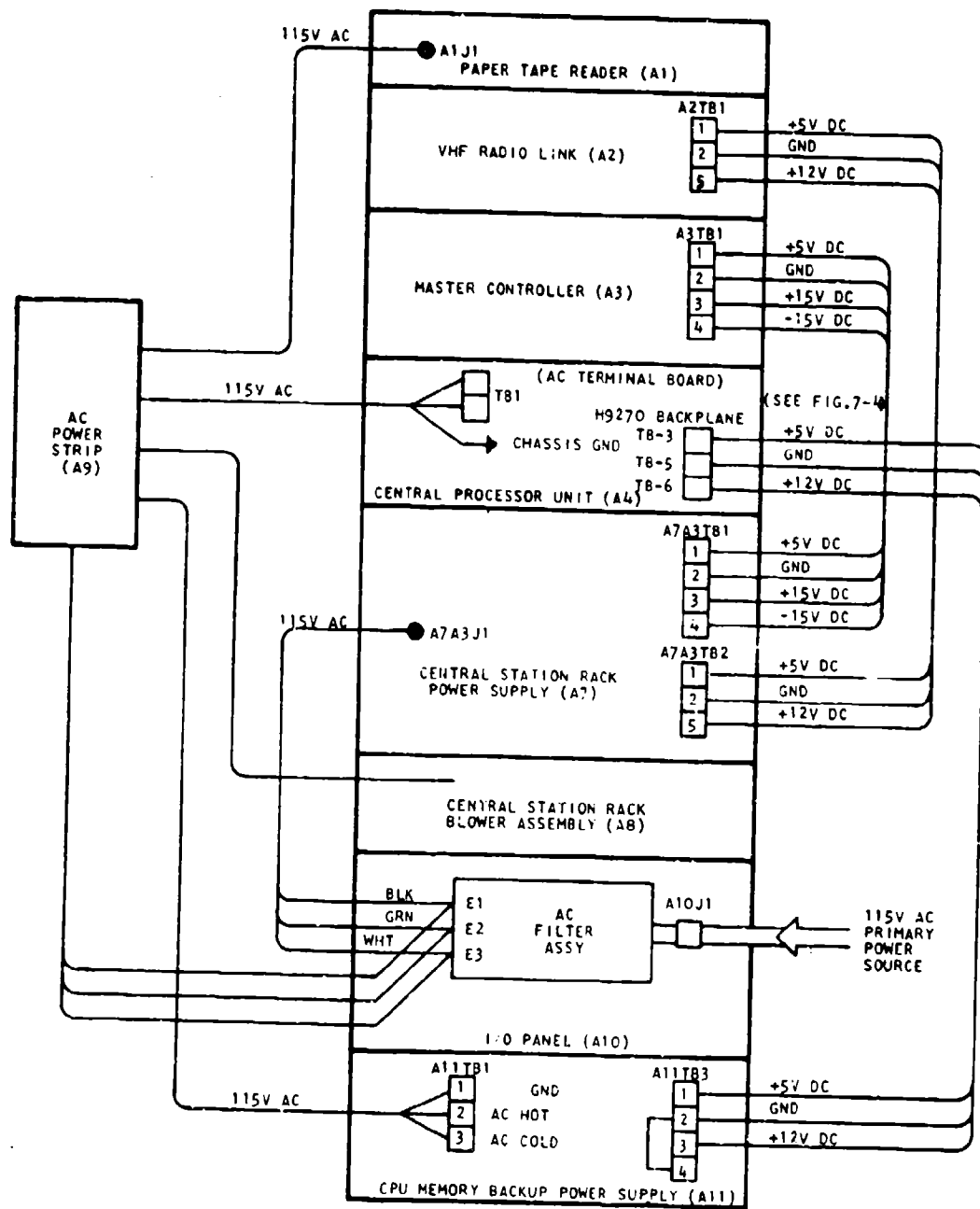
The master station controller, CPU, radio, power supplies, UPS, memory backup, and blower are installed in a 39-inch rack. This is a nonstandard rack which is deeper and shorter than the standard FAA rack. Therefore, some facilities (Houston and Oklahoma City) have chosen to install the LLWSAS equipment in a standard FAA rack. However, the color CRT is not rack-mountable and other arrangements have been made for it. At Houston it is on a nearby table, and at Oklahoma City, it has been mounted on an inclining shelf installed just above the rack and cable trough. Elsewhere, this CRT is mounted atop the 39-inch master rack placing it roughly at eye level. The only other variation in the seven-airport LLWSAS is at Tampa where the UPS has been installed in a standard rack next to the LLWSAS 39-inch rack. Boston is equipped with a small, hand-carry, detachable, rack-mountable, black and white CRT.

Whatever rack type is used, the unit must allow for proper ventilation. This is a necessity for the CPU. Frequent cleaning of the blower air filter is recommended. The master station power supply distribution is shown in figure 26.

The master station VHF antenna is mounted on the tower cab roof at all airports except Kennedy airport. At Kennedy, the antenna is mounted on an observation deck two stories below the roof level. Generally, a roof position is recommended. The antenna is connected to the master station radio card via coaxial cable. All airports except Boston use the dipole-type antenna at the master station. The loop of one dipole is oriented 180° out, with respect to the other loop. This configuration allows nearly omnidirectional radiofrequency (RF) output. The Boston master antenna is an omnidirectional pole type.

#### SPECIALIZED HARDWARE.

Centerfield Wind Gust Measurements. One major by-product of the LLWSAS program has been the sensing of centerfield wind speed gusts and the conditioning, processing, and displaying of the data. Although initial project requirements made no mention of a need to consider wind gusts in LLWSAS, it became apparent that such a consideration would have to be made and that it would become an integral part of the project. During the course of the test, improvements to the original design of the gust factor evolved concurrently with the larger scale project. What has been finalized in the prototype is a sensing, processing, and displaying system significantly different, but believed much improved, over the National Weather Service (NWS) system upon which ours was originally modeled.



80-1-26

FIGURE 26. CENTRAL STATION RACK POWER DISTRIBUTION DIAGRAM

LLWSAS initially used the conventional NWS wind sensor (Electric Speed model F-420) as its centerfield or reference sensor and continued to do so until July 1978. To electronically duplicate what the NWS does in mentally deducing gusts from the analog strip chart (determine the peak wind during a specified interval from the speed chart), the LLWSAS centerfield digital speed values from the F-420 were to be stored in the computer memory for 2 minutes. At display time, the largest speed value was selected from the 2-minute ensemble, but only displayed if it was 9 knots or more greater than the centerfield speed running mean. Two zeros were displayed if the gusts fell below the 9-knot threshold. The technique proved entirely inadequate, however, as the gust factor rarely exceeded the threshold even on gusty days.

When the F-420 was replaced by the Belfort Vectorvane in the major rework of LLWSAS hardware and software in early 1978, there was not much improvement in the frequency of a displayed gust factor. It was then realized that a gust factor could not be determined after analog-to-digital conversion (with the relatively slow LLWSAS scan rate), and the gust factor would have to be determined by inspecting the analog signal. The resulting modification proved to be the technique adopted for the prototype system. The scheme required a sensor modification, fabrication of a new card for the centerfield electronics box, and a modification of the computer software.

Hardware and software development and retrofitting to the six LLWSAS airports were completed in July 1978. Tests have shown that the new technique is a significant improvement to system performance over the old method, and the results now exceed NWS standards.

The centerfield sensor was modified by extracting from the speed generator/ tachometer the raw analog voltage, bypassing the sine/cosine potentiometer, and feeding the signal to the electronics box on a third signal channel (the other two signals being the u-, v-components of the horizontal wind from the potentiometer). For the electronics box, a new card was fabricated called the peak wind detector. (A second generation card is now available combining the peak wind functions of the centerfield station with averaging functions of the five remote stations. This was done to provide quasi-standardization between centerfield and remote stations). The peak wind detector card accepts the raw analog speed voltage and sends to the A/D converter/multiplexer the near-maximum voltage since the last scan. The peak wind detector output to the A/D converter/multiplexer exhibits an irregular sawtooth pattern. The peaks of the teeth represent surges in the wind speed; the negatively sloped backside of the tooth represents the gradual bleed-off of the peak voltage. A new tooth forms when the down ramping voltage is suddenly bolstered by a fresh wind gust. This is shown in figure 27.

The voltage bleed is slow so the peak wind sent to the A/D converter/multiplexer is only slightly less than the peak of the analog signal.

The peak wind is sent to the master station from the centerfield station on a separate channel. At the master station, it is sent to a computer memory register and stored. At update time, the gust register is inspected for the

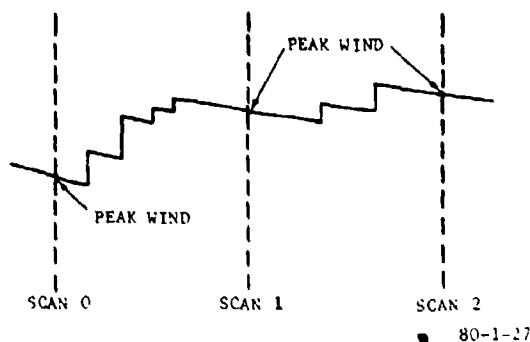


FIGURE 27. HYPOTHETICAL PEAK WIND ANALOG SIGNAL WITH EXAGGERATED BLEED-OFF BETWEEN PEAKS

largest value in the last 15 scans (at the nominal 7.2-second scan rate, 15 scans is just under 2 minutes). If the value of peak wind selected from the registers exceeds the 15-scan running mean by 9 knots, the indicator will display this value of the peak wind; otherwise, zeros.

An illustrative example is shown in table 3. The data were taken from the National Aviation Facilities Experimental Center (NAFEC) test facility on December 17, 1978, when extremely strong winds occurred following a cold front. Only centerfield wind direction, speed, and gust are shown in the table. In scan 1, gusts are displayed as "00" indicating the peak wind in the past 15 scans was less than or equal to the centerfield speed plus 9 knots (centerfield anemometer speed = 31 knots plus 9 knots = 40). The largest value in the registers at the time is not known, but indications are that it was 40 knots because at scan 2 time the centerfield mean speed drops to 30 knots and gusts of 40 knots are displayed. At scan 3 time, gusts increase to 43 knots, obviously due to the newest value in the registers. At scan 4, the wind gusts increase to 52 knots, but this value is not exceeded for the next 14 scans. The mean speed increases slowly to 35 knots at scan 16. (If the software program used here was of the type used at Denver, when the centerfield mean speed reached 35 knots all remote winds would automatically be displayed continuously until the mean speed fell below 25 knots.) After scan 19, both the mean speed and the gusts begin to decrease. The 52-knot gust was the highest ever recorded at NAFEC.

It is interesting at this juncture to compare LLWSAS performance with that of the NWS anemometry, specifically the dial readout in the tower cab. On the date of the case cited above, Kennedy airport also had strong winds. The NWS maximum wind from the model F-420 was 40 knots compared with 52 knots

TABLE 3. CENTERFIELD WIND READOUT FOR NAFEC LLWSAS, DECEMBER 17, 1978

<u>Scan No.</u>	<u>Direction (°)</u>	<u>Speed (kn)</u>	<u>Gusts (kn)</u>
1	300	31	00
2	310	30	40
3	310	32	43
4	310	32	52
5	310	32	52
6	310	33	52
7	310	33	52
8	310	33	52
9	310	33	52
10	310	33	52
11	310	33	52
12	310	33	52
13	310	33	52
14	310	34	52
15	310	34	52
16	310	35	52
17	310	34	52
18	310	34	52
19	300	32	48
20	300	32	46
21	300	32	46

Time approximately 1430 local standard time.  
 Direction rounded to nearest 10°.  
 Speed and gusts in knots.  
 Scan rate 7.2 seconds.

from the LLWSAS Vectorvane. This shows clearly that even considering known overshooting problems of cup-type anemometers such as the model F-420, the NWS sensor has far more severe damping characteristics than the LLWSAS Vectorvane. Apparent increased sensitivity is also produced by the differences in signal conditioning of the LLWSAS speed data compared with the NWS data. This has been shown consistently at other airports also. For example, on January 20, 1979, the Tampa LLWSAS had a peak wind of 37 knots compared with 26 knots from the NWS dials. Apparently, the NWS signal fluctuations as read from the ca' dials are strongly damped, attenuating large amplitude and short period oscillations.

In conclusion, gust factor techniques in the present version of LLWSAS are designed to adhere to the following operational criteria:

1. Gusts are displayed in the right two digital elements on the top line of the cab display when any peak wind from the centerfield station during the last 15 scans of the controller exceeds the centerfield mean wind by 9 knots. Otherwise, "00" is displayed in the appropriate blocks.
2. The peak wind will be continuously displayed for 15 scans, unless:
  - a. on a new scan, the old value is exceeded—in that case, the newest value replaces the old value;
  - b. the centerfield mean speed rises during the 15-scan interval to a value that is within 9 knots of the gust value—in this case, the gust factor changes to "00."
3. The gust factor is also displayed for a maximum of 15 scans:
  - a. to allow for controller recognition of the digital information;
  - b. because there is evidence that a discrete gust maintains its integrity as it moves with the mean wind; and if so, a gust observed at the centerfield station at time zero will be approximately 0.5 mile downwind within 2 minutes, assuming a 25-knot mean wind. This will place the gust closer to the touch-down point of an approaching aircraft at the end of 15 scans.
4. A 9-knot gust threshold (over mean wind speed) is used.
5. The increased sensitivity of Belfort Vectorvane compared with the NWS model F-420 and differences in signal conditioning between the two systems will consistently lead to LLWSAS gusts 10 to 20 percent higher than the NWS sensor dial readout.
6. The LLWSAS digital readout saves controller time in studying the NWS dials to determine gusts. Time spent studying the dials also diverts the attention of controllers (namely, the local controllers) whose undivided attention to aircraft movements is essential.

7. The combined functions of the peak wind detector and averager on one electronics card allows for standardization at all six LLWSAS sites. The centerfield peak wind/averager card is interchangeable with those at remote sites with only a slight modification.

8. Gusts are measured at only one LLWSAS site (centerfield).

TRACON Displays. A second byproduct of LLWSAS has been the development of centerfield wind displays for the TRACON room. At the present time, only the Boston TRACON is equipped with this display. The TRACON one-line indicator has similarities to the cab indicator. It employs the same incandescent filaments and logic. Controller cards are interchangeable.

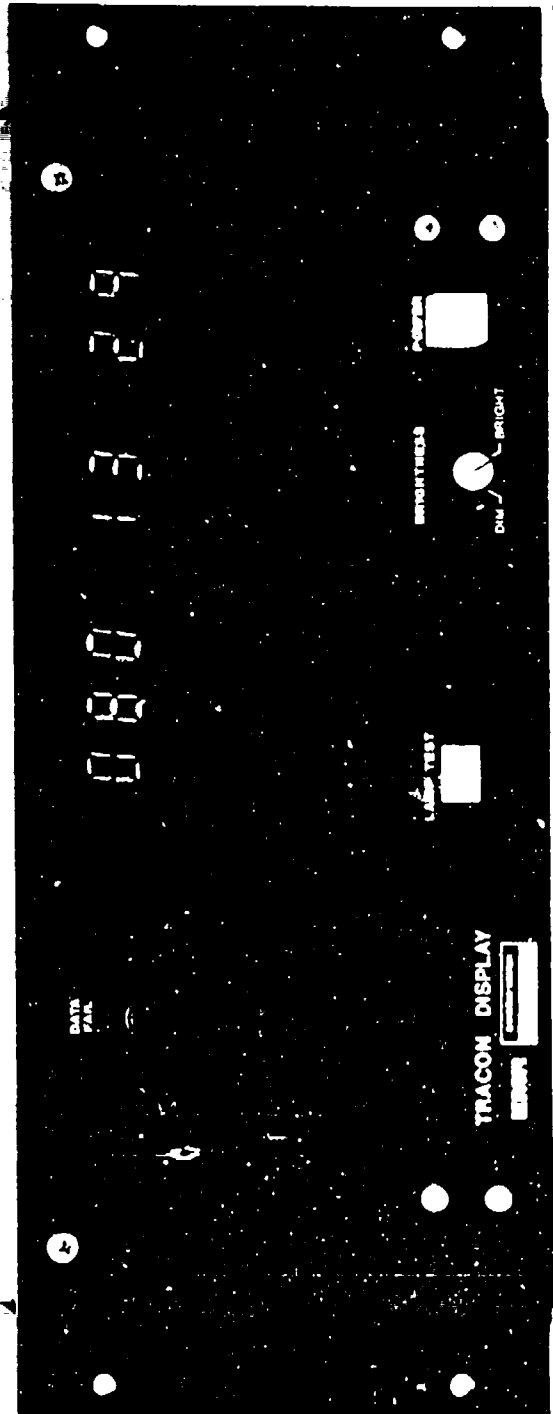
Development of this display was necessary to achieve compatibility between centerfield wind readouts in the tower and TRACON. LLWSAS measures the centerfield wind speed, direction, and gusts using a different sensor than the one used by the NWS. The NWS sensor output is fed to the speed and direction dials in the tower cab and TRACON room. The two sensors differ in dynamic characteristics and may not be collocated. The signal conditioning of the two sensors' outputs differ significantly, resulting in slight, but noticeable, differences in the output speeds, directions, and gusts at any given instant.

The TRACON indicator input signal is received from the CPU via a 20-mA current loop; a loop separate from the wind shear indicator loop. The centerfield wind is continuously displayed and updated every interrogation cycle (7-second nominal rate). The display employs all the external controls of the cab indicator (brightness control, push-to-test, on/off switch, and data fail), except there is no audible alarm function. The display power supply is contained in the same frame resulting in a fairly large box. Figure 28 illustrates the external appearance of the display.

TRACON displays will be installed at the original LLWSAS airports in 1980, except at Oklahoma City which currently has no TRACON room. (Approach control functions are handled at the Tinker Air Force Base Radar Approach Control (RAPCON). The RAPCON obtains a Will Rogers Airport (Oklahoma City) centerfield wind via the NWS "A" teletype. These are hourly observations.)

#### LLWSAS SOFTWARE.

LLWSAS is a real-time, computer-controlled system utilizing a Large-Scale Integration (LSI) microcomputer with 16,000 words, 16-bit semiconductor read/write memory, and an extended arithmetic chip. Interfaced to the microcomputer are two serial line interfaces (for the diagnostic and tower cab displays), a parallel line interface linking the central station controller, and a paper tape reader interface for program loading. In this system, there are eight bits per byte and a word consists of two bytes. The main program, including subroutines, requires 11,968 bytes of memory. The program is written in DEC (Digital Equipment Corporation) PDP11/03 MARCO II assembly language. Data processing routines were originally written in FORTRAN IV before compiling. The FORTRAN program is called BLFRTD.



80-1-28

FIGURE 28. TRACON DISPLAY

The central station controller polls each of the anemometer sites in sequence. A code is assigned to each interrogation transmission, and only the anemometer site with the appropriate code responds to the interrogation message. In one interrogation cycle, 13 discrete data words are returned to the computer. The sequence of these data words is shown in table 4. The data consist of u- and v-wind components from each station plus peak wind (gust) information from the centerfield station (channel 3).

TABLE 4. PARAMETER POLLING SEQUENCE

<u>Polling Order (Channel)</u>	<u>Parameter</u>	<u>Description</u>
1	u <sub>c</sub>	u-component centerfield wind (station 1)
2	v <sub>c</sub>	v-component centerfield wind (station 1)
3	g	peak wind (gusts) centerfield site
4	u <sub>2</sub>	u-component, station 2
5	v <sub>2</sub>	v-component, station 2
6	u <sub>3</sub>	u-component, station 3
7	v <sub>3</sub>	v-component, station 3
8	u <sub>4</sub>	u-component, station 4
9	v <sub>4</sub>	v-component, station 4
10	u <sub>5</sub>	u-component, station 5
11	v <sub>5</sub>	v-component, station 5
12	u <sub>6</sub>	u-component, station 6
13	v <sub>6</sub>	v-component, station 6

Data are tagged and stored in memory registers for later processing.

The time required for the master station controller to complete one interrogation processing cycle is dependent upon:

1. The transmission time required to interrogate 13 data points (approximately 0.54 second each times 13 = 7.0 seconds).

2. The time necessary to reinterrogate specific sites in cases where an invalid transmission occurs on the initial interrogation. Up to three retries are allowed by the controller/computer. If the fourth attempt to obtain a valid transmission fails, the data points in question are tagged as invalid (999/99 is displayed) and the controller proceeds to interrogate the next site in sequence.

3. The time necessary to complete data processing (about 0.2 second).

Under normal conditions (no interrogation retries), an interrogation cycle takes 7.2 seconds.

Received by the computer after each returned data message is a 33-bit formatted stream. The message consists of:

- |   |   |  |
|---|---|--|
| 1. Start bit.   | } | Frame 1<br>Incoming and Outgoing           |
| 2. Seven-bit station address.                                       |   |  |
| 3. Check bit (always 0).  |   |  |
| 4. Parity bit.  |   |  |
| 5. Stop bit.  |   |  |
| 6. Start Bit  | } | Frame 2<br>Incoming and Outgoing           |
| 7. Four-bit data point address.<br>Check bits on outgoing messages. |   |  |
| 8. Four bits of wind data.  |   |  |
| 9. Parity bit.  |   |  |
| 10. Stop bit.   | } | Frame 3<br>11-bit Incoming<br>Message Only |
| 11. Start bit.  |   |  |
| 12. Eight bits of wind data.  |   |  |
| 13. Parity bit.   |   |  |
| 14. Stop bit.   |   |  |

Two sets of parity, start, and stop bits are generated within the UART responding to the initial message received from the CPU upon site interrogation (22-bit outgoing message), and another set is added by the UART after data is received from the anemometer site (33-bit incoming message). For the purposes of this section, only the 12-bit data word in frames 2 and 3 will be discussed.

The data input to the BLFRTD FORTRAN subroutine is the 12-bit digital word received by the CPU from the UART. Each word represents either the u-component wind, v-component wind, or peak wind from the centerfield station. Data words for the wind components are in the form of numerical counts ranging from 0 to 4,095, corresponding to the dynamic range of the sine/cosine potentiometer of the sensor:  $\pm 5.93$  volts d.c. (or  $\pm 86.6$  knots in meteorological units) is scaled to  $\pm 5$  volts. Minus 5 volts d.c. equals 0 counts and +5 volts d.c. equals 4,095 counts. The peak wind signal varies from 0 to 11.86 volts and is scaled to  $\pm 5$  volts. This corresponds to a 2,048 to 4,095 range in counts. Counts are converted to engineering units (volts, knots, and degrees) by the BLFRTD subroutine.

Program version 5A is presently used at Tampa, Houston, New York's Kennedy, and Oklahoma City. Version 5B is used at Denver only. Program 5B contains a slight modification to 5A to operate in the high-wind conditions frequently observed in the lee of the Rocky Mountains. Program version 6A is in operation at Atlanta. It contains a modified algorithm to reduce false alarms generated when remote winds are affected by local obstructions. Programs 5B and 6A will be described at the end of this section. Program 7A is in use at Boston. It is identical to 5A, except it contains specialized software to drive updated versions of diagnostic, cab, and TRACON room displays. (It is the intention of LLWSAS project engineers to combine the functions in programs 5A, 5B, and 6A into one software program for a retrofit to the six-airport LLWSAS. Later equipment modifications at these airports are to be followed by development and retrofit of program 7A (table 5) which will complete standardization at all airports). Programs 5A and 7A are summarized in flow chart form in figures 29 through 33.

Currently operating, proposed, and obsolete program versions are briefly described in table 5. Because of subtle differences in the way data are processed for the cab and diagnostic displays, discussion of each will be separate. Data for cab displays will be discussed first. In all operating program versions, data from the anemometer sites are converted from counts to engineering units in the CPU. Data are initially in the form of u- and v-horizontal wind components (figure 34) and are converted to speed and direction using

$$S_i = K \sqrt{u_i^2 + v_i^2} \quad i = 2, 3, \dots, 6 \quad (1)$$

and

$$D_i = \tan^{-1} \left( \frac{v_i}{u_i} \right) \quad i = 2, 3, \dots, 6 \quad (2)$$

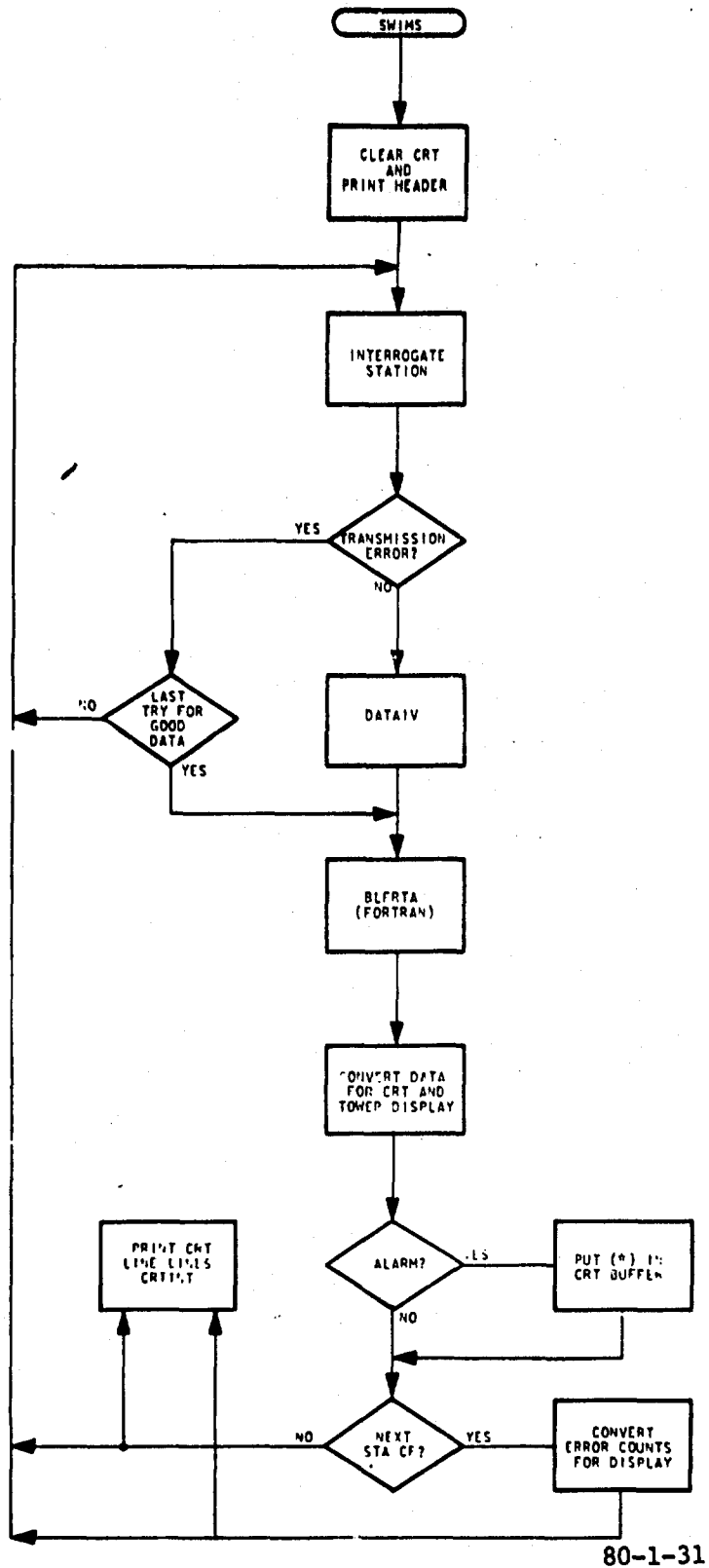
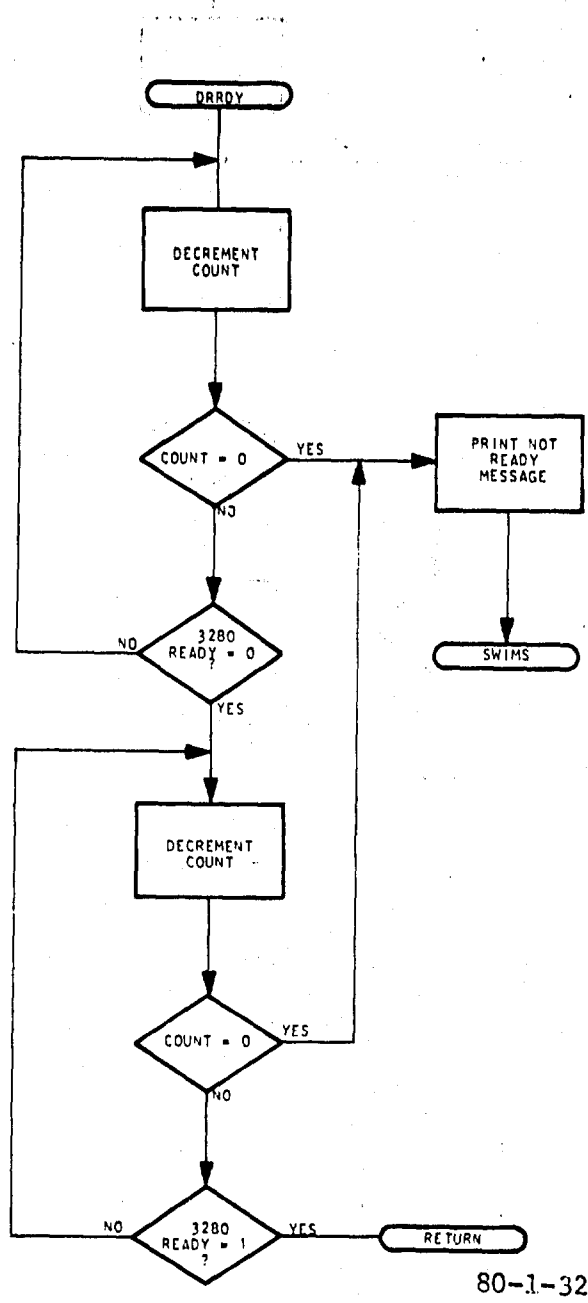
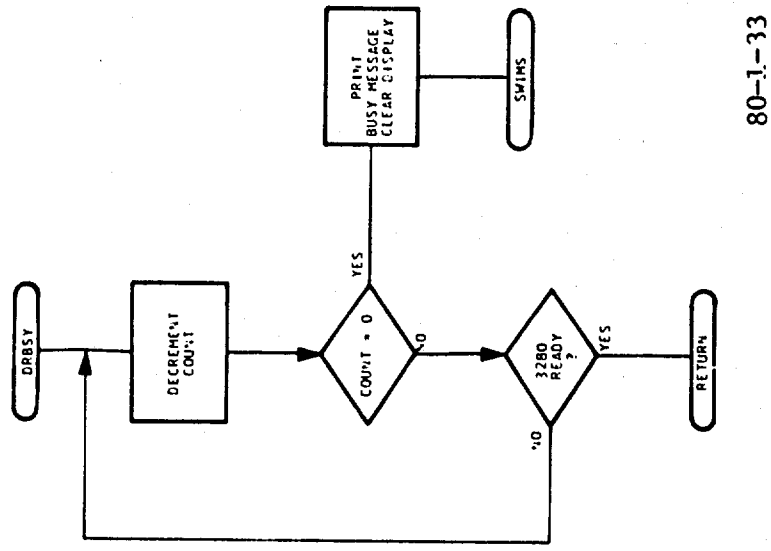


FIGURE 29. LLWSAS PROGRAM FLOW DIAGRAM



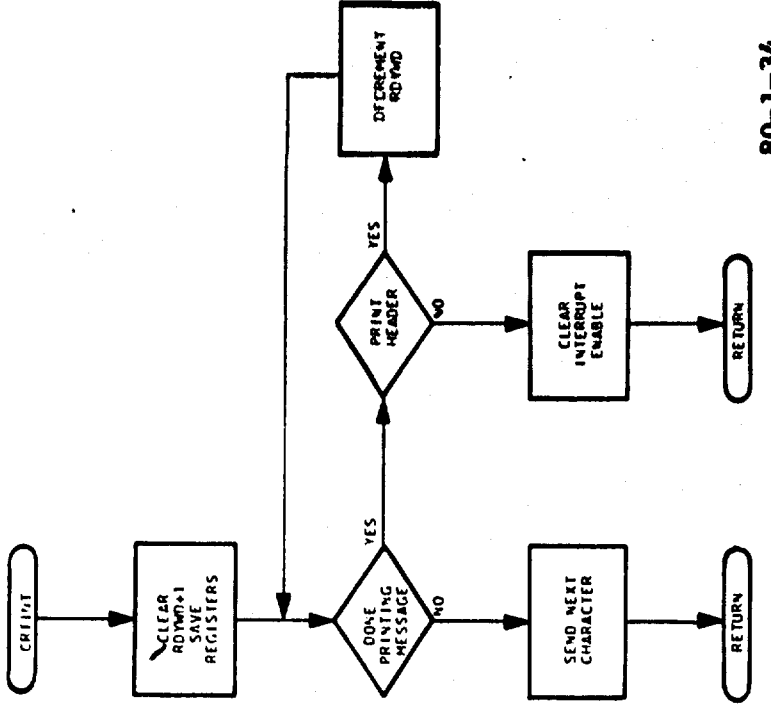
80-1-32

FIGURE 30. MASTER-CONTROLLER-READY SUBROUTINE FLOW DIAGRAM



80-1-33

FIGURE 31. MASTER-CONTROLLER-BUSY SUB-ROUTINE FLOW DIAGRAM



80-1-34

FIGURE 32. INITIATE-CRT-DATA-TERMINAL SUBROUTINE FLOW DIAGRAM

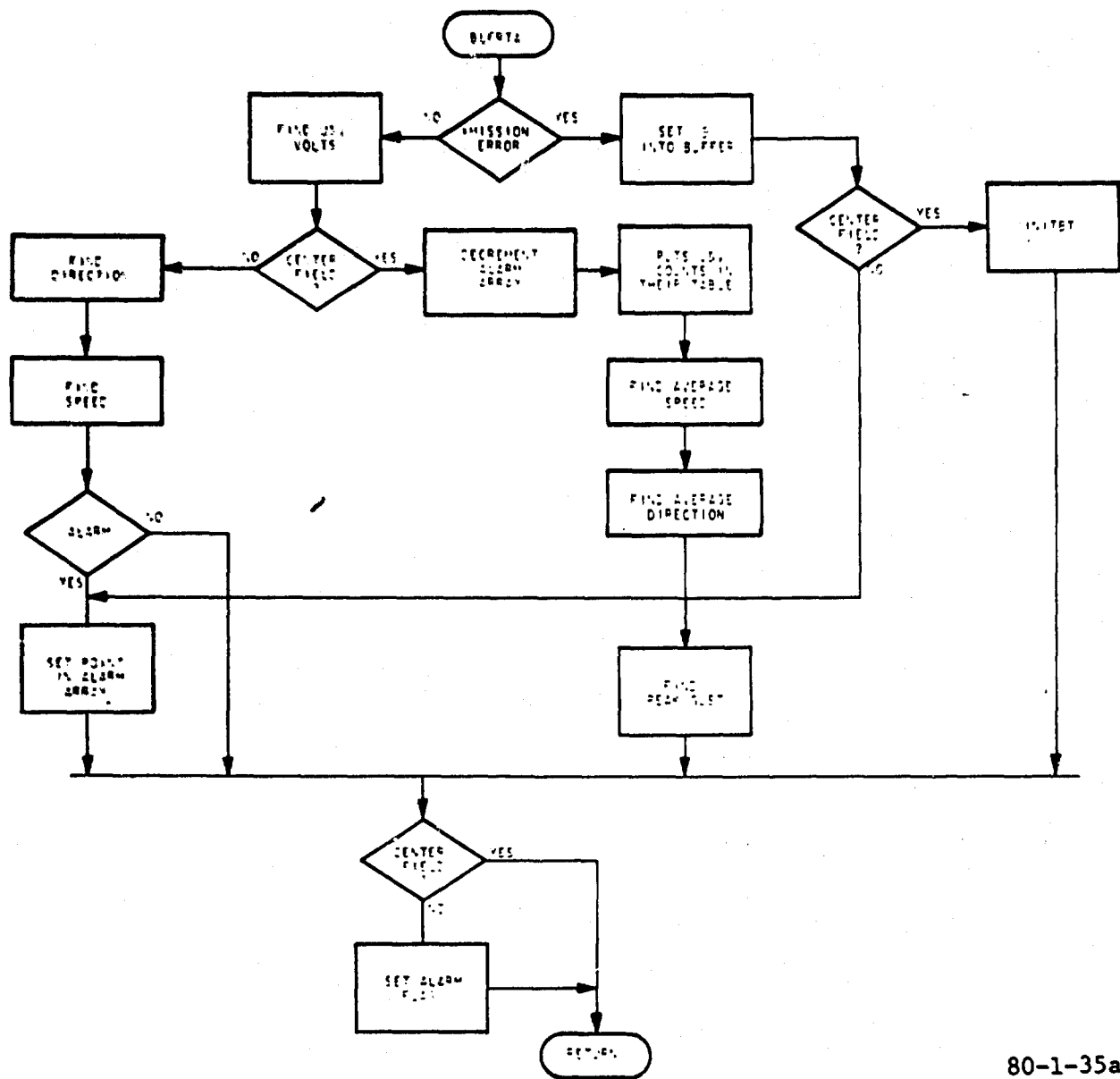
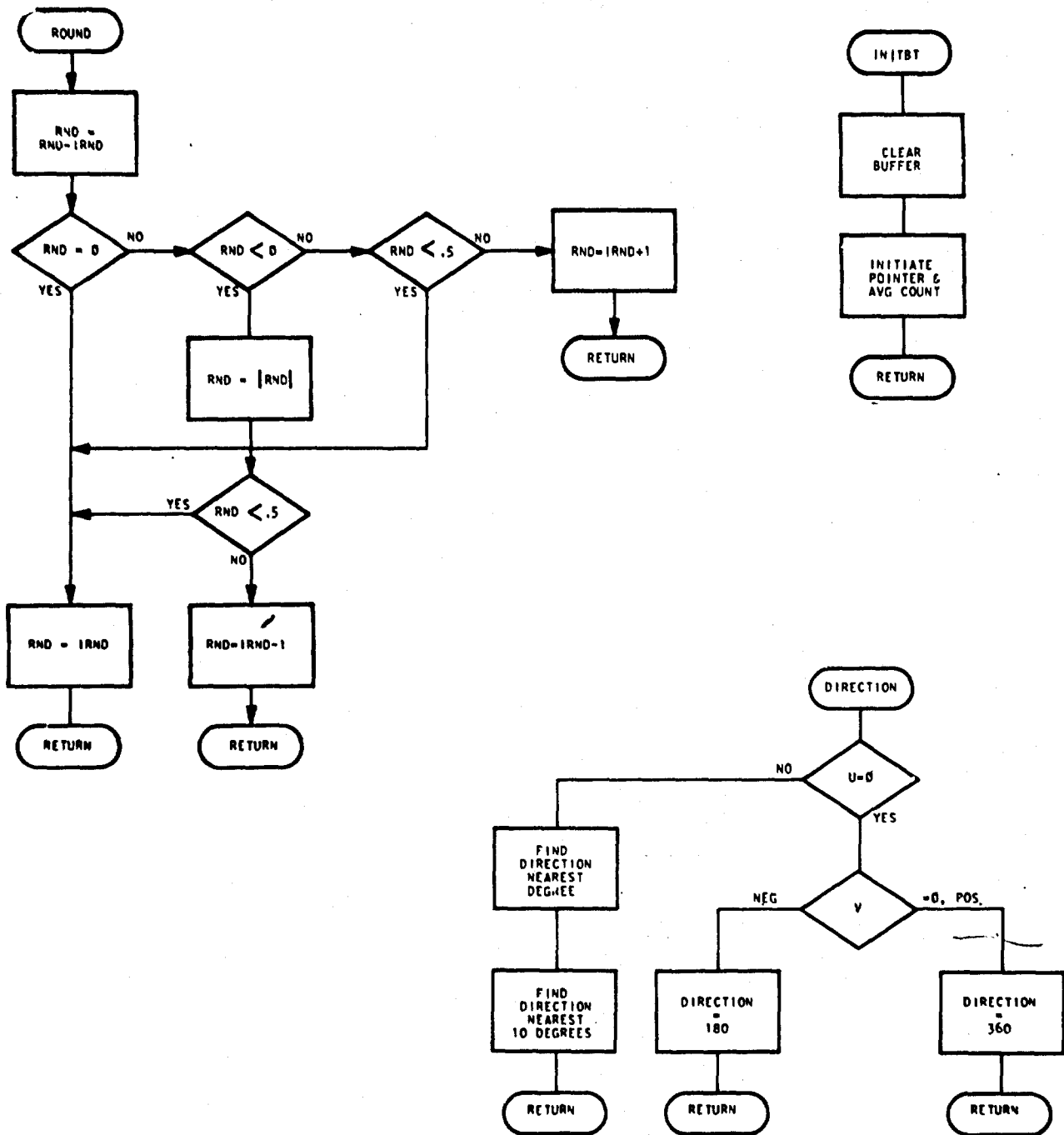


FIGURE 33. BLFRTD FORTRAN DATA PROCESSING FLOW DIAGRAM (SHEET 1 OF 2)



80-1-35b

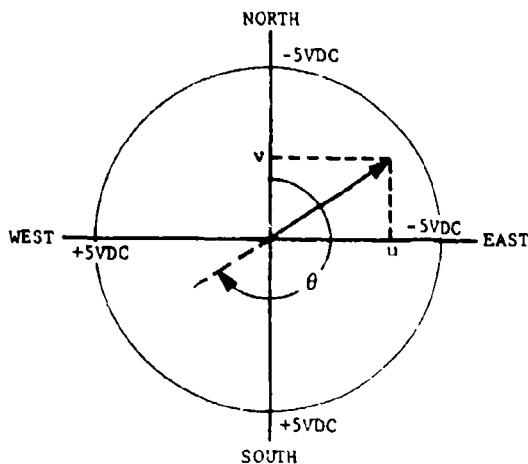
FIGURE 33. BLFRTD FORTRAN DATA PROCESSING FLOW DIAGRAM (SHEET 2 OF 2)

TABLE 5. LLWSAS SOFTWARE PROGRAM VERSIONS

Program No.	Description	NAFEC	TPA	ATL	OKC	IAH	JFK	DEN	BOS	Remarks
1	Early test program.									Obsolete
2	Early test program.									Obsolete
3	Early test program.									Obsolete
4	Test program used in data collection mode.	T								Operationally obsolete; functional at NAFEC with hardware modifications.
5	Drives IKE displays, no recording or communication link, no expander box, 30-second alarm hold, remote display on CFA failure, reformatted CRT.									Obsolete
5A	Same as 5 except with peak wind (gust) channel.	0	0		0	0	0			
5B	Same as 5A except continuous remote display if $\bar{S}_c \geq 35$ knots.	T						0		
5C	Same as 5A except allows data collection on floppy disk.	P,T								In development stage.
6	Same as 5 except has turbulence alarm exclusion routine.	T								Operationally obsolete; can be used if peak wind channel is shorted.
6A	Same as 5A except has turbulence alarm exclusion routine.	0		0						
6B	Combines features of 5A, 5B, and 6A.		P	P	P	P	P	P		In development stage.
7A	Same as 5A except drives EMR displays.								0	
7B	Same as 6B except drives EMR displays.		P*	P*	P*	P*	P*	P*	P	In development stage.

\* - Will replace 6B at these airports when necessary hardware modifications are made.  
 0 - Currently operational.  
 P - Proposed as operational.  
 T - Test

respectively, where  $K = 14.64$ . Symbol explanations are given in table 6. The resulting wind speeds and directions are stored in memory.



$$\text{SPEED} = \sqrt{u^2 + v^2}$$

$$\text{DIRECTION} = \text{TAN}^{-1} \left( \frac{v}{u} \right) = \theta$$

80-1-29

FIGURE 34. VECTOR COMPONENT PAIR ( $u$ ,  $v$ ) AND CORRESPONDING SCALED PEAK VOLTAGES ON EACH LEG

The data from the centerfield station are manipulated slightly differently. Before computing speed and direction, a 15-scan running mean ( $\bar{u}_c$ ,  $\bar{v}_c$ ) is determined. Overbars indicate mean values. Fifteen scans represents about 2 minutes under normal conditions. (The scan or polling time is increased if a station failure occurs.) Components from periphery stations have been conditioned by an averager or low-pass filter described previously under Remote Stations. This is used to filter out small-scale fluctuations while retaining mesoscale fluctuations associated with wind shifts and keeping filter lag at a minimum. At the reference or centerfield station, the objective is not only to smooth out small-scale wind fluctuations but also to duplicate objectively the NWS technique of tracking a visual 2-minute mean wind determination from a strip chart. This is the technique used to obtain wind speeds for hourly and special observations ultimately reaching users via teletype outputs. The fabrication of a low-pass filter for the centerfield outputs with a 0.01 hertz (Hz) cutoff frequency would have resulted in a large, costly device with unstable outputs. It was, therefore, decided to adopt the mathematical rather than electronic approach. The 2-minute average adheres to recommended International Civil Aviation Organization (ICAO) standards (reference 14).

TABLE 6. LIST OF PARAMETERS

$u_i$	$i = 2, 3, \dots, 6$ u-component wind (remote site)
$v_i$	$i = 2, 3, \dots, 6$ v-component wind (remote site)
$u_c$	u-component wind (centerfield site); overbar indicates 15-scan mean
$v_c$	v-component wind (centerfield site); overbar indicates 15-scan mean
$\Delta u_i$	$= (\bar{u}_c - u_i)$ $i = 2, 3, \dots, 6$ u-component difference
$\Delta v_i$	$= (\bar{v}_c - v_i)$ $i = 2, 3, \dots, 6$ v-component difference
$V_i$	$= K(\sqrt{\Delta u_i^2 + \Delta v_i^2})$ $i = 2, 3, \dots, 6$ vector difference
$S_i$	$i = 2, 3, \dots, 6$ remote wind speed
$D_i$	$i = 2, 3, \dots, 6$ remote wind direction
$g$	peak wind (gust)
$\bar{S}_c$	mean (15 scan) centerfield wind speed
$\bar{D}_c$	mean (15 scan) centerfield wind direction
$g_{max}$	maximum $g$
$G$	gust factor $= g_{max} - \bar{S}_c$
$N$	sample size counter
$u_i, v_i$	$i = 2, 3, \dots, 6$ and $\bar{u}_c, \bar{v}_c$ ; u, v scaled voltages
$i$	(subscript) remote station identifier: 2, 3, ..., 6
$c$	(subscript) centerfield station identifier
$D_i$	$= (\bar{D}_c - D_i)$ $i = 2, 3, \dots, 6$ direction differences (used in program 6A only)
$K$	$= 14.64$ (a scaling constant)

The 15-scan averaged centerfield wind components are used to determine speed and direction according to

$$\bar{S}_c = K\sqrt{\bar{u}_c^2 + \bar{v}_c^2} \quad (3)$$

and

$$\bar{D}_c = \tan^{-1} \left( \frac{\bar{v}_c}{\bar{u}_c} \right) \quad (4)$$

$\bar{S}_c$  is rounded to the nearest 1 knot and  $\bar{D}_c$  rounded to the nearest 10 degrees. At the end of the data processing for a polling cycle, the rounded values of  $\bar{S}_c$  and  $\bar{D}_c$  are transmitted to the tower cab indicator and displayed on the top line. This output is ultimately intended to replace that of analog dials as presently used. Determination of gusts will be discussed later.

The most significant function of the data processing is the comparison of remote site winds with the centerfield winds or the computation of the vector differences from the five output pairs. For this function, the remote station  $u_i$  and  $v_i$  values and the reference station  $\bar{u}_c$  and  $\bar{v}_c$  values are retrieved from storage. The vector difference for each remote-centerfield pair is computed using

$$V_i = K\sqrt{\Delta u_i^2 + \Delta v_i^2} \quad i = 2, 3, \dots, 6 \quad (5)$$

where  $V_i$  has the units of knots and  $\Delta u_i$  and  $\Delta v_i$  are defined as in table 6. Graphically,  $V_i$  is the magnitude of the resultant vector after the subtraction of the remote site wind vector from the centerfield wind vector. Notice that the direction of the resultant vector  $V_i$  is not important in LLWSAS, only the scalar magnitude. There has been confusion on the part of some users that  $V_i$  having units of knots implies LLWSAS computes only the "speed shear." This is not the case since (5) indicates that  $V_i$  is a function of both  $u$  and  $v$  which in turn are both functions of the station speed and direction.

It is also important to note that  $V_i$  is not a measure of wind shear. Wind shear is  $V_i$  per unit distance between the station pair assuming a linear change. Since LLWSAS does not take into account the distance between remote and centerfield stations, wind shear is not computed. However, at airports where there is symmetry between remote and reference stations, an "airport wind shear" is implied. At airports where there is a lack of symmetry, an "airport wind shear" factor is not directly inferred. However, there is no serious problem with an unsymmetrical network as long as all remote stations meet the minimum station spacing requirements as specified in the section on Anemometer Siting Criteria.

After  $V_i$  is computed, a determination is made as to whether its value exceeds a preset threshold of 15 knots. If the value of  $V_i$  exceeds 15 knots, an alarm condition is registered for the remote station whose data has been used in the  $V_i$  computation. When an alarm condition is issued, the speed and direction data for the appropriate remote station are displayed on the appropriate line of the cab indicator, hitherto blank. Simultaneous with the initial remote station data stream, two audible beeps will be sounded in the cab indicator. Once the initial stream of data has been displayed, it will continue to be displayed for six additional scans whether or not  $V_i$  exceeds 15 knots on the second through seventh scan. This is to allow controller recognition of the alarm condition. The implicit assumption is made that once an alarm is registered it will persist at that station, unless it is caused by random turbulence in high-wind conditions or the wind shear event is marginally hazardous (just barely exceeds the 15-knot threshold). The alarm condition for a given remote will hold with routine updates at least six scans beyond the last time  $V_i > 15$  knots. If any additional stations go to alarm status, the same chain of events will be followed; i.e., initial remote data stream, audible alarm, and at least six additional scan displays and update sequences. More than one remote station may be in alarm status at any given time.

The special electronics circuitry handling the peak wind signal has been described under LLWSAS Hardware. The peak wind between scans is transmitted to the master station on channel 3. The peak wind or gust is given the symbol "g." The value of g will be stored in memory for up to 15 scans. If during the course of the 15-scan period the old value of g is exceeded by a fresh value, the new value replaces the old and is subsequently stored for 15 more scans. This, then, is  $g_{max}$ . If after 15 scans,  $g_{max}$  is not increased,  $g_{max}$  is assigned the next lowest value of g in memory, and this new value of  $g_{max}$  is retained until it is 15 scans old.

A gust factor is computed every scan by subtracting  $\bar{S}_c$  determined in (3) from  $g_{max}$ .

$$G = g_{max} - \bar{S}_c \quad (6)$$

If G is greater than 9 knots, then  $g_{max}$  is displayed in data block 3 of the cab indicator's top line. Otherwise, "00" is displayed.

This completes the discussion of data processing for the cab indicators. Variations in data processing for the diagnostic display will now be discussed. All data that appear on the tower cab displays are also output to the diagnostic display (figure 35). The screen reports the wind direction and speed information for each anemometer on a separate line. The top line reports the centerfield anemometer information and is identified as CFA. The boundary anemometers are on subsequent lines and are identified by number only. However, in order to adequately detect and troubleshoot system problems, much more information is also output to the maintenance scope. All station wind directions (rounded to the nearest degree) and speeds are displayed regardless of the value of  $V_i$ . Gusts are displayed only if the gust factor (G) exceeds 9 knots. Alarm status is indicated by an asterisk (\*) on the appropriate line

in cases of vector difference alarms. The six-scan alarm hold condition does not apply to the diagnostic scope, and there is no audible alarm.

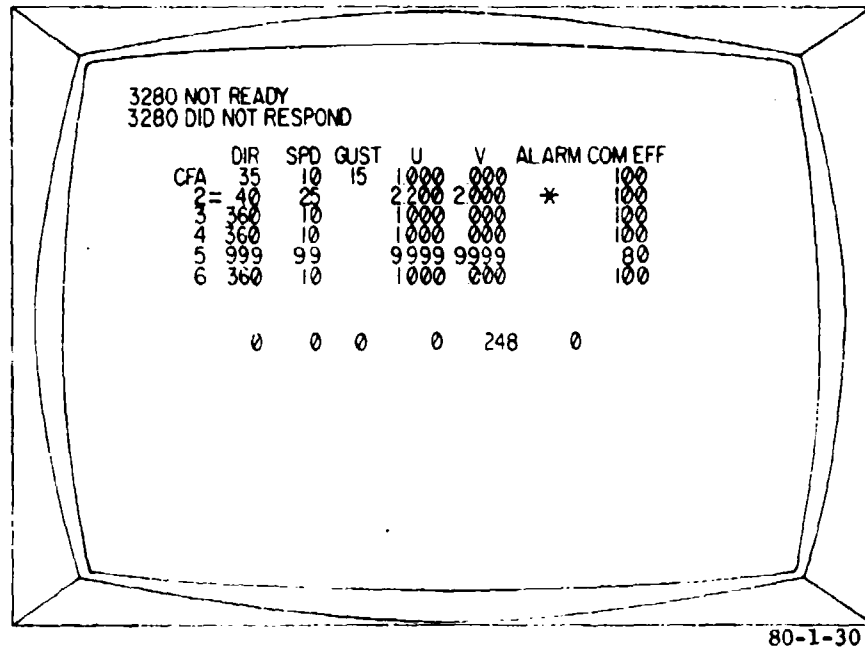


FIGURE 35. DIAGNOSTIC CRT DISPLAY FORMAT

In addition to the display of direction and speed from all sites, the scaled u- and v-component voltages are also displayed. Resolution is to the nearest millivolt. For the centerfield readouts, instantaneous u and v voltages are displayed, whereas the displayed direction and speed are 15-scan means. Thus,  $D_C$  and  $S_C$  values are not to be directly computed from the displayed u and v values as may be done with remote site values.

Two types of transmission error counts, short term and long term, are derived and output on the diagnostic display.

Short term is a count of the number of successful polls on the first try in the last 100 scans (in percent). This is the short-term nonaccumulative error count of communication efficiency (COM EFF). This information is output to the far right column on the diagnostic scope. Both "hard and soft" transmission problems are accounted for in this count. The count is updated every 100 scans.

Long term is a count of the number of unsuccessful tries to obtain u- and v-component signals from a given remote station (up to a maximum of 8 counts per scan, 12 for centerfield, if there is a complete failure to retrieve data from a station (hard failure)). This is the long-term accumulative count. These errors are accumulated up to 9,999 on the bottom line of the diagnostic scope. After 9,999 errors or after a program reload, the count recycles to 0. If a hard failure occurs, 9's will appear in appropriate direction and speed blocks on the maintenance and tower displays and scaled voltage blocks on the maintenance display only. If the transmission failure is soft (i.e., good data is retrieved on the second or third try), the error count will be incremented, but no 9's will appear in the data blocks on either display.

As mentioned earlier, there are two special versions of the LLWSAS program 5A which are modifications for operational use at airports with peculiar terrain or meteorological factors. The first of these is program 6A or the so-called turbulence alarm exclusion program designed to reduce false alarms caused by spurious wind fluctuations. These fluctuations may be induced by rugged terrain or tall obstacles in the vicinity of the anemometer site. Terrain irregularities and obstructions are common at Atlanta where the program is now in use. Such roughness causes wind deflections and ultimate short-lived alarms if standard program 5A is used. The "false" shear alarms are local and not in the category of aircraft hazards. Nevertheless, they are annoying to controllers. The turbulence alarm exclusion program modifies the basic vector difference algorithm in program 5A by adding wind direction difference calculation ( $\Delta D_i$ ), where

$$\Delta D_i = \bar{D}_c - D_i \qquad i = 2, 3, \dots, 6 \qquad (7)$$

The wind hazard alarms will be issued only if one of the following criteria are satisfied:

1. When  $\Delta D_i < 30^\circ$  it is necessary that  $V_i > 25$  knots,
2. When  $30^\circ \leq \Delta D_i \leq 60^\circ$  it is necessary that  $V_i > 20$  knots, or
3. When  $\Delta D_i > 60^\circ$  it is necessary that  $V_i > 15$  knots.

Operation of this program has had a substantial effect of reducing terrain-induced wind alarms at Atlanta, while preserving real wind hazard alarms caused by sustained wind shifts.

The second special version of program 5A is the one in use at Denver. This program version is called program 5B. Denver is in the lee of the Rocky Mountains and is frequently subjected to extremely strong winds associated with the so-called Chinook or foehn wind condition, especially during cold weather months. These strong winds have considerable imbedded turbulence which randomly trigger short-lived alarms at any remote station when program 5A is used. In light winds, program 5B is identical to 5A. In strong winds, to inhibit the frequent sounding of the audible alarms, program 5B turns on

all remote outputs for continuous display whenever the centerfield wind speed exceeds 35 knots. A shear condition is registered by flashing digits, but no audible alarm is sounded. This display mode persists until the centerfield wind speed falls below 25 knots, when program 5B again operates like 5A.

Current plans are to standardize LLWSAS software as previously summarized. In addition to the thrust of this standardization effort, the following modifications will be made to the software:

1. Add a counter to the program to count the number of hard failures (the number of occurrences when 999/99 is displayed or the number of occurrences when a transmission failure is registered after three reinterrogations of a remote site).
2. Display the running or moving percentage of communication efficiency in the last 100 scans rather than in 100 scan blocks.
3. Add a seventh remote station output on the diagnostic display so that the spare remote box can be used as a simulation site for test purposes.
4. Change program 6A algorithm to a linear relationship between direction difference and vector difference rather than the step function relationship now used. This implies that when  $\Delta D_i$  is between  $0^\circ$  and  $60^\circ$  the program will trigger an alarm only if  $V_i > (150 - \Delta D_i)/6$ . Otherwise,  $V_i$  must be  $>15$  knots. This is shown graphically in figure 36.

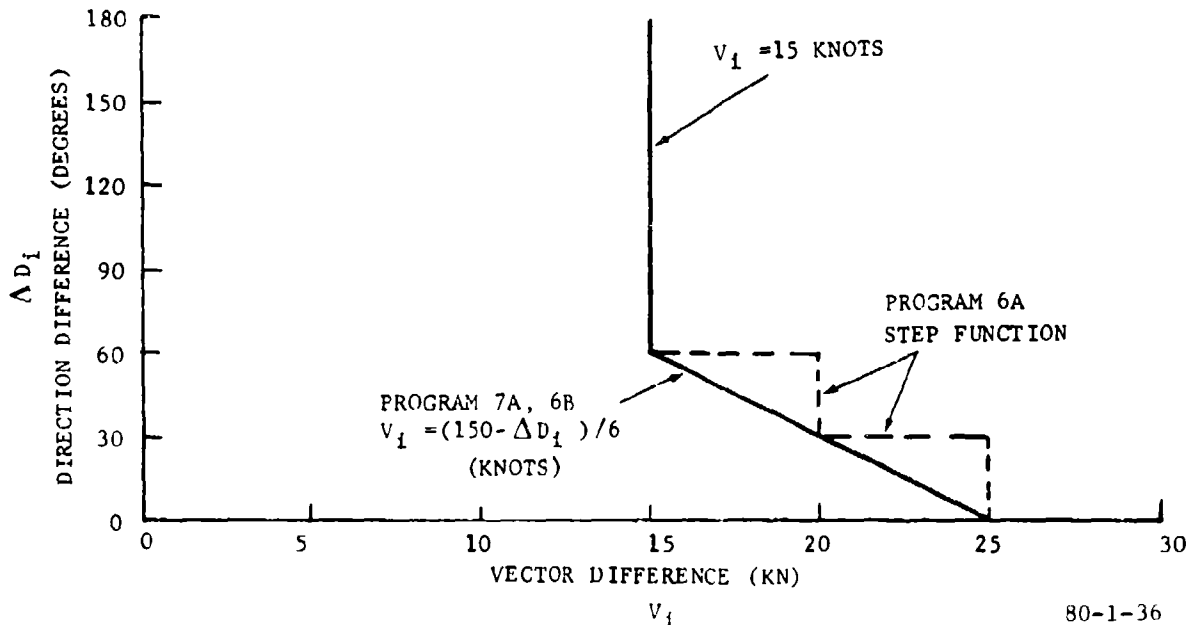


FIGURE 36. RELATIONSHIP BETWEEN DIRECTION DIFFERENCE AND VECTOR DIFFERENCE IN PROPOSED ALGORITHM CHANGE FOR PROGRAMS 6B AND 7B

## ANEMOMETER SITING CRITERIA.

INTRODUCTION. The effectiveness of the LLWSAS is dependent not only on the reliability of the electronic equipment but also upon the location of the sensor and its electronics package. The sensor must be positioned to measure representative winds, detect sustained wind shifts, give timely warnings of potentially hazardous wind shear, facilitate data communication, and be easily maintained.

In selecting LLWSAS anemometer sites, principally airport periphery sites, several factors were found important. A set of guidelines of a meteorological nature used to maximize system performance was weighted against a set of siting constraints of a logistical nature.

### System Performance.

1. Minimizing the influence of terrain and obstructions to facilitate measurement of representative winds.
2. Locating sensors far enough from runway thresholds to assure timely warnings.
3. Maintaining recommended spacing between remote and centerfield sensors to detect wind shifts.
4. Avoiding areas of jet wash and wing tip vortex (wake turbulence) impingement to avoid spurious data spikes.
5. Maintaining network symmetry to normalize wind vector difference calculations.

### Logistical Constraints.

1. Obstruction clearance.
2. Line of sight between remote and master station antennae.
3. Property ownership of proposed site.
4. Proximity of a.c. power.
5. Access by maintenance personnel.

During site surveys at the seven LLWSAS airports, logistical factors took precedence over system performance factors which were essentially unknown at the time. The resulting reduction in system performance ultimately required repositioning many sensors. Repositioning consisted of raising the sensor, relocating the sensor, or both. Table 7 shows the breakdown by airport.

TABLE 7. SENSORS REPOSITIONED DURING THE COURSE OF THE LLWSAS TEST

<u>Airport</u>	<u>Raised</u>	<u>Relocated</u>	<u>Raised &amp; Relocated</u>
TPA	1	0	1 (1)
ATL	2	3	0
IAH	4	0	2
OKC	0	0	0
DEN	2	3	0
JFK	0	1 (1)	1
BOS	0	0	0

Values in parentheses indicate sensors repositioned for reasons other than meteorological. One site at Tampa was moved because of runway construction, and another site at Kennedy was moved because the pier end upon which the sensor was originally located was damaged. There remained 16 occasions when sensors required repositioning to satisfy performance criteria. This involved 13 (about 36 percent) of the LLWSAS sites.

EFFECTS OF TERRAIN AND OBSTRUCTIONS ON SYSTEM PERFORMANCE. When the near-surface wind is sensed over flat terrain devoid of natural and/or manmade obstructions, such as trees, hills, valleys, or buildings, the lack of relief and obstructions facilitates the measurement of representative winds. However, except for the Midwestern United States, few airport locations are characterized by such smoothness, especially around the airport periphery.

Most often, one can expect the following conditions near airport boundaries where remote sensor facilities are located:

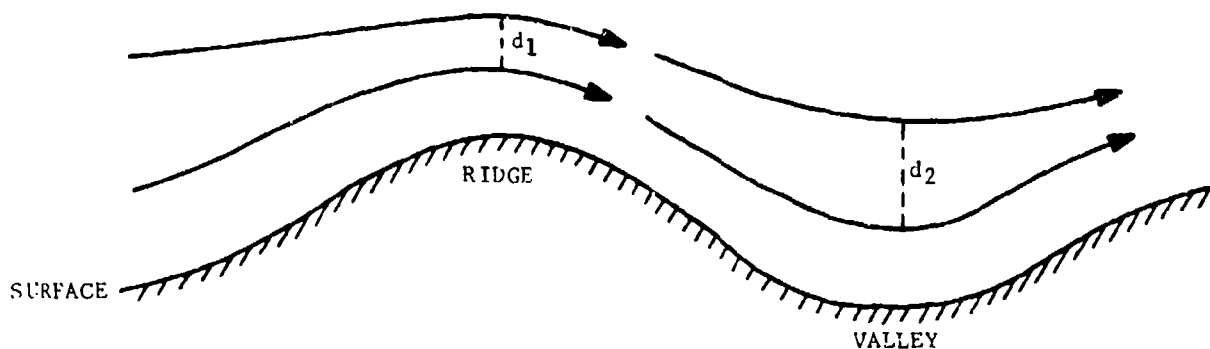
1. Rough ground surface caused by hills, depressions, or escarpments.
2. Tall trees; sometimes in patches, sometimes in a dense forest.
3. Buildings tall enough to influence the local wind.
4. Highway and/or railroad overpasses and associated irregularities.
5. Water bodies and the influence of the land-water interface.

All of the aforementioned factors make proper anemometer siting difficult as most introduce wind irregularities. False vector difference alarms can occur when output from a poorly placed remote wind sensor is compared with the unobstructed wind flow at centerfield.

It is interesting to note that some of these wind irregularities may cause real problems for pilots, especially on landing approach. Nevertheless, for the purposes of LLWSAS, sites with irregularities should be avoided whenever possible.

Unfortunately, it is not possible to make a general recommendation if high relief effects are encountered. There is inadequate documentation as to the exact nature of the wind flow in highly irregular terrain, except to say that the wind should also be expected to be highly irregular. For a start, some generally known wind behavior will be reviewed.

Case 1--Hills, Depressions, and Escarpments (Ground Undulations). In figure 37, the spacing between streamlines ( $d_1$  and  $d_2$ ) is proportional to the speed of the wind which is blowing perpendicular to a ridge and trough line. A jet (unrepresentatively high wind) would be found above the ridge (confluence zone). Conversely, a wind shelter (unrepresentatively low wind) would be observed in the valley. Accordingly,  $d_1 < d_2$ . Considering the unavoidable possibility of this type of terrain at an airport, it would be preferable to locate a sensor on the ridge; avoiding the trough or ravine at all costs. If the depression is broad, such as the case at Atlanta's southwest site, a location in the depression is permissible if the sensor is raised to or slightly above the level of the neighboring higher terrain.



80-1-37

FIGURE 37. AIRFLOW IN A RIDGE AND VALLEY TERRAIN CONFIGURATION

Airflow over an escarpment or cliff situation is a variation of Case 1 (figure 38). If the airflow is down the escarpment, a sensor located at the high point but near the escarpment edge would experience only minimal upstream diffidence effects (deceleration of the wind).

More serious is the local jet produced when air flows up the ridge (figure 39). It is important to locate the sensor as far back from the cliff edge as possible, but positioning the sensor at the top of the cliff is preferable to locating it at the ridge base. This is shown in figure 40 (a-d) which is based on laboratory experiments conducted by Bowen and Lindley in 1977 (reference 15). Atlanta's northwest site has similar relief and has a sensor at the high point. Although a 50-foot embankment edge is 100 feet east of the sensor, it is the only possible site in this corner of the airport.

The wind direction is also affected by ridges, troughs, and embankments. This effect is most pronounced if the wind is blowing at an angle to the axis of the ridge, trough, or escarpment. The wind is forced to blow along the axis but very likely corrects to equilibrium a short distance downstream from the terrain irregularity.

Case 2--Tall Trees. Most airports are cleared of tall vegetative obstructions near active runways and taxiways; however, the area at or near the airport boundary is often not clear. It is very possible to encounter tall trees either singly, in clumps, or in a solid forest near the airport boundary. These trees may be the evergreen type (providing a solid obstruction year round) or the deciduous type (providing a solid boundary in the warm months and a semisolid to solid boundary in the cold months).

For sensor locations in an area that is heavily forested with trees of fairly uniform height, the anemometer should be 20 feet higher than the tallest trees and the sensor position should not be closer than 500 feet from the forest edge. Figure 41 can be used as a guide. Such "in forest" locations will require the clearing of a small tree patch for an access road and mast location. Note that a very tall mast may be required.

It is important to achieve data compatibility from site to site at a given airport. For example, if the centerfield anemometer is located 20 feet above ground level, as is usually the case, and the data from this sensor are compared with data from a remote sensor located at 50 feet above ground level but in open terrain, there may be an incompatibility since the wind generally increases with height and this natural vertical shear is most pronounced near the ground. Vertical shears of 2 knots per 30 feet, lasting several hours are not uncommon anywhere, and shears two to four times this value are possible for periods up to several minutes. This means, in the extreme case, that if remote and reference sensors are separated 30 feet in the vertical, an 8-knot vector difference due to vertical speed shear will be induced into the LLWSAS, implying that the 15-knot vector difference threshold will be reduced to 7 knots. Frequent false alarms could result.

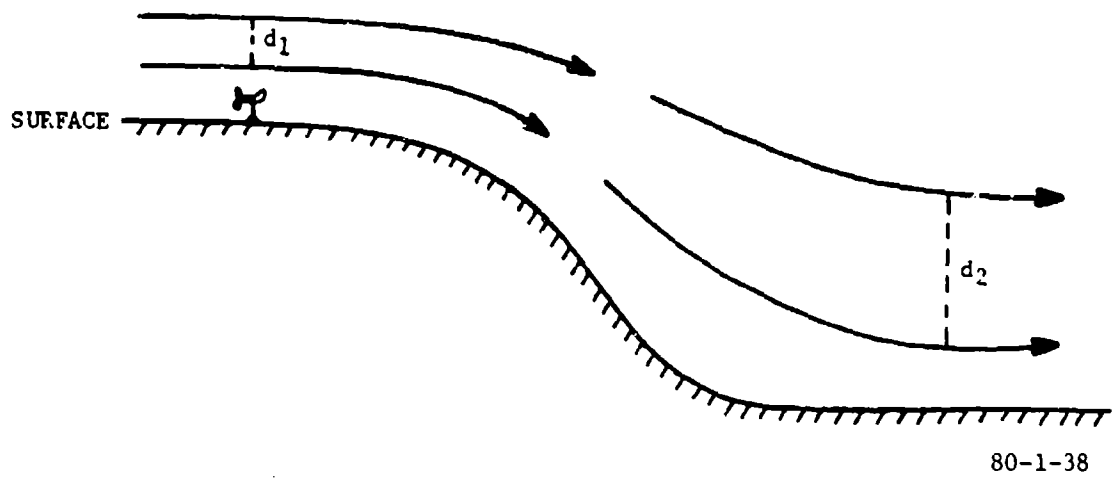


FIGURE 38. STREAMLINE PATTERN WHEN AIR FLOWS DOWN AN INCLINE

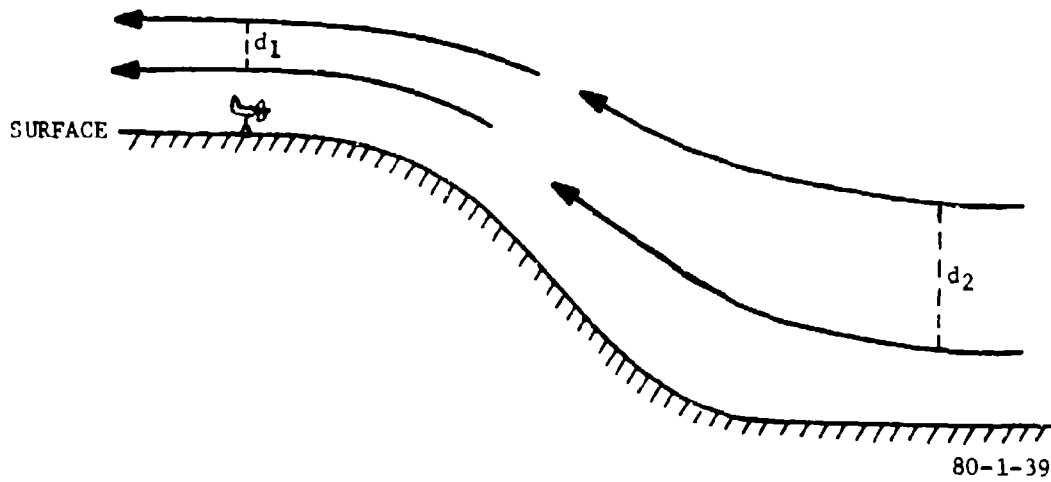
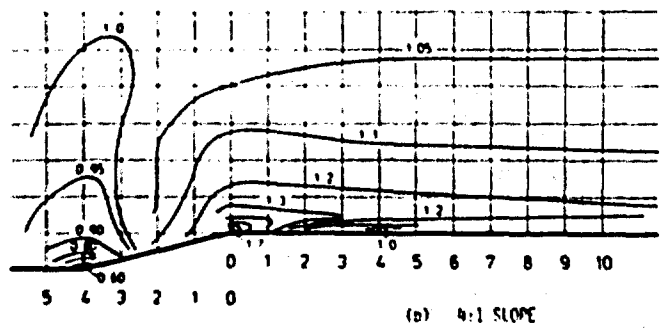
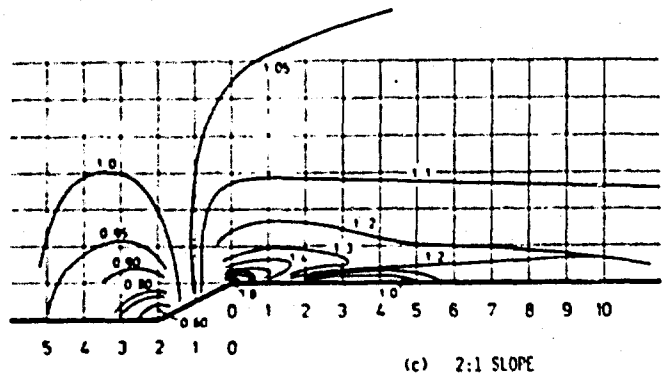
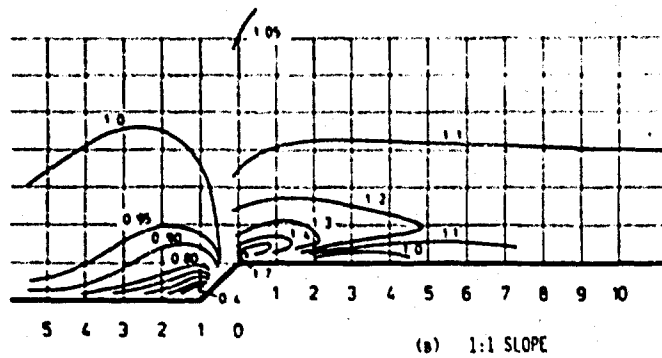
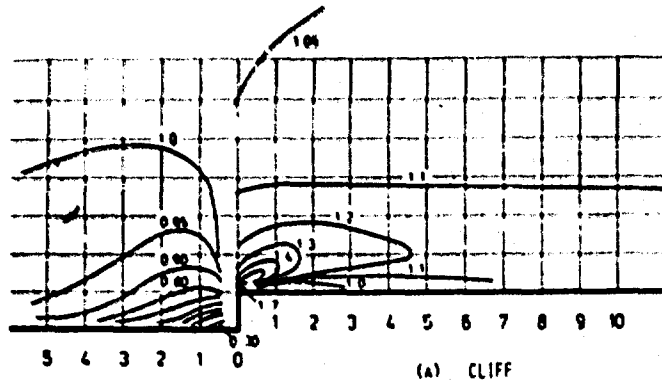


FIGURE 39. STREAMLINE PATTERN WHEN AIR FLOWS UP AN INCLINE

WIND SPEED AND TURBULENCE CHARACTERISTICS



80-1-40

FIGURE 40. CONTOURS OF EQUAL AMPLIFICATION FACTOR OVER VARIOUS ESCARPMENT SLOPES

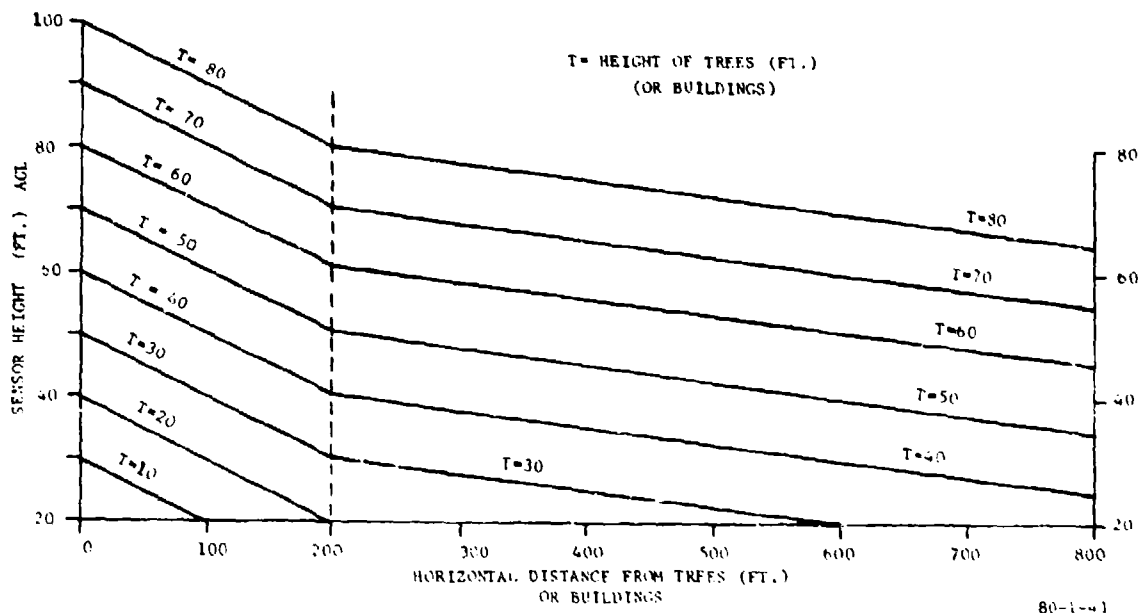


FIGURE 41. SENSOR LOCATIONS AND HEIGHTS RELATIVE TO TREE LINES AND BUILDINGS

This rationale also applies to an anemometer location which has an isolated obstruction (tree clumps or buildings) in one direction and open terrain in the other direction. When the wind blows in the direction opposite to that shown in figure 42, vertical speed shear will induce a lower vector difference threshold (assuming the centerfield sensor is 20 feet above ground level). Sensor height compatibility requirements are satisfied; however, when an anemometer is located in an area with obstructions in all directions or above a solid forest because the ground level has, in effect, been displaced upward to the top of the trees where heights are considered uniform. With irregular tree tops, the sensor should be 30 feet or more above the tops instead of 20 feet, but it is difficult to objectively assess irregularity to determine the sensor height above the tops. Large clearings in a dense forest should be avoided for sensor locations, since these will produce extremely irregular (turbulent) and virtually undefinable wind conditions.

Airports surrounded by tall forests with an existing LLWSAS network are Houston International Airport and NAFEC Airport. Tests at NAFEC have shown that anemometers located above the mean height of nearby trees, but in a cleared zone near the trees, frequently sense low winds when the ambient wind flows over the trees before impinging upon the sensor. This is caused by forest-produced diffluvence (shown in figure 43 by diverging streamlines). Even if the criteria in figure 41 are used to determine the sensor height, there will be some influence on the wind by the upstream obstruction. This is also the case for easterly flow at Houston's west site.

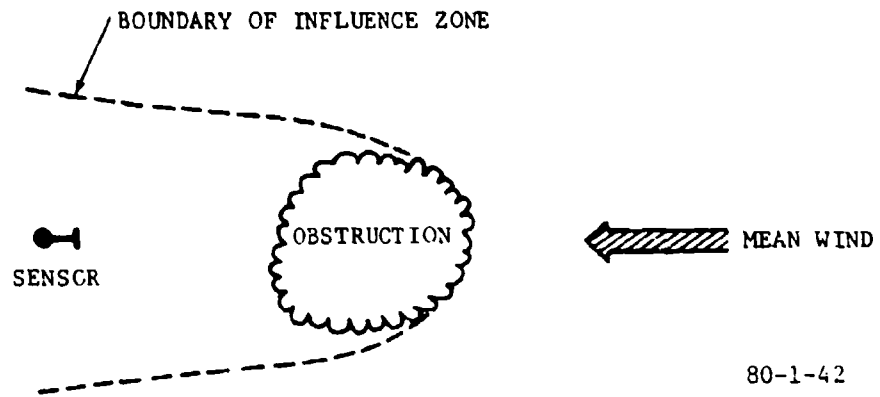


FIGURE 42. AREA OF INFLUENCE CREATED BY OBSTRUCTIONS UPWIND FROM A SENSOR

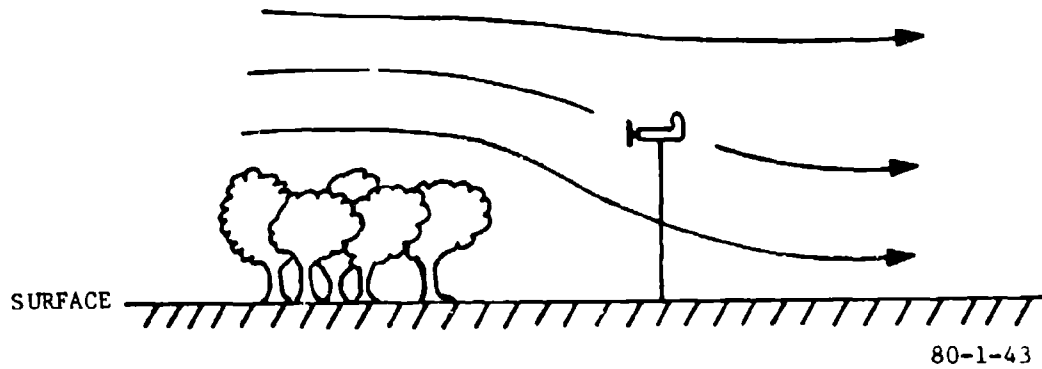


FIGURE 43. STREAMLINES IN AN AIRFLOW TRANSITION FROM FOREST TO OPEN TERRAIN

If an obstruction to the wind exists at a preferred sensor location and there is a choice between alternate sites, it is preferable to locate the sensor further away from the runway threshold along the centerline axis rather than closer. This should be done to increase rather than decrease the warning capability of LLWSAS. The closer a critical anemometer is to a runway threshold, the less time there is available for shear detection and distribution of data to pilots.

Case 3—Buildings. Buildings present similar airflow problems as trees, except buildings disturb the local flow more because they have sharper edges. They too are randomly located, have various sizes and shapes, yet are generally less frequently encountered when choosing a prospective anemometer site. They should rarely present any problem for the centerfield anemometer location because buildings are infrequently located at this part of the airfield. However, if a single, small building is encountered at any proposed site, the same general rules apply to choosing an alternate site, as in the case of small tree patches. Use of figure 41 will suffice in many cases.

At the airport boundary, buildings are sometimes more numerous. In an environment where buildings are closely spaced and vary in height and a sensor facility is located among the buildings, it will be very difficult to obtain representative data. Such near-building sites are to be avoided and an alternate site chosen. For example, in the LLWSAS field test at Atlanta, it was impossible to find an adequate site on the north side of the airport because of high-density residential and commercial buildings of widely differing heights. It is not a viable alternative, with the present LLWSAS software, to locate an anemometer on a tall building in this situation because this anemometer is to be compared with a lower centerfield reference sensor implying induced vertical shear bias due to the different heights of the sensors. In addition, building-top sites are in a wind jet regime induced by airflow over the obstruction. Building-top sites are not recommended. At Atlanta, the north side of the airport is not covered by the LLWSAS network, but sites exist at the northeast and northwest corners of the airport which cover this quadrant.

Anemometer sites near residential areas also present the hazard of vandalism. Two anemometer sites at LLWSAS airports were targets for repeated vandalism during the LLWSAS test (two acts of vandalism at Tampa; six at Kennedy). Public access to remote sites should be discouraged.

Case 4—Highway Interchanges, Railroad Overpasses, and Other Irregularities. Most airports are ringed with transportation networks and have complex interchanges where a prospective anemometer site is desired. Considering the infinite terrain configurations possible for such networks, it suffices to say that if they present high relief or significant obstructions to the wind, they should be avoided. However, if the transportation network has low relief and is clear of obstructions, sensor location should be chosen at least 100 feet from road traffic or 300 feet from rail traffic.

Case 5—Water Bodies. The LLWSAS test project has involved work with sensor locations near large water bodies; e.g., New York's Kennedy Airport and Boston's Logan Airport. In some cases, the runway threshold is very close to the water's edge and a desired anemometer site is over water. The problem has been solved at New York and Boston by locating the anemometer on an approach light pier over the water. The sensors are located 20 feet above the water (not 20 feet above the pier). Similar sites are suggested for proposed LLWSAS facilities at Washington's National Airport and New York's LaGuardia Airport.

At Boston, the airport is protected from high water (water surrounds the airport on two sides) by a 20-foot seawall. A ground-based sensor location at Boston is positioned several hundred feet from the seawall to minimize the effect of airflow disturbed by the seawall impinging on the anemometer. A 20-foot anemometer is adequate since the site is otherwise clear and flat.

Anemometer sites on buoys are not recommended.

#### SENSOR LOCATION IN RELATION TO RUNWAY THRESHOLDS TO ASSURE TIMELY WARNINGS.

LLWSAS detects horizontal wind shears associated with all meteorological phenomena. However, because of the preset 15-knot vector difference threshold, LLWSAS test results have shown that vector difference alarms are registered primarily by four meteorological events:

1. The thunderstorm; namely, the storm's gust front
2. The cold front
3. Strong turbulence in high winds
4. The seabreeze front

The purpose of implementing the LLWSAS program was to detect the progressive (moving) wind shift zone associated with thunderstorm gust fronts and strong cold fronts. The other two weather features sometimes produce alarms, but these alert events are treated as by-products and were not intended for detection in the original system design. Test results have shown, however, that shears associated with high turbulence may be troublesome to pilots and annoying to passengers, but only rarely are they unflyable hazards (excepting the Denver Chinook wind condition). Seabreeze fronts are sustained, progressive (moving) wind-shift lines often requiring a change in runways. They are not an aircraft hazard if pilots are alerted to their existence. Vector differences in seabreeze/fronts may frequently exceed the vector difference threshold at New York's Kennedy Airport and Boston's Logan Airport in the late spring or early summer, but rarely does the vector difference exceed 20 knots. There was further discussion of these two events in the section discussing meteorological phenomena.

In order to provide adequate warning, LLWSAS remote anemometers must be located some distance from the active runway threshold so that sensors can detect the shift in wind before the pilot reaches decision height. Decision height is generally just above the middle marker site (if an ILS runway) or 2,800 to 3,000 feet from the threshold. Unfortunately, most

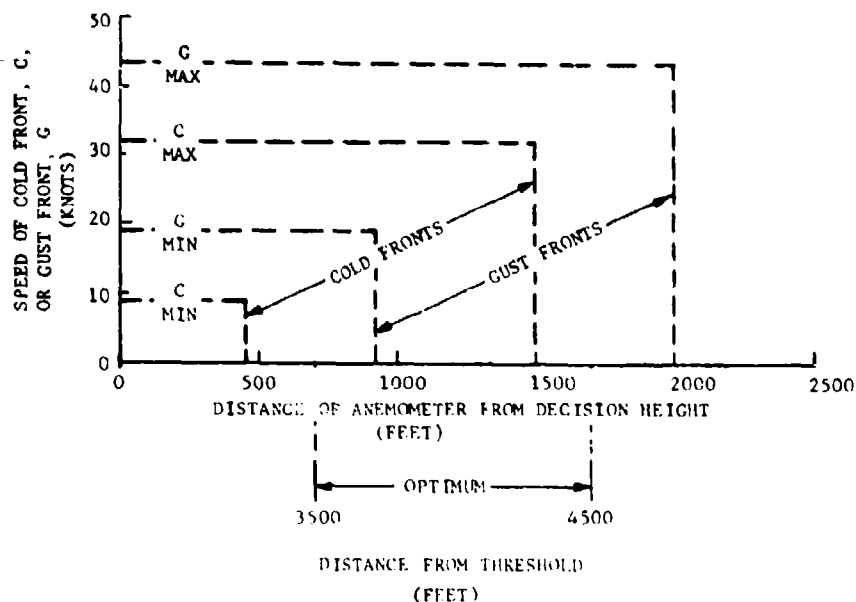
airport boundaries extend only to the middle marker site and the preferred LLWSAS remote site lies just beyond the middle marker; i.e., outside the airport boundary in many cases.

To determine the preferred zone for the anemometer position, some facts pertaining to the meteorological phenomena and the system response time are presented. Cold fronts and thunderstorm gust fronts typically approach an airport from the north through the west quadrant (except gust fronts associated with tropical thunderstorms in low latitudes). This factor determines which remote anemometers are considered "critical." Factors to be considered in determining the remote site location are the speed of the shear boundary, electronic delay in displaying information, air traffic controller (ATC) delay in distributing the information, and pilot/aircraft response to a vector difference alarm.

Table 8 shows estimated total delay time based on electronic and human responses. The product of the delay time and the propagation speed of the wind shift line determines the characteristic line in figure 44. When typical speed ranges of cold fronts and gust fronts are projected onto the ordinate from the characteristic line, the result is a range of optimum sensor locations (400 feet minimum to 2,000 feet maximum) relative to the decision height point. To narrow this zone a bit, a 1,000-foot range was arbitrarily chosen to straddle the overlapping projected speed factors of the cold front and gust front. Relative to the runway threshold, this 1,000-foot range suggests sensor placement in a 3,500- to 4,500-foot zone (solid block over the ordinate scale), or 700 to 1,700 feet from decision point. Figure 44, then, represents the distance a shear zone would move in 32 seconds. Speed ranges are typical but some out-of-range exceptions do occur. In northern latitudes and in the Great Plains, where weather systems generally move faster than in southern latitudes, sensor placement out to 1 mile from the threshold (or toward the upper portion of the range suggested) is recommended.

TABLE 8. DELAY FACTORS INHERENT IN LLWSAS

Lag induced by remote low-pass filters.	10 seconds
Polling cycle (update frequency).	7 seconds
Controller response (alarm time to acceptance by pilot)	10 seconds
Pilot/aircraft response.	5 seconds
<hr/>	
Total estimated delay time	32 seconds



80-1-44

FIGURE 44. DISTANCE OF CRITICAL ANEMOMETER FROM DECISION HEIGHT PROJECTION ON SURFACE (FEET)

Putting this principle to practice in the LLWSAS test presented a rather difficult situation in siting decisions, often requiring a compromise. It is preferable to locate the LLWSAS remote site on the airport property for easy access to a.c. voltage, for security reasons, for quick and direct access by service personnel, and because the site is often flat and clear. Since such logistical considerations were given precedence in initial siting, many remote sensors were positioned at or near the middle marker, an average of 2,800 feet from the threshold. This is 700 feet closer to the threshold than the recommended distance. At the seven field test airports, only two of the thirty-five remote anemometers were located off airport property; both at the Denver facility on the property of the Rocky Mountain Arsenal (U.S. Army). Emphasis on airport sites rather than off-airport sites avoided the problems involved in leasing or purchasing private property. Such transactions normally take considerable time, an element not available to LLWSAS planning engineers. However, an effort should be made in future systems to locate critical remote anemometers the recommended distance from runway threshold.

A viable alternative might be to utilize a pressure-jump sensor technique (Bedard, et al., 1979, reference 16) as an advance warning device. This system is not suggested as a replacement for LLWSAS because it infers the wind shear rather than the more direct method in LLWSAS. However, it could serve as a remote warning device in conjunction with LLWSAS since the pressure sensors are not site sensitive as are the anemometers. The concept of combining these different sensing techniques is currently being investigated at NAFEC.

REMOTE SENSOR LOCATIONS RELATIVE TO THE CENTERFIELD SENSOR: THE ORIGIN OF THE 15-KNOT VECTOR DIFFERENCE THRESHOLD. So far, the location of a remote sensor to LLWSAS has been discussed in terms of its relationship to local obstructions and terrain factors and its recommended distance from threshold. It is also of paramount importance in LLWSAS to maintain a certain distance between critical remote sensors and the centerfield or reference sensor. The sensor spacing is a direct result of the atmospheric wind properties which are to be sensed.

Surface wind shift lines associated with thunderstorms and cold fronts have a finite horizontal thickness. Although the thickness varies somewhat from case to case, it is evident from 7 years of data collected from the Oklahoma City instrumented tower (in part reported by Goff, 1976, and Goff, et al., 1977, references 5 and 17), that the width of most gust fronts is in the 0.4- to 2.0-nmi range (figure 45) measured near the ground. The average width is 1.1 nmi. In designing LLWSAS, however, sensor spacing was configured so as to contain the total wind shift zone between the LLWSAS sensor first detecting the wind shift and the centerfield sensor. To achieve this, an attempt was made to make the spacing between these sensors at least as great as the widest of strongly sheared fronts (those exceeding 15-knot vector difference). To use a smaller spacing is to risk the possibility of a shear alarm miss. The number of potential misses is inversely proportional to the distance between this sensor pair.

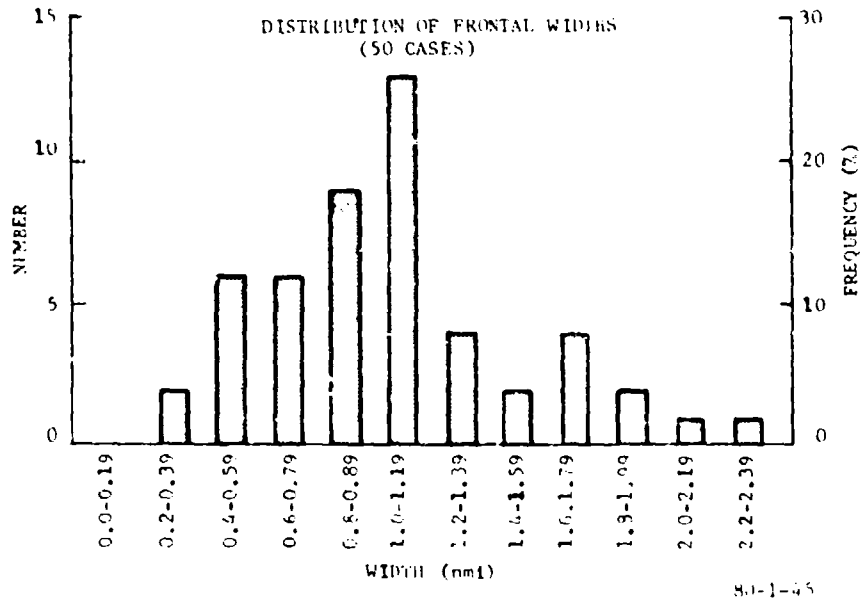


FIGURE 45. DISTRIBUTION OF FRONTAL WIDTHS (50 CASES)

In the paragraphs that follow, it will be shown how a critical width is determined and how the 15-knot vector difference threshold originated. Table 9 is a list of 23 shear cases reported by Goff (reference 5) in defining general characteristics of thunderstorm outflows. By using the objectively-analyzed time-height plots in the report's appendix, the width of the gust front and its associated vector difference and horizontal shear can be determined. Table 9 is a compilation of these statistics. Strong outflows are distinguished from weak outflows. The strength determination, while somewhat subjective, was based on the statistical properties of the outflows (prefrontal updraft magnitude, strength of the cold air outflow, temperature discontinuity, and storm strength). Notice that the vector difference of all strong outflows (column B) exceeds 15 knots, whereas only a few of the weaker outflows have vector differences more than 15 knots; none more than 20 knots. This is the origin of the 15-knot vector difference threshold; the lower limit of strong outflows based on the Oklahoma data.

Tables 10 and 11 are similar to table 9 in format but contain additional cases accumulated since the initial report. Data in table 10 (containing both strong and weak outflows) were extracted from the study by Goff, et al. (reference 17), and table 11 contains new (unpublished) data. Like table 9, tables 10 and 11 use the Oklahoma City tower as a data source. Cases in table 10 are all thunderstorm outflows (except the May 29, 1976 "heat burst"); whereas, table 11 contains data from gust fronts and several strong cold front cases. The latter are marked by a double asterisk (\*\*) on the left side. A total of 50 cases is presented. Note that the strong cold front cases have frontal characteristics similar to the thunderstorm gust front cases. Most cold fronts, however, are in the weak category and are characterized by gradual wind shifts (time domain) implying wider wind-change zones. These weak cases are not shown in the table.

Summarizing the strong wind shift cases presented in the three tables, the surface vector difference ranges from 15.5 to 37.1 knots and the width of these shear boundaries ranges from 0.35 to 2.37 nmi. It is the vector shear (column C) though that poses the hazard to aircraft; and since LLWSAS is not designed to measure vector shear directly, the design of the system must compensate for this apparent deficiency.

A maximum vector shear of  $53.8 \text{ hours}^{-1}$  has been calculated from the data (December 29, 1976, case C from table 11). This corresponds to an aircraft airspeed change of over  $2 \text{ knots/second}^{-1}$  sustained for 9 seconds, assuming an aircraft ground speed of 140 knots (typical approach speed, commercial jets) and no pilot input. There are several other cases where nearly as much airspeed change has been sustained for a much longer period. Notable is the June 6, 1975, case (table 11), where a  $1.8 \text{ knot/second}^{-1}$  change was sustained for 17 seconds. Thirteen cases (26 percent) will produce airspeed changes in excess of  $1 \text{ knot/second}^{-1}$  assuming no pilot input.

To determine LLWSAS design criterion for vector shear, the width of the shear boundary (column A) is plotted against the boundary vector shear (column C) in figure 46. The figure is a log-log plot. There is a high negative

TABLE 9. FRONTAL CHARACTERISTICS (DATA FROM GOFF, 1976)

<u>Date of Event</u>	<u>A</u> Surface Width of Shear Boundary (nmi)	<u>B</u> Surface Vector Difference (kn)	<u>C</u> Boundary Shear (hr <sup>-1</sup> )	<u>D*</u> Aircraft Transition Time (sec)
Strong Outflows				
May 14, 1974	0.99	23.5	23.7	25.5
July 2, 1972	1.02	37.1	36.4	26.3
May 6, 1972	1.44	21.0	14.9	37.1
May 27, 1972	1.13	20.8	18.4	29.1
May 31, 1971	1.75	27.2	15.5	45.2
June 17, 1972	0.98	15.5	15.8	25.3
June 7, 1971	1.75	33.2	18.9	45.2
May 23, 1974	1.26	25.4	20.2	32.5
June 16, 1973A	1.05	27.2	25.9	27.0
June 16, 1973B	0.63	27.2	43.2	16.2
June 10, 1971	0.86	21.5	25.0	22.2
June 2, 1971	1.89	19.8	10.5	48.7
June 4, 1973	0.71	31.4	44.2	18.3
Weak Outflows				
June 14, 1972	0.87	12.6	14.5	22.5
June 12, 1971	0.59	13.6	23.1	15.2
May 23, 1972	1.70	14.0	8.2	43.8
May 12, 1972	0.66	12.6	19.1	17.0
May 23, 1974A	1.19	11.6	9.7	30.6
May 23, 1974B	1.04	17.5	16.8	26.9
April 19, 1972A	0.70	11.6	16.6	18.0
April 19, 1972B	1.18	17.5	14.8	30.5
May 26, 1972	0.98	19.4	19.8	25.3
April 21, 1972	2.37	17.8	7.5	61.1

\*Assumes aircraft ground speed of 140 knots.

TABLE 10. FRONTAL CHARACTERISTICS (CASES FROM GOFF, ET AL. 1977)

<u>Date of Event</u>	<u>A</u> Surface Width of Shear Boundary (nmi)	<u>B</u> Surface Vector Difference (kn)	<u>C</u> Boundary Shear (hr <sup>-1</sup> )	<u>D*</u> Aircraft Transition Time (sec)
May 10, 1976	1.07	21.4	21.9	27.5
May 12, 1976	1.09	22.4	20.5	28.1
May 22, 1976	1.02	21.8	21.3	26.5
May 26, 1976A	2.16	23.5	10.9	55.8
May 26, 1976B	0.59	19.4	32.6	15.2
May 29, 1976A	0.37	15.7	42.5	9.6
May 29, 1976B**	1.08	8.7	8.1	28.0
May 30, 1976	0.59	16.4	27.9	15.2
June 13, 1976A**	1.40	13.8	9.8	36.2
June 13, 1976B	0.87	16.3	18.7	22.5
June 23, 1976**	1.08	11.0	10.2	27.8

\*Assumes aircraft ground speed of 140 knots.  
 \*\*Weak Fronts

TABLE 11. FPONTAL CHARACTERISTICS (UNPUBLISHED CASES)

<u>Date of Event</u>	A	B	C	D*
	<u>Surface Width of Shear Boundary (nmi)</u>	<u>Surface Vector Difference (kn)</u>	<u>Boundary Shear (hr<sup>-1</sup>)</u>	<u>Aircraft Transition Time (sec)</u>
June 6, 1975	0.66	31.0	47.0	17.0
June 2, 1977	0.67	26.0	38.8	17.3
June 28, 1977	1.08	21.3	19.8	28.0
Sept. 24, 1977**	0.91	20.8	22.8	28.5
Sept. 13, 1977A**	0.52	21.3	41.0	13.4
Sept. 13, 1977B**	0.42	19.4	46.2	10.8
August 10, 1977	1.64	20.4	12.4	42.4
May 30, 1977	1.22	22.1	18.1	31.5
May 20, 1977A	1.45	24.8	17.1	37.5
May 20, 1977B	1.95	21.9	11.2	50.2
April 20, 1977	1.33	23.5	17.6	34.4
January 28, 1977**	1.15	19.8	17.2	29.6
Dec. 30, 1976A-J**	0.81	17.5	21.6	20.9
Dec. 29, 1976A**	0.49	17.4	35.6	12.6
Dec. 29, 1976B**	0.85	18.0	21.2	22.0
Dec. 29, 1976C**	0.35	18.8	53.8	9.0

\*Assumes aircraft ground speed of 140 knots.

\*\*Cold front.

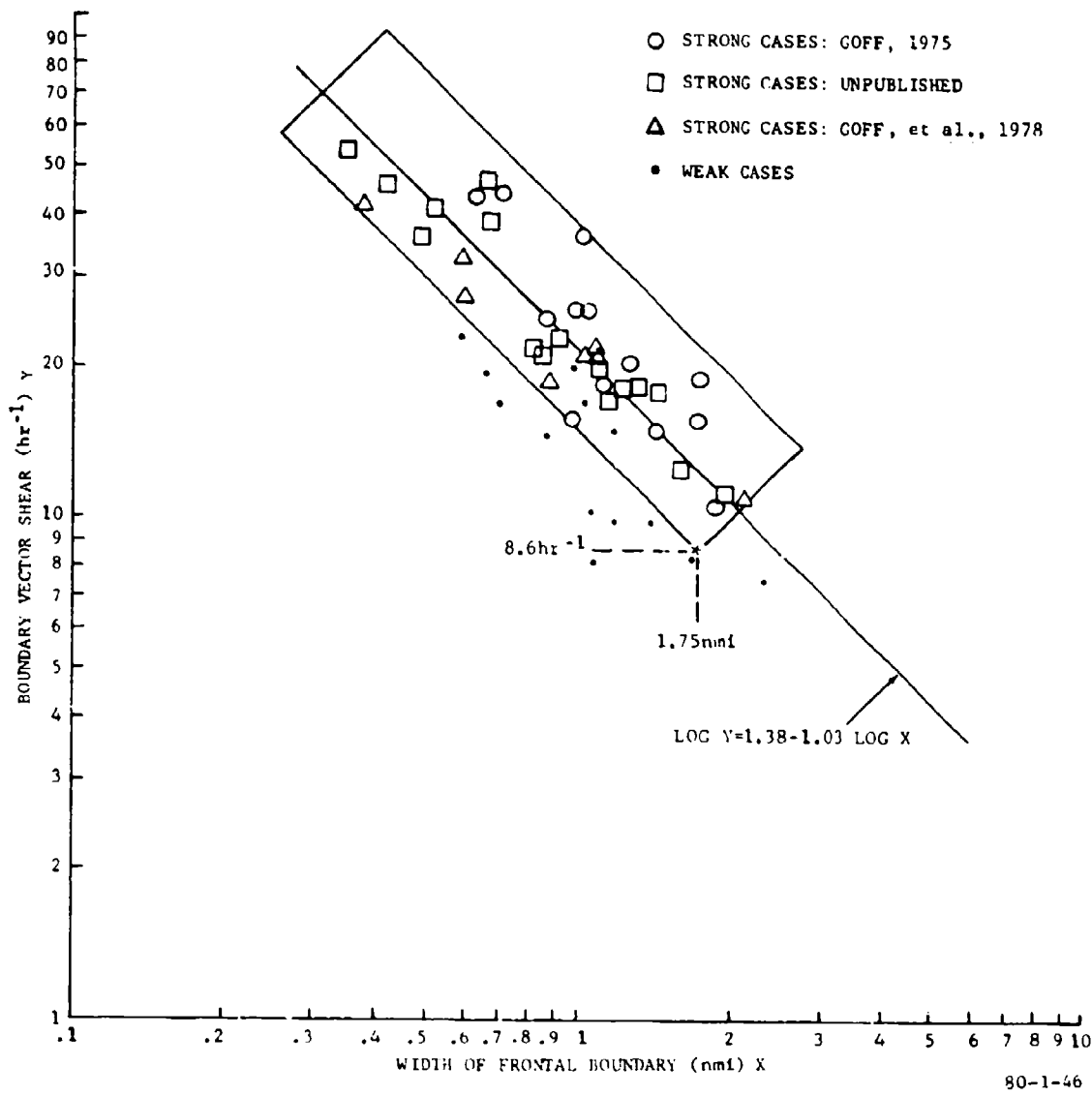


FIGURE 46. RELATIONSHIP BETWEEN FRONTAL WIDTH AND VECTOR SHEAR (50 CASES)

correlation between frontal width and associated shear. The best fit curve to the data is the middle left-to-right sloping line which has the equation

$$\log Y = 1.38 - 1.03 \log X \quad (8)$$

where X and Y are the frontal width and vector shear, respectively. Two parallel curves are also shown in figure 46. They represent an envelope about the strongest cases. The cases that fall outside the envelope are all weak outflows. In order to accommodate possible system error and slightly lower values of vector shear in a strong front, a threshold boundary vector shear of  $8.6 \text{ hours}^{-1}$  is chosen as the cutoff between strong and weak cases. This corresponds to a critical frontal width of 1.75 nmi as shown by the asterisk in the lower left corner of the envelope. These criteria then (vector difference = 15 knots, vector shear =  $8.6 \text{ hours}^{-1}$ , and frontal width = 1.75 nmi) represent the explicit and implicit LLWSAS threshold criteria. The frontal width threshold (1.75 nmi) is then the minimum critical remote-to-centerfield sensor spacing.

Three wind shear cases have frontal width larger than the optimum sensor spacing. However, the implied vector difference per unit distance is still greater than the  $8.6 \text{ hours}^{-1}$  threshold (shown by arrows extrapolating original graph positions to the  $X = 1.75$  nmi line).

It is apparent that the number of misses increases as sensor spacing decreases. If  $X = 1.50, 1.25, 1.00,$  and  $0.75$  nmi, the number of respective misses is 3 (5 percent), 5 (13 percent), 11 (27 percent), and 24 (45 percent).

Several times in preceding paragraphs, reference has been made to the so-called critical anemometer. This is the wind sensor that most frequently detects the leading edge of the wind shift. In northern latitudes this sensor is most often in the northwestern airport quadrant. At airports located near large cool water bodies, seabreeze or lakebreeze fronts may approach the aircraft from the direction of the water body, and the sensor closest to the water is also a critical sensor. In the southern latitudes the upper atmospheric flow is often from the east. It is this flow that determines the motion of thunderstorms, and for this reason, sensors on the east side of the airport are also considered "critical" and should be located so as to adhere to the criteria developed in this section. In the Midwestern and Southern United States, strong supercell thunderstorms move generally southwest to northeast. Therefore, at Oklahoma City, Atlanta, and Houston, the southwest sensor, too, is a critical sensor.

Table 12 lists the critical sensors for the seven-airport LLWSAS network. Superscripts indicate the type of wind discontinuity likely to impinge upon the critical sensor.

Table 13 shows current remote-to-centerfield spacing at the seven LLWSAS airports. A total system estimate miss rate is given. Figure 47 is a graphical representation of the miss rate to sensor-spacing relationship. The miss rate increases exponentially as the spacing decreases. Data are taken from figure 46.

TABLE 12. CRITICAL SENSORS FOR THE SEVEN-AIRPORT LLWSAS NETWORK

<u>Airport</u>	<u>Critical Sensors</u>
Atlanta	NW <sup>1/4</sup> , SW <sup>2</sup> , NE <sup>1/4</sup>
Tampa	NW <sup>1</sup> , E <sup>4</sup> , NE <sup>1/4</sup>
Oklahoma City	NW <sup>1</sup> , W <sup>1/4</sup> , SW <sup>2/4</sup>
Houston	SW <sup>2</sup> , W <sup>1</sup> , E <sup>4</sup>
Boston	NW <sup>1/4</sup> , SE <sup>3</sup> , NE <sup>1</sup>
New York City	NW <sup>1/4</sup> , W <sup>3</sup> , NE <sup>1/4</sup>
Denver	NW <sup>5</sup> , N <sup>1</sup> , E <sup>5</sup> , SW <sup>5</sup> , NE <sup>5</sup>

1. Fronts, squall lines.
2. Supercell thunderstorms.
3. Seabreeze, lake breeze fronts.
4. Tropical thunderstorms.
5. High plains thunderstorms.

TABLE 13. REMOTE-TO-CENTERFIELD SENSOR SPACING IN THE SEVEN-AIRPORT LLWSAS

<u>Remote Sensor</u>	<u>Sensor Spacing (nmi)</u>						
	<u>TPA</u>	<u>ATL</u>	<u>OKC</u>	<u>DEN</u>	<u>IAH</u>	<u>JFK</u>	<u>BOS</u>
N	-	-	-	3.37*	-	-	-
NE	1.35*	1.76*	1.71	1.41*	-	1.47*	1.09*
E	1.30*	-	-	1.76*	1.75*	-	-
SE	-	1.37	1.18	-	1.59	0.95	1.32*
S	1.28	0.37	-	-	1.70	-	-
SW	-	1.10*	1.12*	1.21*	1.27*	1.11	1.10
W	0.56	-	2.17*	-	-	2.63*	1.07
NW	1.60*	1.11*	1.68*	2.29*	1.59*	3.00*	1.01*
Average	1.22	1.12	1.59	2.01	1.58	1.83	1.12
Miss Rate**	8	20	3	4	3	1	20

\*Critical Sites

\*\*Estimated System Miss Rate % (from figure 47)

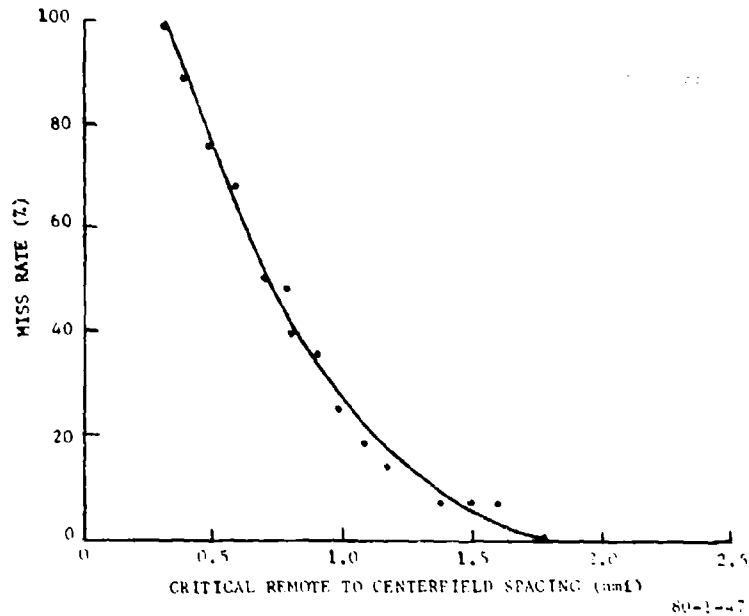


FIGURE 47. ALARM MISS RATE VERSUS CRITICAL REMOTE-TO-CENTERFIELD STATION SPACING

EFFECTS OF JET WASH AND WINGTIP VORTEX IMPINGEMENT. It should be obvious that sensor locations affected by jet wash will inhibit the sensing of representative winds and will produce false alarms. Except for the centerfield locations, one should hardly ever have to face this problem. Remote sites should always be well away from active runways and taxiways. The tacit assumption is also made that LLWSAS centerfield locations in proximity to the NWS airfield anemometer have been surveyed by the NWS and will be free of jet blast effects. At LLWSAS test facilities, incidents of jet blast effects have never been observed. However, at future facilities if the LLWSAS centerfield sensor is not to be located at the NWS site for some reason, FAA survey personnel should take every precaution to assure that jet wash will not ever impinge upon the sensor.

Wingtip vortex impingement has been a very real problem for LLWSAS remote sensors, especially those vortices shed by wide-body aircraft. Vortices are a problem in light wind conditions or in the situation when the sensor is near centerline and the mean wind is roughly parallel to the centerline axis (Garodz, 1977, reference 18). Vortices may add tremendous amounts of kinetic energy to the mean wind under certain conditions, but the vortex dissipates rapidly when the mean wind is high and when the vortex circulation makes contact with the ground. Sensors are more susceptible to strikes the higher they are above the ground. To insure that vortices would not produce an unacceptable number of false alarms, low-pass filters or averager cards were

added to the remote electronics package during the course of the test. This filter virtually eliminated all reports of false alarms due to vortices, except for occasional strikes at Atlanta's southwest and southeast sites, where vortices shed by wide-body jets apparently persist longer than the cutoff period of the filter. Both sites were eventually moved off centerline, and the problem has not resurfaced. (The southeast site was moved from the 09L to the 09R centerline. Runway 09R is used primarily for departures in a westbound operation.)

In future systems, a remote site should be located 800 feet off centerline, if possible, following the guidelines established during the test of the Vortex Advisory System (VAS) at O'Hare. This is not necessary, however, if the sensor is more than 1 mile from threshold and lower than 40 feet above ground. The suggestion is not an absolute requirement because the low-pass filters appear to eliminate most vortex-induced false alarms.

NETWORK SYMMETRY. Sensor symmetry refers to the character of the LLWSAS airport network--the property of having all remote sensors more or less evenly spaced from the centerfield sensor. Network symmetry is important because the LLWSAS computer does not compute wind shears (vector difference per unit distance), only the vector difference. The computer has no information as to the spacing between sensors. However, an "airport wind shear" value is implied in the vector difference calculations if all remote stations are roughly equidistant from the centerfield station. A wind shear threshold is not used in LLWSAS in the attempt to standardize software between airports.

Acquiring network symmetry at an airport may be a difficult proposition, highly dependent on the airport runway configuration and the location of the centerfield sensor relative to the runways. LLWSAS test airports at Houston and Boston are symmetrical, whereas Denver and Kennedy are not (see table 13).

SUMMARY: APPLICATION OF CRITERIA IN CHOOSING A PROSPECTIVE ANEMOMETER SITE.

Perhaps the best way to show how the meteorological criteria are blended and weighted in anemometer site selection would be to apply the criteria to a hypothetical airport complex. Shown in figure 48 is such an airport. Runways 13-31 and 08-26 are major runways each with a middle marker. The runways are 9,000 feet long. Centerline axes ( $C_L$ ) are indicated by dashed lines.

The following is a step-by-step application of meteorological siting criteria:

1. Determine the location of the centerfield anemometer site. Geographically centered locations are recommended.
2. Draw three concentric circles with the centerfield location as the circles' center. The circles should represent 0, 5, and 10 percent miss rates which have been predetermined from figure 47. The circles should be 1.75, 1.5, and 1.25 nmi from the centerfield station, respectively.



3. Determine which prospective sites are critical by consulting the nearby office of the NWS or by contacting the LLWSAS Project Manager, R. Craig Goff, or Ernest Schlatter, Program Manager, at NAPEC. Assume that 75 percent of all gust fronts and 25 percent of all cold fronts are potentially hazardous in terms of wind shear. Generally speaking, remote stations in the west and northwest quadrant of the airport are critical most of the time, except in the Florida Peninsula and near the Gulf of Mexico where stations on the northeast through southeast side of the airport are also critical. Remote stations facing large cold water bodies (Atlantic Ocean and Great Lakes) are also critical at those airports within 25 miles of the coastline.

4. Determine the figure 44 site criteria for critical sites by plotting zones 3,500 to 4,500 feet from each threshold. The zones should be 1,500 to 2,000 feet long, but should not inscribe an area 800 feet either side of centerline. The 800-foot criteria is not important and may be narrowed if the runway is infrequently used for approaches or the prospective site is more than 1 mile from the threshold.

5. Select all critical sites first by proper weighting of criteria in 2 and 4. Note that a site should be further from threshold rather than closer if the two criteria are by and large mutually exclusive.

In the example shown, it may be advantageous to begin by selecting the northwest site, adding the others in a symmetrical pattern afterwards. In figure 48, site 4 in the northwest quadrant is selected first (solid dot). It is 800 feet off centerline, along the 2 percent imaginary miss rate circle and about 2,000 feet from the runway 13 middle marker (possibly the nearest a.c. power source). Since the northwest site is assumed critical 75 percent of the time, the airport miss rate is 1.5 percent (2 percent of 75 percent) for this site alone.

The west site is selected next. It can tolerate a higher miss rate because it is assumed critical only 25 percent of the time. The proposed site is near the 10 percent miss rate circle, but only 2.5 percent is added to the airport miss rate (10 percent of 25 percent). Since these are the only critical sites, the total airport miss rate is 4 percent (the airport's miss rate should not exceed 5 percent, if possible). The west site position is 2,000 feet from the middle marker or a.c. power source. Notice the site can be moved closer to a.c. power without significantly increasing the airport miss rate. Also notice both the northwest and west sites have been selected by weighting the figure 47 criteria more heavily than figure 44 criteria. The converse may be true if the centerfield anemometer is biased toward a critical side(s) of the airport.

The remaining sites (all noncritical) may be selected by placing more emphasis on factors related to symmetry and logistics (access by road, proximity to a.c. power).

Site 6 should be selected next to cover the approaches to runways 31 and 26. A location anywhere in the hatched zone of figure 48 is adequate. The suggested location maintains airport symmetry and is close (1,000 feet) to the a.c. power source at the runway 31 middle marker. Sites 2 and 5 fill the gaps between other sites. They are not runway oriented.

No mention has been made in this section of the highly significant factor of terrain in site selection. It has been assumed in the hypothetical case that the terrain around each proposed remote site is flat and clear of obstructions. However, this may not be the case in practice. If terrain is a serious constraint, adjustments must be made in either the ground location of the mast and/or the height of the sensor, and all logistical factors are of secondary importance.

#### LLWSAS DATA COLLECTION AND ANALYSIS.

DATA COLLECTION METHODOLOGY. Digital wind direction and speed data were collected during part of the LLWSAS operational test. The data were used to verify the ability of LLWSAS to detect horizontal shears associated with weather fronts and to compare airport anemometer outputs for assurance that the anemometer sites were not unduly influenced by local terrain and obstructions. As a result of this data collection and subsequent analysis, several sites were relocated during the course of the LLWSAS test.

Although the objectives of the data collection were eventually met, the gathering of wind data and the editing and archiving of the raw records for ultimate analysis were only accomplished after a great deal of effort. In terms of original design criteria, the data collection was intended to be a rather sophisticated, almost fully-automated process. At all six LLWSAS airports, a dual floppy disk was interfaced to the master station computer. Data were output to a single diskette on a given day, but output was automatically switched to the alternate diskette on midnight of the following day. Date (Julian day), time, and u- and v-component wind data were recorded. A keyboard command to initiate recording and an entry to set the correct Julian date and time were the only manual requirements. To make certain a diskette would not fill with data before the midnight switchover, only every other scan of the LLWSAS sites was output to the floppy. Thus, the nominal recording rate was 20 seconds. (Each diskette has 2,002 sectors, and four logical records are recorded per sector. During the LLWSAS data recording operation, the remote site polling rate was 10 seconds. This equals 8,640 records per day. Only 8,008 records can be recorded per diskette, per day, at the 10-second recording rate, thus, the constraint to record only every other scan.)

At NAFEC, an auto-dial system, magnetic tape drive, and teletype were interfaced to a computer. Shortly after midnight of every day, the NAFEC computer was to command the auto-dial system to call each LLWSAS airport and retrieve the data recorded on the previous day's diskette. This communication link was via signal-conditioned commercial telephone line. The data stream flowing to NAFEC would be edited by the computer and recorded on 1/2-inch magnetic tape. Any shear alarms or data anomalies would be flagged and printed on the teletype.

NAFEC personnel, when arriving on station that morning, would have a hard copy, quick check of all LLWSAS data recorded the previous day. The retrieval of data by the auto-dial system would not affect ongoing airport data collection since the real-time data recording had switched to the alternate diskette at midnight.

Because of the priority of installing and debugging LLWSAS equipment at so many airports, the NAFEC portion of this scheme was not implemented. Instead, the assistance of local Airway Facilities personnel was requested. This involved the changing of diskettes daily and the periodic transfer of diskettes to NAFEC via mail. This system eventually was successful despite numerous problems. A total of 181 data diskettes were collected at the six LLWSAS airports. (Boston was not included in this data collection and processing effort.)

DATA ANALYSIS. Machine processing of the LLWSAS data sets involved the use of two utility and four analysis programs. The objective of the programming task was not to determine the climatology of the wind at each airport (this was not possible because of the small size of the data sets), but rather to determine the representativeness of the wind at each site, the adequacy of sensor spacing, the character of data output during vector difference alarms, and the effect of existing obstructions on the wind. Despite the small quantity of data collected, the analyzed product was instrumental in promulgating important changes during the course of the test and evaluation.

The following four analysis programs were developed:

1. Compute the record-by-record vector difference between each remote site and the centerfield site and compute 5-minute averages of the u- and v-components of the wind vector.
2. Determine the distribution of vector differences by remote/centerfield pair.
3. Compute the bivariate distribution of speed and direction by station.
4. Plot airport scale surface wind flow patterns using objective analysis.

Table 14 demonstrates the use of program 1, the vector difference information computed between each remote station and the centerfield station. The data shown were recorded at Tampa on July 13, 1977, during a thunderstorm. The table shows the vector differences computed from data recorded every other scan (~21 seconds) for roughly 11 minutes. The assignment of scan 0 to the 155814 data is arbitrary. At scan 0, vector differences are low and the values are representative of a 30-minute past history at Tampa. Between scan 2 and 22, the vector differences at station 4 northeast (NE) increase nearly monotonically to 24.20 knots, exceeding the 15-knot vector difference threshold at about 160030. Underlined values in table 14 are those exceeding the alarm

TABLE 14. VARIATION OF VECTOR DIFFERENCES DURING A THUNDERSTORM PASSAGE AT TAMPA, FLORIDA, JULY 13, 1977

Time Scan (LST)	Vector Differences (kn) Centerfield to				
	(W) Station 2	(NW) Station 3	(NE) Station 4	(E) Station 5	(S) Station 6
155814 0	1.45	0.13	1.64	2.82	2.73
155835 2	3.43	1.32	0.62	7.37	4.04
155856 4	2.50	0.69	1.81	7.59	3.58
155917 6	0.72	0.25	4.59	7.09	3.72
155937 8	0.48	1.38	6.73	5.33	3.22
155957 10	0.11	0.91	7.48	5.63	4.71
160018 12	1.61	2.93	10.72	2.78	2.92
160038 14	0.46	3.41	13.54	3.16	3.09
160059 16	2.42	6.17	19.27	1.20	3.48
160120 18	1.14	6.50	<u>19.21</u>	0.89	2.29
160141 20	3.17	4.69	<u>17.75</u>	3.33	6.36
160203 22	6.60	14.59	<u>24.20</u>	4.95	5.56
160224 24	3.41	11.86	<u>17.33</u>	2.68	4.87
160244 26	4.57	11.77	<u>15.61</u>	2.64	5.55
160305 28	5.29	7.76	<u>16.85</u>	4.50	7.34
160325 30	2.36	4.78	11.52	5.05	6.15
160346 32	4.31	1.93	13.52	4.66	6.63
160407 34	4.72	9.38	15.37	3.19	9.40
160427 36	4.10	12.60	<u>16.98</u>	4.21	9.53
160448 38	4.51	14.23	<u>15.16</u>	7.54	9.17
160509 40	7.58	10.15	<u>15.09</u>	10.21	10.60
160530 42	6.54	13.09	<u>14.18</u>	4.79	6.82
160551 44	0.75	11.87	8.16	2.45	3.10
160612 46	8.39	<u>15.89</u>	9.51	4.79	6.55
160633 48	4.89	<u>16.58</u>	5.92	7.53	9.46
160654 50	8.89	11.29	5.98	6.23	8.36
160714 52	8.32	14.61	8.81	5.87	8.49
160735 54	7.68	14.86	6.54	4.88	8.72
160755 56	9.20	<u>17.75</u>	8.91	5.91	10.67
160816 58	5.76	9.25	3.83	3.35	3.67
160836 60	5.52	6.51	7.14	1.73	5.42
160857 62	7.88	8.08	2.87	4.04	5.60
160917 64	6.44	9.52	2.64	2.08	3.66

threshold. Using interpolation, an alarm would have been registered in the tower cab at scan 15 signifying the passage of the gust front at the northeast station. At scan 29 or 30, the vector difference falls below the threshold and the alarm condition halts. The alarm condition is renewed at scan 34 and ends at scan 41 or 42. About 5 minutes have elapsed during which time the gust front continues to propagate toward the airport. At scan 46, an alarm commences at station 3 northwest (NW), lasts for 3 or 4 scans, ceases, then is refreshed for 1 or 2 scans (Nos. 55 and 56).

The intermittency of alarms at station 2 point to an early air traffic controller objection to the LLWSAS software. Prior to the summer of 1978, alarms were governed solely by the value of the vector difference. Alarm intermittency caused controller confusion and possible annoyance. Based on the data from this case and others like it, the software was changed in 1978 to hold the alarm condition for 6 scans beyond the last scan having a computed vector difference greater than 15 knots. This reduces intermittency substantially.

There were no other alarms registered in the case presented in table 15. Data indicate the potentially hazardous part of the thunderstorm affected only the north side of the airport. In an operational mode, approaches to Tampa's runways 18R and 18L would have been interrupted for 8 1/2 minutes. (The centerfield wind remained from the south throughout the period. Departures would have been unaffected by the thunderstorm.) This case is remarkably similar, though less severe, than the Kennedy case causing the Eastern 66 accident.

Program 2 (distribution of vector differences by station) is helpful in determining the adequacy of anemometer siting. Figure 49 is an example of distributions for Houston, Texas, on October 10, 1977. Data for the distributions were collected on a fair-weather day (no thunderstorms, fronts, or other wind discontinuities). Inspection of figure 49 indicates that all distributions are approximately similar, except the distribution for station 3 east (E) whose distribution peak is offset toward higher values of vector difference. The offset distribution compared with the others illustrates a minor sheltering problem at this site when the wind is from the northeast quadrant. The sheltering causes a 2- to 2.5-knot vector difference bias. Low, widely scattered evergreen trees exist northeast of the station 3 sensor.

Distributions were also inspected for shape characteristics. If the mean vector difference at all stations is high, a near normal distribution is expected. Any wide departure from a nonzero skewness is an indication of sheltering or turbulence caused by terrain roughness. In the case presented in figure 49, the distribution mode (peak) is low and nonzero skewness is expected.

Distribution tails are good indications of the effect of terrain roughness. If one distribution has a long tail, relative to the others, wide excursions of the wind speed and/or direction are implied at this station. Station 4 shows some evidence of relative dispersion probably caused by vegetation-induced turbulence northeast of the sensor. Neither of the suspected problems





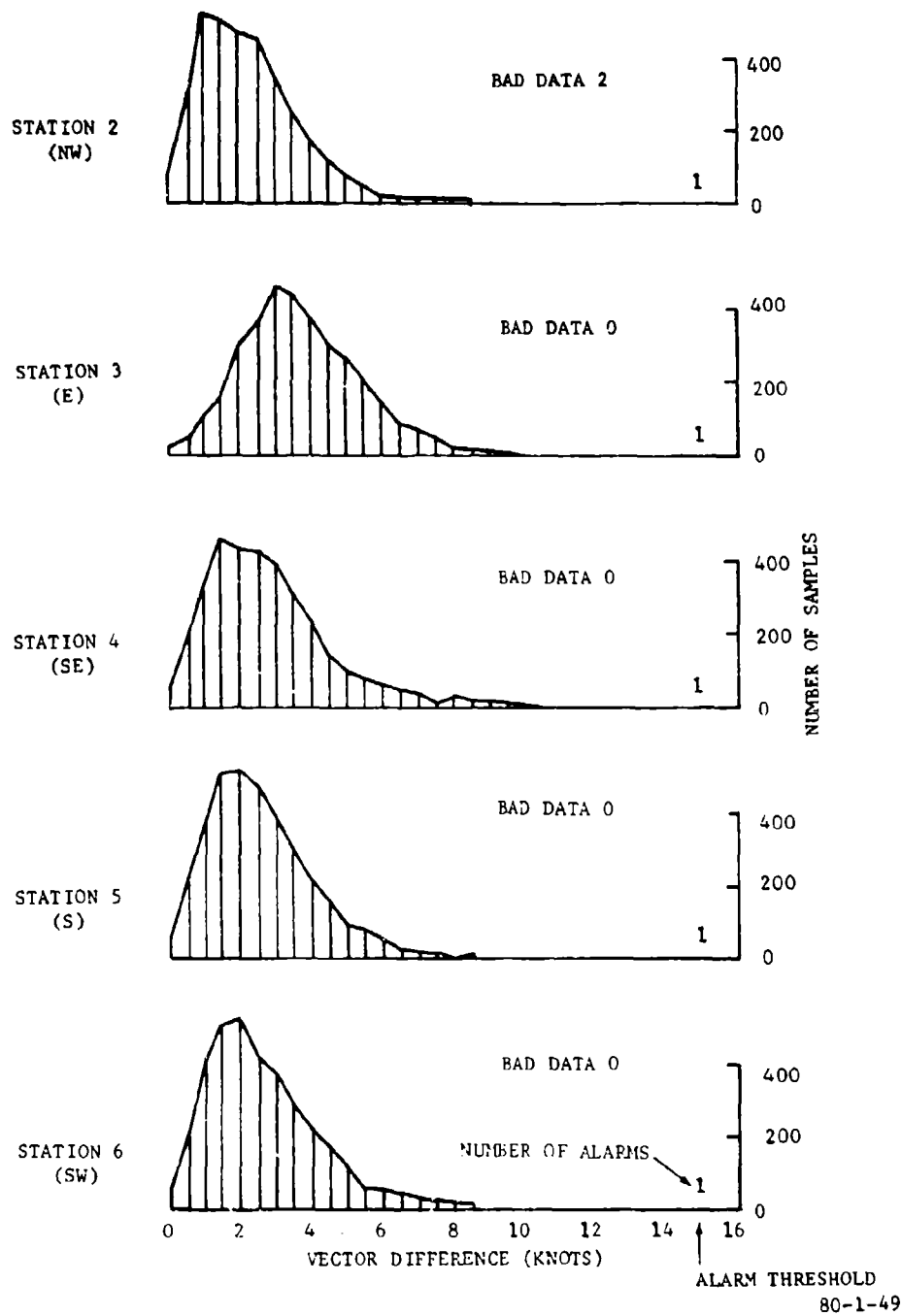


FIGURE 49. DISTRIBUTIONS OF VECTOR DIFFERENCES FOR HOUSTON, TEXAS, OCTOBER 10, 1977

at stations 3 or 4 were considered significant enough to warrant a site relocation; however, both anemometers were raised from 20 to 40 feet in July 1978.

An auxiliary function of program 2 is to count hard transmission failures. For the 20-hour data sample from Houston used for the figure 49 distributions, the centerfield station failed once (indicated by one out-of-range vector difference at each station), and station 2 had two failures. All other stations reported zero transmission errors.

Program 2 was used to process data from all other airports. Results confirmed the need to make the site adjustments discussed under Anemometer Siting Criteria.

The bivariate distribution of wind speed and direction (program 3) is used for the same purpose as program 2, to check the adequacy of siting. The results are difficult to interpret and were not as useful as the distributions in program 2. Typical distributions of speed and directions on a fair-weather day (July 3, 1977) at Tampa, Florida, are shown in table 15. Twenty-degree direction class intervals represent the vertical axis.

Wind speeds in 1-knot class intervals represent the horizontal axis. The distributions for speed classes from each of the six LLWSAS stations are grouped in a given direction class. The station numbers are shown on the left. In the example used, most of the observations are grouped in three directional classes from which a rough estimate of airport wind direction ( $300^\circ$ ) is determined.

Some properties of the distributions are immediately obvious from table 15 and figure 50. Station 5 E has a distribution peak at higher speeds (table 15) than other stations in the  $260^\circ$  to  $280^\circ$  class interval. This is because it is the only Tampa station with a smooth fetch for this wind direction. The centerfield station shows similar characteristics in the  $240^\circ$  to  $260^\circ$  class interval. Station 3 NW has a bimodal distribution with an accumulation of observations at low speeds for the two-direction class intervals spanning  $240^\circ$  to  $280^\circ$ . Figure 50 is a plot of distribution sums for each direction class interval (see right side of table 15). Although most distributions are similar (as desired), stations 2 west (W) and 5 E have a bimodal distribution, the centerfield station distribution is offset about  $20^\circ$  to lower values of wind direction, and station 3 NW has a slight peak in its distribution tail due to wind tending to blow along the path of least resistance; i.e., down the 18-36 centerline clear cut zone. Despite these differences, system performance is not significantly impaired. Similar analysis of Tampa data, when the mean airport wind was from the south, did reveal a severe sheltering problem at the south site. The sensor was subsequently raised 16 feet to place it above nearby obstructions. Program 3 was used to determine wind representativeness at other airports also.

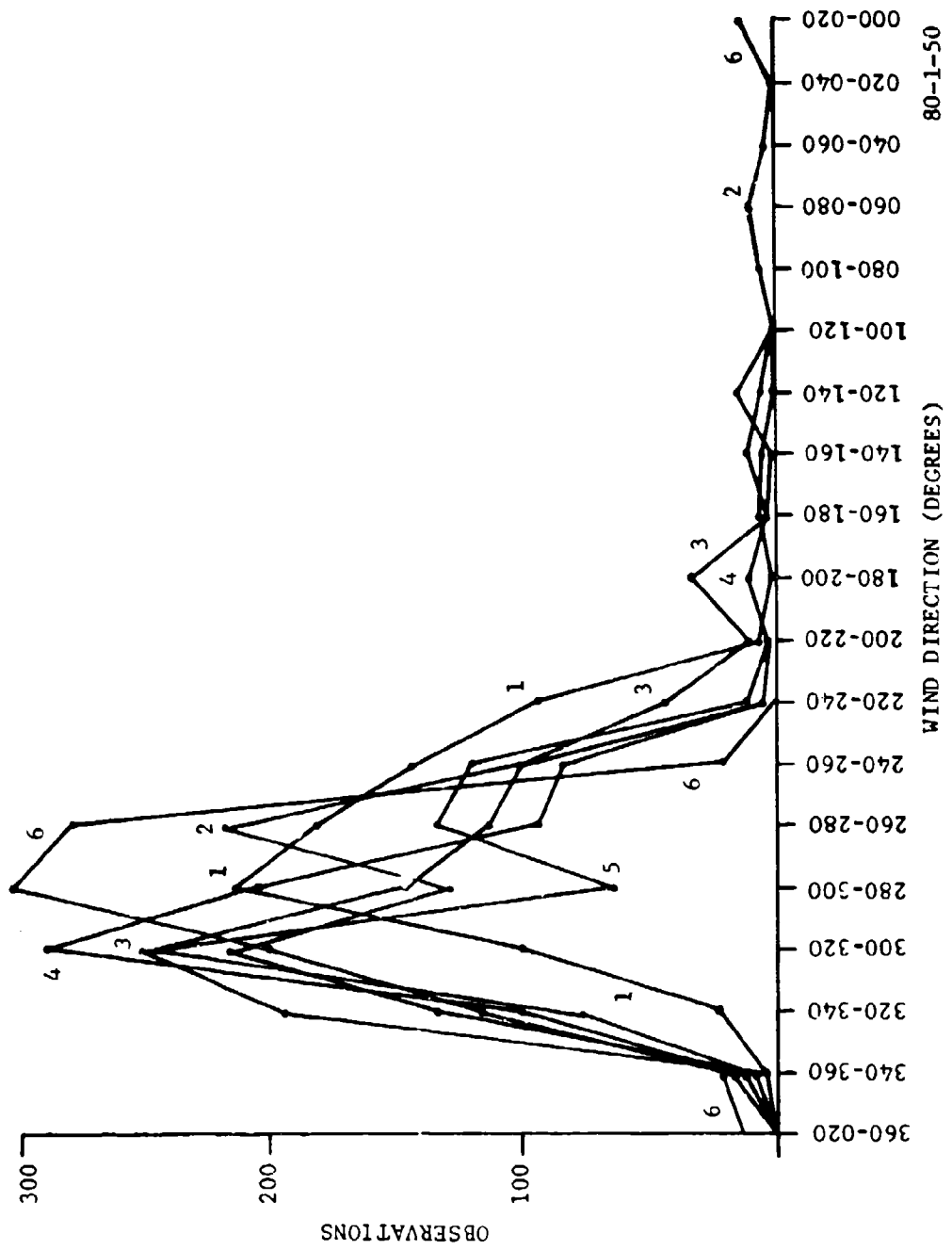


FIGURE 50. DISTRIBUTION OF WIND DIRECTION FOR TAMPA, FLORIDA, JULY 1977

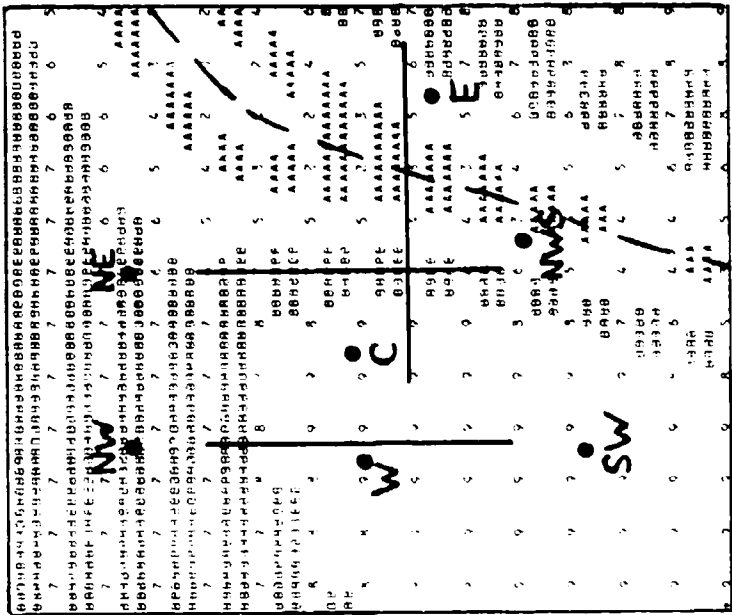
Objective analysis and plotting of the surface wind observations (program 4) is a numerical method developed by Barnes, 1974, (reference 19) and modified for use on the NAFEC general-purpose computer. Two examples of the line printer output are shown in figures 51 and 52. Figure 51 illustrates objectively-analyzed data from Tampa for a thunderstorm case on June 29, 1977. Figure 51(a) is the analyzed wind direction, and figure 51(b) is the wind speed. LLWSAS site locations, the NWS anemometer, and runways are shown in bold print. Hand-drawn streamlines are superimposed in figure 51(a). The center of the wind shift zone associated with the gust front is indicated by a heavy dashed line in figure 51(b). Although the gust front is weak in terms of horizontal shear, the example demonstrates the ability of the LLWSAS to detect potentially hazardous shears before they reach the airport center. The analysis was also useful in determining the adequacy of station locations and spacing. In this case, the gust front is approaching the airport from the southeast. The east station first detects the wind change, and ample warning is given to any pilots that might be using Tampa's principal runways (18R-36L and 18L-36R). The objective analysis indicates that the width of the front is about 1.25 miles, or less than the average station spacing, at Tampa and, therefore, within the guidelines established and justified in the Anemometer Siting Criteria section which discussed station spacing.

A similar machine-plotted objective analysis appears in figure 52. These data were gathered at New York's Kennedy Airport during a seabreeze front passage on May 19, 1978. The front is moving slowly from southwest to northeast and has propagated past all of the LLWSAS stations except the north (N) station. Although no inbound or outbound operations were interrupted during the front's passage over the airport (sky clear, visibility unlimited), the initial detection of the front at the southwest (SW) sensor gave air traffic controllers about 10 minutes leadtime to coordinate a runway change with other major airports (LaGuardia and Newark) in the metropolitan area. Although this seabreeze front is similar to the Tampa case in figure 51, seabreeze fronts as a rule are much weaker than thunderstorm gust fronts.

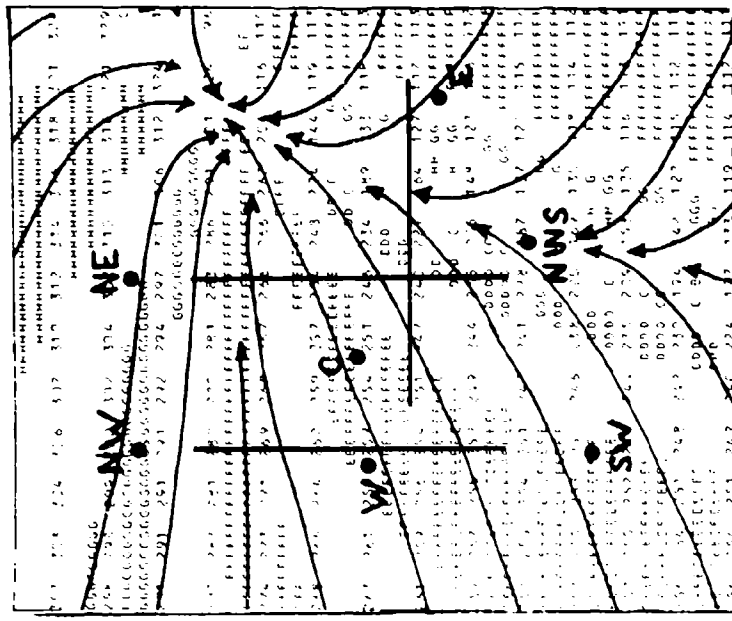
#### AIRPORT SENSOR CONFIGURATIONS, SPECIAL SITING FACTORS, AND QUALITATIVE TEST RESULTS.

TAMPA INTERNATIONAL, FLORIDA. The Tampa LLWSAS was the first installed (June 1977) because west central Florida has the highest frequency of thunderstorms in the United States and because the airport is the closest to the principal contractor's factory headquarters. The latter permitted quick debugging of hardware and software problems encountered in early stages of the LLWSAS test.

Tampa has three principal runway axes--two oriented north-south and one oriented east-west. The airport is bounded on the east and south by residential areas, on the north by a mixed open and commercial plant area, and on the west by Tampa Bay. Terrain is essentially flat, and vegetation alternates between patches of open, scrub brush (10 to 15 feet high) and tropical forest (30 feet high).

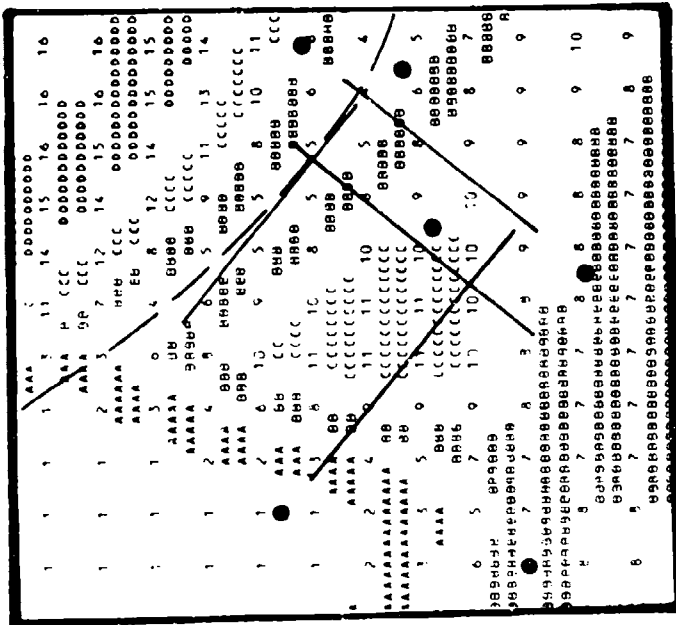


(b) SPEED

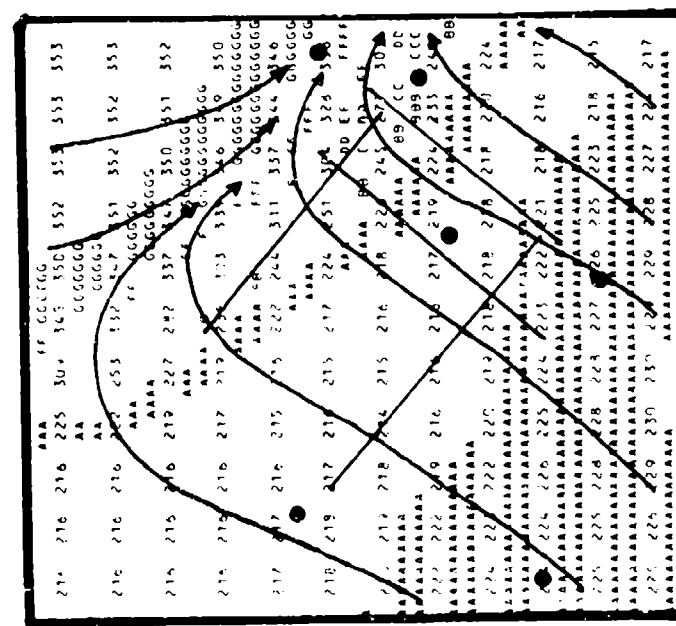


(a) DIRECTION

FIGURE 51. OBJECTIVELY ANALYZED WIND DIRECTION AND SPEED DATA FOR A THUNDERSTORM GUST FRONT PASSAGE AT TAMPA, FLORIDA, JUNE 29, 1977



(a) DIRECTION



(b) SPEED

FIGURE 52. OBJECTIVELY ANALYZED WIND DIRECTION AND SPEED DATA FOR A SEABREEZE FRONT AT KENNEDY AIRPORT, NEW YORK, MAY 19, 1978

Anemometer positions (figure 53) are in the northwest, northeast, east, southwest, and west quadrants of the airport in addition to the centerfield position near the airport's geographical center.

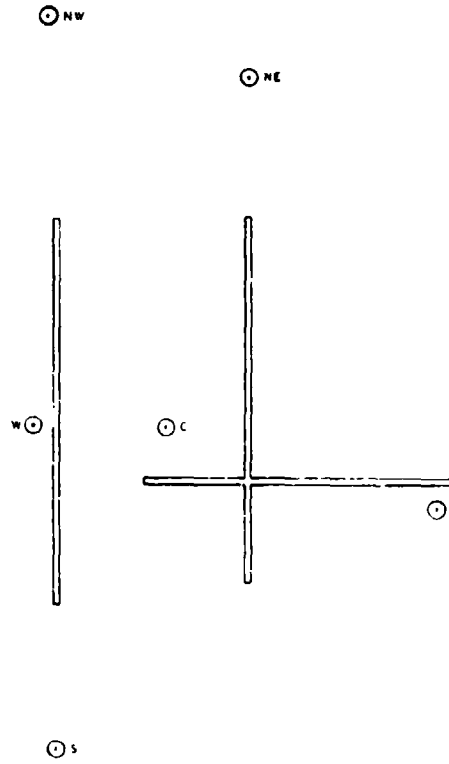


FIGURE 53. AIRPORT RUNWAY MAP WITH ANEMOMETER LOCATIONS, TAMPA INTERNATIONAL AIRPORT, FLORIDA

The northwest anemometer is 1/2 mile north of Hillsborough Road, to the east of Benjamin Road, 200 feet off centerline. The anemometer is 40 feet above ground on a utility pole. There are no wind obstructions to the north or south, there are a few 30-foot trees east of the site (none closer than 500 feet), and a 20-foot high, large surface area building is 600 feet northwest. There are no major obstructions within 1,000 feet west of the site. The site

is considered good in terms of sensing representative winds. The present site was moved 3,200 feet north in November 1978 because of an anticipated extension of the 18R-36L runway. It is presently in a better position to sense representative winds and to give earlier warnings of shear than the old site. The site is not secure, but being some distance from residences and along a frequently traveled road, vandalism should not be a problem. (Experience has shown that only sites accessible by the public but remote from general public view or located in an area where there is hostility to the airport by the local residents have any incidence of vandalism.) The northwest site is a critical site, especially in the winter when strong squall line thunderstorms may approach from the north. Otherwise, it is not a critical site for wind hazard detection. The optimum position for this site should be 1,000 feet further north and 500 feet further west; however, this location is off airport property in an industrial development zone and, thus, inadequate for anemometer siting.

The northeast sensor is near the middle marker to 18L, along centerline, just south of Hillsborough Road. The sensor is 20 feet above ground on a Vega tower. The area to the north is commercialized with low buildings, the south is open. To the east and west, widely scattered 25-foot trees and low brush exist beyond the centerline clear zone which is about 1,000 feet wide. These obstructions to the north and principally to the east and west cause some sheltering of the anemometer (no more than 2 to 3 knots). When the winds are light, from the east or west over the airport, the wind at the northeast site tends to flow along the path of least resistance, diverting north or south, depending on the unobstructed azimuth. Thus, when speeds are below 8 knots, there will be large-angle differences between this sensor and the centerfield. This sheltering and wind deflection is not considered significant and should never cause false alarms. The northeast site is occasionally the critical sensor due to thunderstorms building along the seabreeze line and moving east or southeast toward Tampa in the late afternoon. The site is on airport property and is secure.

The east site is most often the critical anemometer at Tampa since most tropical thunderstorms that form along the seabreeze line move from the east. The sensor is 20 feet above ground on a Vega tower positioned south of runway 09-27, near the 27 threshold. It is in an excellent position to sense representative winds, but it is in a poor position to give adequate warnings of wind shifts before they cross the 27 threshold. No adequate sites exist further east. However, runway 09-27 is not frequently used by commercial aircraft. The terrain around the site is essentially clear except for a helicopter maintenance building, 700 feet southwest, and a clump of 25- to 30-foot trees, roughly 700 feet east-southeast. There is virtually no sheltering effects because obstructions are not large or close to the site. The site is on airport property and is secure.

The south site is near the middle marker for runway 36L. The site is positioned inside a chain-link fence area on airport property but is remote from day-to-day airport activities, and the area outside the fenced square is accessible to the public by foot travel through adjacent swampy terrain.

Because of its remote location, there have been two acts of vandalism at this site; the sensor and remote box were shot at on one occasion, and the sensor was stolen on another occasion. The sensor is on a 16-foot aluminum pipe guyed-extension fastened to a 20-foot utility pole and, thus, 36 feet above the ground. The original sensor position was atop the utility pole without the extension, but tall trees to the south caused severe sheltering and resulted in frequent false alarms with strong southerly winds. The 16-foot extension has reduced the number of alarms virtually to zero, but the sensor is still sheltered to some degree with south winds due to the 25- to 30-foot trees. A better site (with a 50- to 60-foot mast) is along the high voltage Florida Power and Light run, parallel to Cypress Road extension; but this location is off airport property, is unsecure, and is relatively inaccessible. The current sensor position is in a zone clear of obstructions to wind to the north and relatively clear to the east and west quadrants. The sensor is only rarely a critical sensor.

The centerfield sensor is roughly 500 feet east of the Hillsborough County Airport Authority vault building off the airport access road. The sensor is atop a 20-foot Vega tower. The site is geographically centered compared with the NWS anemometer site which is near the threshold to runway 36R, about 1 mile southeast. The LLWSAS site is in an open area, and the only possible sheltering is due to scattered trees and the small vault building 500 to 1,000 feet away in the west-to-north quadrant. The terminal complex is too far away to disturb the wind more than a few knots with moderate mean wind speeds. The only major problem with this site is the electrical a.c. power connection. Alternating current power feeds from a circuit breaker in the vault building. The building, always locked, is not directly accessible by FAA personnel. Provisions are being sought to connect the LLWSAS equipment to a power outlet external to the vault building.

The west site is roughly midway, adjacent to and west of runways 36L-18R. The sensor is atop a steel pipe which is affixed to a transmissometer tower. There is some sheltering with west winds because of obstructions (bushes and trees) to the west. More importantly, the site is so close to the centerfield site (0.56 nmi) that its usefulness is diminished. (See section on Anemometer Siting Criteria.) However, the sensor is not one of the airport's critical sensors, and the decommissioning of this site is being discussed.

HARTSFIELD INTERNATIONAL, ATLANTA, GEORGIA. The Atlanta LLWSAS was installed in August 1977. Problems ensued immediately. The roughness of the local terrain around the airport caused frequent false alarms. Equipment problems resulted in numerous system failures. Both resulted in a protracted test bed debug period. Consequently, LLWSAS at Atlanta was not suitable for operational usage until late spring of 1978.

The system conforms to general equipment configurations at other airports. The above mentioned terrain roughness around the airport, however, has resulted in the need for five sensor adjustments during the test to meet the need of sensing representative winds. One additional sensor movement was required to prevent wing tip vortex impingement.

Atlanta has three principal parallel runway axes oriented east-west. The airport is the second busiest commercial airport in the world, and runway 08 is the busiest runway in the world. The airfield is ringed on three sides by dense residential and commercial buildup. The problem of wind obstructions by buildings is compounded by a vegetative cover outside the airport periphery composed of 50- to 60-foot trees and terrain undulations of 60 to 80 feet. The airport property does not extend far beyond the runways; thus, terrain roughness, trees, and buildings are encountered in the immediate vicinity of the airport boundary and preferred sensor locations were either nonexistent or required several relocations before an adequate site was found.

The northwest sensor is on a 20-foot Vega tower near the middle marker for runway 08 (figure 54). The sensor site is adjacent to (50 feet back from) a 40-foot embankment along Interstate 85. The embankment runs roughly north-northeast to south-southwest. Thus, winds from any easterly direction (except when blowing exactly perpendicular to the embankment) are laterally deflected by the terrain, causing wind direction biases. In addition, such winds will produce a small wind jet caused by convergence when blowing over the embankment. No other anemometer site is available, however, as extensive surveys in the College Park community to the west have taken place with negative results. The northwest sensor is the critical sensor for virtually 75 percent of the wind shear cases. The northwest sensor measures representative winds coming from the 240° to 010° (through north) quadrants.

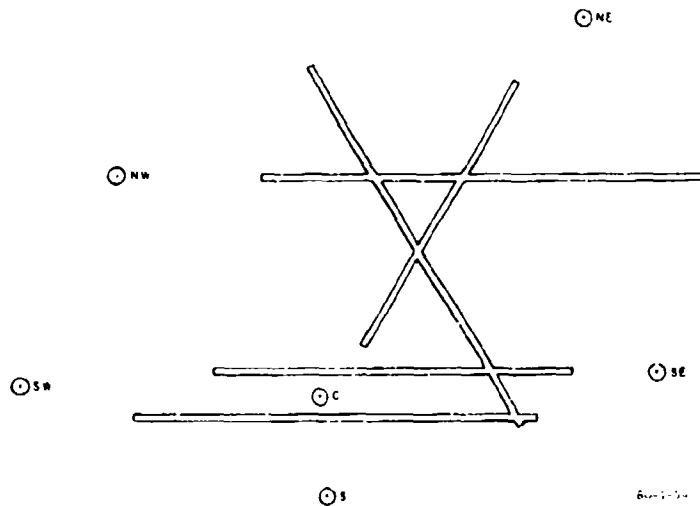


FIGURE 54. AIRPORT RUNWAY MAP WITH ANEMOMETER LOCATIONS, HARTSFIELD AIRPORT, ATLANTA, GEORGIA

The southwest anemometer is properly positioned to sense representative winds, but this was only achieved after two sensor relocations. The site is 40 feet above ground on a utility pole in a wide, shallow depression 800 feet north of the middle marker for runway 09R or midway between the 09R and 09L centerlines. It is the critical sensor roughly 15 percent of the time. Except for the slightly depressed ground terrain relative to the runway to the east and ground to the west, the surface in the immediate vicinity of the sensor is flat and free of vegetation of significant height. The 40-foot height of the sensor reduces the chance of wind decelerations caused by relatively low surface elevation compared to nearby terrain.

The sensor was originally adjacent to the 09R middle marker on a 20-foot Vega tower. Compared to other airport sensors, this position measured lower winds because of the low surface elevation. To correct this deficiency, the sensor was raised to 40 feet on a utility pole in May 1978. This resulted in sensing more representative winds, but also allowed for occasional wing tip vortex impingement and associated false alarms. In January 1979, the sensor site was moved off-centerline 800 feet north. This site is now considered adequate.

The south site is in an open, grassy field near the Atlanta VORTAC. Aside from the VORTAC facility 500 feet northwest, there are no major obstructions to the wind at this site. The sensor is on a 20-foot Vega tower. The location is considered excellent, based on comparisons of data from this site with data from the centerfield site. However, this site is very close to the new position of the centerfield anemometer (0.37 nmi) and its decommissioning is being discussed. The site is hardly ever critical.

The southeast site is on a 20-foot Vega tower on the approach to runway 27R, about 3,000 feet from threshold. The site is on a flattened knoll. There are no obstructions within 1,000 feet. Although the terrain drops off to the east, the slope is gradual and only minimally affects the wind. There is no problem with jet blast effects which might be anticipated closer to the threshold. The original location for this sensor was atop a 20-foot utility pole near the middle marker for runway 27L. That position was subjected to unrepresentative winds produced by nearby trees, terrain irregularities due to Interstate-285 excavation, and the Clark Howell Highway overpass as well as frequent vortex impingement. The sensor was moved in May 1978, and the new site is considered adequate.

The northeast site has presented persistent problems during the course of the test. It was originally located near the middle marker for runway 26 on an abandoned approach light tower. The nearby terrain is very rugged and the centerline clear zone is only 300 feet wide bordered by 50-foot trees. Single-story residences are scattered nearby. So severe was the sheltering when the mean airport wind was from the north or south, that the northeast sensor often indicated calm winds. This resulted in frequent false alarms. In March 1978, the sensor was raised 40 feet higher or roughly up to the boundary of restricted airspace. This action improved the situation, but severe sheltering was still apparent. In June 1978, this site was totally abandoned, and the sensor was moved 1.3 nmi northwest to an open area adjacent

to the shipping terminal employee parking lot along Doug Davis Drive. The site is considered adequate in terms of sensing representative winds. Although obstructions exist in all quadrants, they are all more than 600 feet away. Their presence, however, creates considerable turbulence, especially in light wind conditions (less than 10 knots) causing large wind direction fluctuations and some sheltering. The mean wind direction, though, compares favorably with the centerfield site. False alarms occur infrequently.

The centerfield site is offset to the south side of the airport midway between the 09-27 runway parallel. It is 20 feet above ground on a mast affixed to the midpoint transmissometer tower. The site is considered excellent for sensing representative winds.

The centerfield sensor was originally located near the NWS anemometer south of the 08-26 runway. It was moved in the spring of 1979 because of airport construction activity. Its new position improves the performance of LLWSAS considerably as the old site was too close to Atlanta's most critical north-west sensor (see section on Anemometer Siting Criteria).

HOUSTON INTERCONTINENTAL, TEXAS. The Houston LLWSAS was installed in August 1977. Subsequent to a short debug period during which software problems common to all airports were solved, the Houston system enjoyed a protracted period of successful equipment operation unmatched at other airports. Between November 1977 and January 1979, LLWSAS at Houston experienced only two minor electronic problems. Total system downtime was only 1 hour in 14 months. This record resulted in quick air traffic controller acceptance and high credibility.

However, data collected at Houston and later analyzed showed that the remote site winds were severely affected by local obstruction factors (tall trees). This effect was not noticed by controllers because strong wind conditions over the airport regime, which might have produced false alarms at sheltered sites, are not the general rule at Houston. Sheltering, that was evident to NAFEC engineers, indicated the need to raise or relocate all anemometers. This was accomplished in July 1978. In this effort, the centerfield anemometer was relocated to a position nearer the geographical center of the airport.

Houston Intercontinental has two runway axes, 08-26 and 14-32, in a V-pattern opening to the southeast. The airport is in a rural area, 15 miles north of the city of Houston. The airport terrain is flat, but the field is ringed by a dense evergreen forest. Trees are up to 70 feet tall. Originally, all sensors were 20 feet above the ground.

The southwest anemometer site (figure 55) has the best exposure to wind. It is located along Aldine Westfield Road in an area that is relatively free of tall trees. The sensor is now 40 feet above ground on a utility pole, and is the critical sensor about 20 percent of the time. The anemometer measures representative winds in all quadrants.

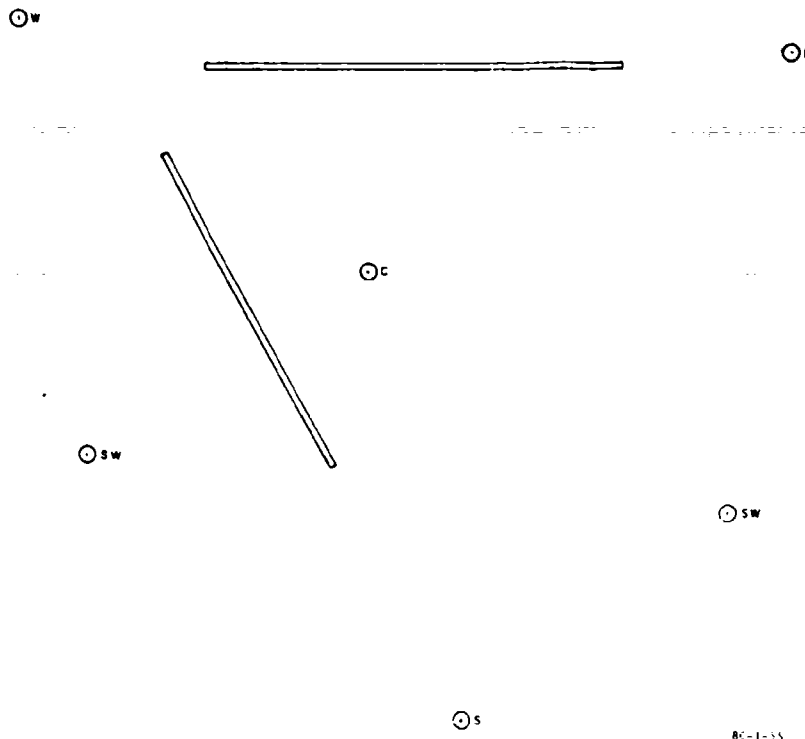


FIGURE 55. AIRPORT RUNWAY MAP WITH ANEMOMETER LOCATIONS, HOUSTON INTERCONTINENTAL AIRPORT, TEXAS

The northwest sensor is the critical sensor about 70 percent of the time. It is also located on Aldine Westfield Road adjacent to the north boundary access road. The sensor is now 50 feet above ground on a utility pole. There is adequate exposure to representative winds at sensor level when the wind is from the north, west, or south. However, a thick forest with tree heights up to 55 feet exists 400 feet east of the sensor. This causes a 10 percent speed reduction and may result in some false alarms with strong east winds. The present position of the sensor is midway between the imaginary X-pattern of the approaches to runways 08 and 14. It is about 3,500 feet from both thresholds. The original position of the sensor was adjacent to (400 feet north) the No. 24 approach light tower to runway 08. The sensor was only 20 feet above ground, and being in close proximity to a tall forest line to the west, extreme sheltering was evident. In addition, the original position of this critical sensor, like the northwest sensor at Atlanta, was too close to the original position of the centerfield sensor (0.7 nmi). Sheltering plus the close remote-to-centerfield sensor spacing caused numerous shear alarm misses. This sensor and the centerfield sensor were moved to their present positions in July 1978. Both problems were solved in moving the sensors to their new locations.

The east anemometer is adjacent to the localizer for runway 08, thus it is near the approach zone for runway 26. Some sheltering is possible from scattered trees to the north and east. The sensor has good exposure to winds from the west and south. The sensor is 40 feet above ground on a utility pole. The original sensor height was 20 feet, but the sensor was raised in July 1978 to minimize sheltering. The east sensor is critical for occasional summertime tropical storms. These storms are not often severe.

The southeast sensor is in a remote location but is on airport property. It is about 2 miles east of the runway 32 approach, adjacent to a drainage channel known as Richardson (or Reinharts) Bayou. In dry weather, access to the site is possible by conventional vehicle over an unimproved road, but in or after wet weather, access is possible only by four-wheel-drive vehicle or on foot. The sensor is atop a 40-foot utility pole. The exposure to wind from any quadrant is considered good since the vegetation in this portion of the airport consists of scattered-to-dense forest, but trees are typically only 20 to 25 feet high. Best exposure exists in the east-to-west through north quadrants. The most dense forest is to the south.

The south site is the poorest site in terms of exposure, but the sensor is only rarely the critical sensor. The anemometer is mounted on a 40-foot utility pole. Its position is about 3,000 feet from the threshold to runway 1 north of Greens Road. Trees 300 feet away, south of Greens Road, are taller than 60 feet generally, and rather severe sheltering occurs with south winds. Exposure is excellent when the wind is from other directions.

The centerfield site at Houston is a geographically central position located southwest of the Kennedy Boulevard/Jetero Boulevard interchange. The sensor is on a 50-foot utility pole. The area to the east and southeast of the sensor is heavily forested (70-foot trees), but the forest line is 625 feet away at the closest point. Due north and south of the sensor the terrain is clear, although to the north the terrain surface is irregular in the interchange area. The terminal area is over 2,000 feet north of the sensor, and there is no significant affect from these buildings. Most serious, however, is the affect of a large tree grove to the west and southwest of the sensor. At the closest point, 60-foot trees are 300 feet from the sensor resulting in some sheltering with west and southwest winds. Sheltering at the centerfield site is considered intolerable by air traffic controllers. The Houston Airport Authority intends to remove most of the 9 acres of trees involved. When this is accomplished, the problem should be resolved, but until that time, air traffic controllers will use the NWS output for operational wind and will issue LLWSAS wind when alarms occur.

The NWS anemometer site was the original position of the LLWSAS centerfield sensor, but this position was biased to the west side of the airport and was too close to the northwest sensor site (even at its present location).

The present position of all sensors represents a desirable symmetrical network pattern so that all remote sites are more or less evenly spaced from the centerfield sensor. The network has average station spacing of 1.58 nmi or just slightly less than ideal.

WILL ROGERS, OKLAHOMA CITY, OKLAHOMA. Sensor positions at this airport are considered model perfect. The terrain is flat and unobstructed, and more than adequate warning is given to wind shears by the key critical anemometer (the first sensor to detect shears in most approaching thunderstorms) which is roughly 2 miles west of the airport. Its position relative to runways is shown in figure 56. The airport's LLWSAS equipment was installed in July 1977. Although the LLWSAS electronics at Oklahoma City has undergone a long period of debugging to achieve reliability, sensing of representative winds and timely warnings of shear events has never really been questioned.

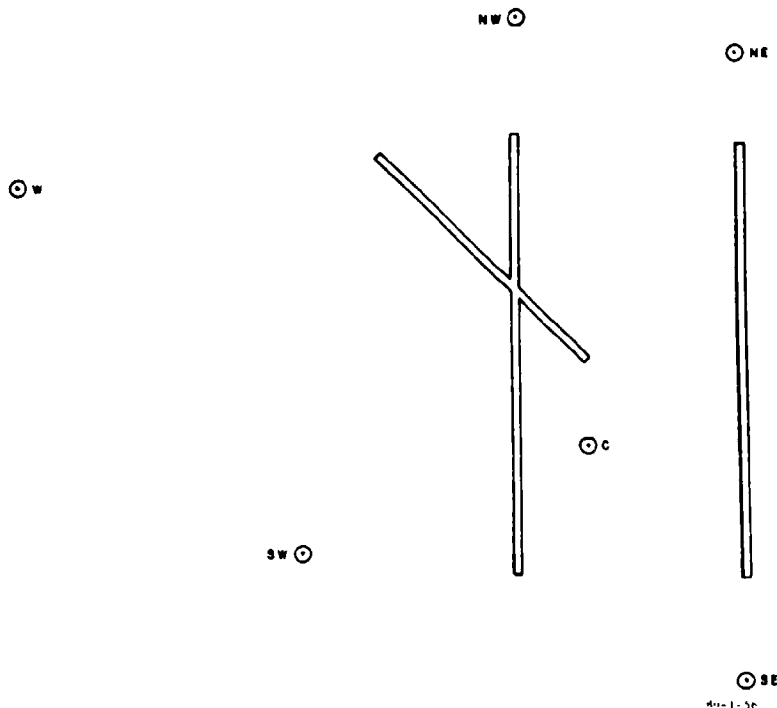


FIGURE 56. AIRPORT RUNWAY MAP WITH ANEMOMETER LOCATIONS, WILL ROGERS AIRPORT, OKLAHOMA CITY, OKLAHOMA

Oklahoma City airport has two primary north-south runways about 1 mile apart and one intersecting, lesser-used runway 14-32. Remote sensors are located roughly 3,000 feet from thresholds to runways 35R (southeast), 17R (northwest), and 17L (northeast). The southwest sensor is west of the 35L threshold at the FAA Academy VORTAC site. The small VORTAC building is located northwest of the LLWSAS sensor. Oklahoma City's west sensor is 2.2 miles due west of the 17R threshold at the FAA radio beacon facility off Newcastle Boulevard (Route 152). The terrain is flat and clear except for the small radio beacon building 200 feet west-southwest.

The location of the west sensor so far from the runways is ideal for Oklahoma City because most severe thunderstorms rapidly approach the airport from the west or northwest. For a gust front approaching Will Rogers airport from the west at 20 knots, a 5- to 6-minute warning of hazardous shear is possible for aircraft approaching runway 17R (and this will be a very frequent scenario in the spring storm season).

The centerfield sensor is east of the abandoned portion of Meridian Road midway between and halfway down runways 17R-35L and 17L-35R. The sensor has excellent exposure to winds in all quadrants except the south. With south winds there is minimal sheltering from a small grove of 25-foot trees 1,000 feet away.

All sensors at Oklahoma City are on 20-foot utility pole masts.

DENVER STAPLETON, COLORADO. Stapleton Airport is located in the generally treeless, flat, high prairie east of Denver center city. With the exception of one remote site, there are few obstructions to near-surface airflow, and siting of sensors has not been a problem. Of the seven LLWSAS airports, however, Denver is unique in two aspects. First, its proximity to the Rocky Mountains and the area's high plains-type climatology are strong influences on weather patterns, producing shear events of character unique to this area in the lee of the Rocky Mountains. Second, Denver's runway pattern is enscribed by boundaries shaped like an inverted T compared with conventional rectangular or square boundary patterns. In order to protect the airport and provide timely warnings, some sensors are quite distant from the centerfield reference sensor. This has presented no particular problem in communication or service-ability, but does result in a lack of LLWSAS network symmetry.

Denver Stapleton has been constructed on a relatively high plateau about 20 miles east of the Rocky Mountain foothills. To the west of the airport there is a distinct 3- to 5- mile wide depression running roughly north-south at the base of the Rocky Mountain foothills. Center city Denver is actually in this depression, carved by the South Platte River and its tributaries. To the east of downtown Denver, the terrain rises several hundred feet before beginning the gradual slope toward the Mississippi River several hundred miles to the east. Stapleton is near the top of this plateau. This subtle terrain feature would not even be worthy of mentioning under normal circumstances, but construction of the airport on relatively high ground, compared to the immediate surroundings coupled with the unique high plains climatology, induces unusual airflow patterns ultimately affecting LLWSAS.

It is not necessary to delve into a detailed explanation of the Denver area climatology. It suffices to say Denver is strongly influenced by wind undulations created as air flows over the high peaks of the Rocky Mountains. Regardless of the airflow near the surface, the upper atmospheric airflow is almost always west-to-east. Therefore, mountain waves, which retain their identity as they move out over the prairie, will usually be present and will ultimately affect the near-ground airflow, including Stapleton field.

This atmospheric/orographic phenomenon is compounded by another flow feature which relates more to the nature of Stapleton's local terrain. In light wind conditions, an air drainage pattern is established at Stapleton. Drainage simply means that cold air, which is denser or heavier than warm air, tends to flow to the lowest level possible, and conversely, warm air is pushed to higher levels. In the early evening when the ground cools rapidly after a sunny day, the near-ground air is cooled and begins to flow off the airport plateau into the South Platte Valley. This is a near-ground, light wind east-to-west flow. In the morning, the opposite happens.

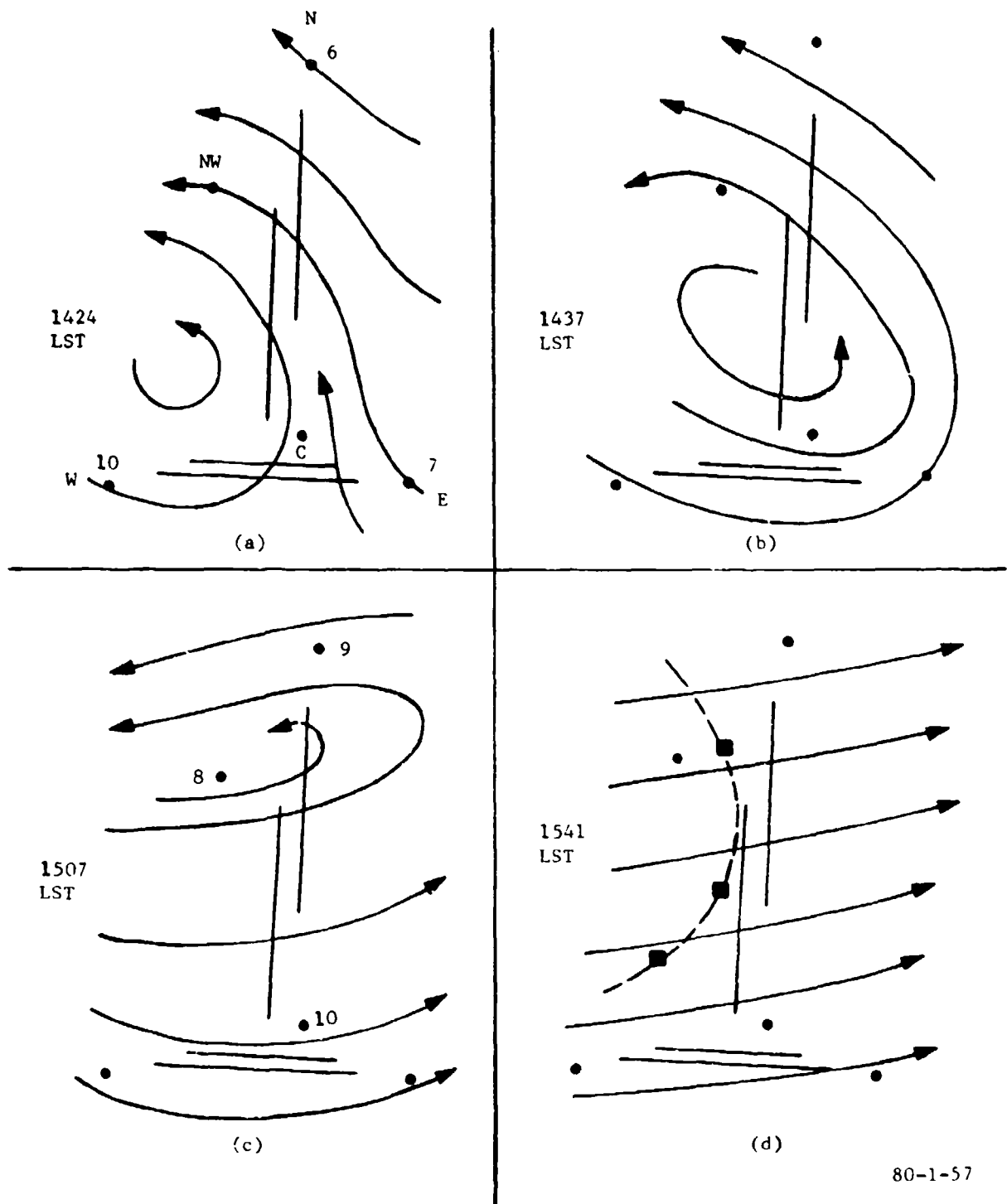
One can now see that the influences of the mountains, air drainage, fronts, thunderstorms, and local ground roughness, whether occurring singly or together, may produce an exceedingly complex airflow pattern at Denver. Such complexities have caused confusion and suspicion of winds observed among air traffic controllers at Denver, but actual presence of the complex flow has been verified both by data collected at the airport and by personal observations.

To cite an example, an unusual flow pattern was observed on May 7, 1979. Figure 57(a) shows the streamline pattern for 1424 local standard time (LST). A large eddy was centered southwest of the airport. Winds ranged from 6 to 10 knots at all stations, but directions varied considerably. Starting about 1410, there were frequent alarms at the northwest and north sites. The weather was clear.

Figure 57(b) shows that by 1437, the eddy moved to the airport center, and figure 57(c) shows that it moved toward the airport's north boundary by 1507. Notice the strong shear between the northwest and north sites (only 1.3 nmi apart) in figure 57(c). The north site was in constant alarm status during this period. By 1541 as shown in figure 57(d), the eddy moved off airport property, and the flow at all stations was from about 250° to 260°. The dashed line was the eddy's track over the 75-minute period. Such flow complexities are to be expected at Denver.

All of Denver's anemometer sites utilize utility poles for masts: the northwest anemometer is 30 feet above ground level (AGL), the north anemometer is 40 AGL, the northeast and southwest sensors are 50 feet AGL, and the other two anemometers are both at 20 feet AGL. The north and northwest sites are on Rocky Mountain Arsenal (U.S. Army) property (figure 58). The northwest site was moved to its present location in August 1978, because its old position was too close to the north end of runway 17R to provide adequate warning to pilots of storms moving in from the west.

The south and west anemometers were recently relocated. The original west anemometer position at 20 feet AGL on a utility pole near the intersection of 25th Street and Quebec was found to be severely affected by the sheltering factor with west winds. A line of single-family residences and 35-foot trees exist 200 feet west of the sensor. In August 1978, the sensor was raised to 41 feet atop a new utility pole.



80-1-57

FIGURE 57. COMPLEX AIRFLOW AT DENVER STAPLETON AIRPORT, MARCH 7, 1979

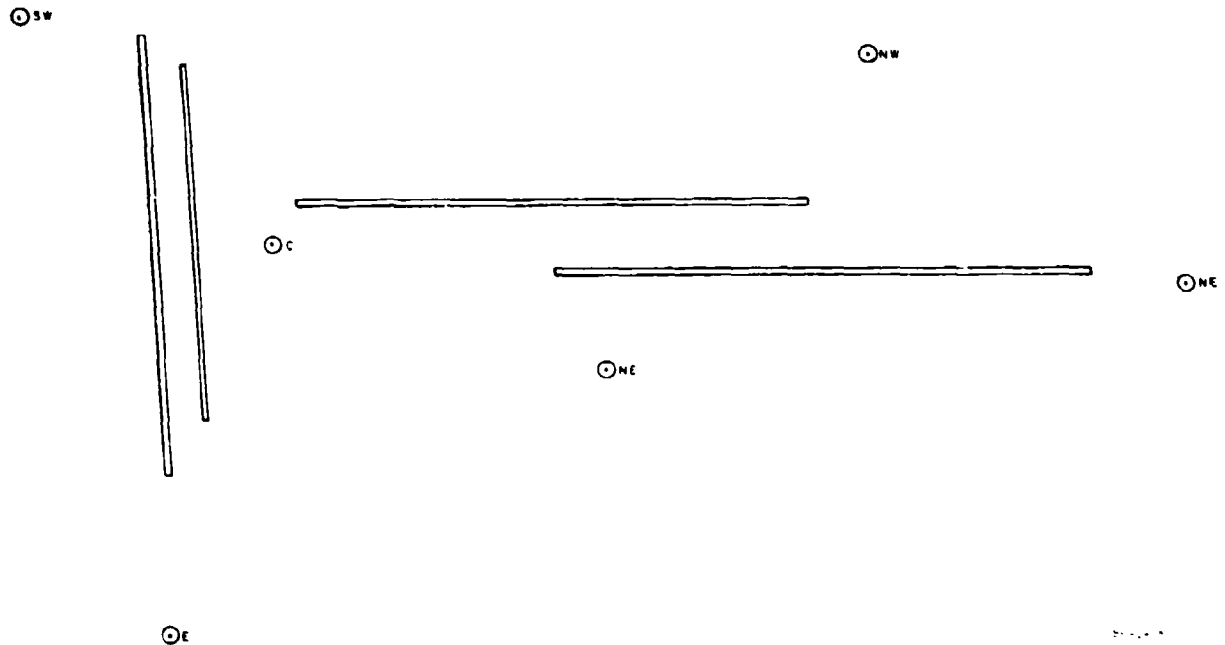


FIGURE 58. AIRPORT RUNWAY MAP WITH ANEMOMETER LOCATIONS, DENVER STAPLETON AIRPORT, COLORADO

In the spring of 1979 this site was moved to a position northeast of the Montview Boulevard/Syracuse Street intersection. The site was redesignated the southwest site. The move was necessary when the south site (near the 35L middle marker) was decommissioned to make way for construction of a new taxiway. The new southwest site, in effect, combines the functions of the old south and west sites. At this time, a new sensor position, designated the northeast site, was installed just west of the Havana/47th Street intersection to fill a gap in the original LLWSAS network on the northeast side of the airport. The northeast site is in open terrain, except for some large area buildings 30 feet tall, 400 feet east. A 50-foot mast, however, should sense fairly representative winds from the east.

The north and centerfield sites are ideal requiring no special comment.

J. F. KENNEDY INTERNATIONAL, NEW YORK. Kennedy Airport was equipped with LLWSAS in September 1977. Numerous problems, some unique to this facility, occurred during the course of the debug period. The LLWSAS equipment achieved desired reliability by the spring of 1978 and was commissioned for air traffic operational usage (contractor maintained) on June 15, 1978.

Kennedy Airport is situated in South Queens Borough, New York, and is bordered on the north side by a densely populated area; on the west and east sides by

inland bays, marshes, and drainage channels; and on the south side by Jamaica Bay. The terrain around the airport periphery is essentially flat.

Kennedy has two 04-22 runways and two 13-31 runways. Runway 22L was the runway in use at the time of the wind shear-related fatal aircraft accident on June 24, 1975 (reference 20). Although Kennedy's property boundaries are roughly rectangular, the principal hub of aircraft activity is in the east quadrant of the airport because several runways cross there. Therefore, four of the six LLWSAS sensors are concentrated in this area as illustrated in figure 59.

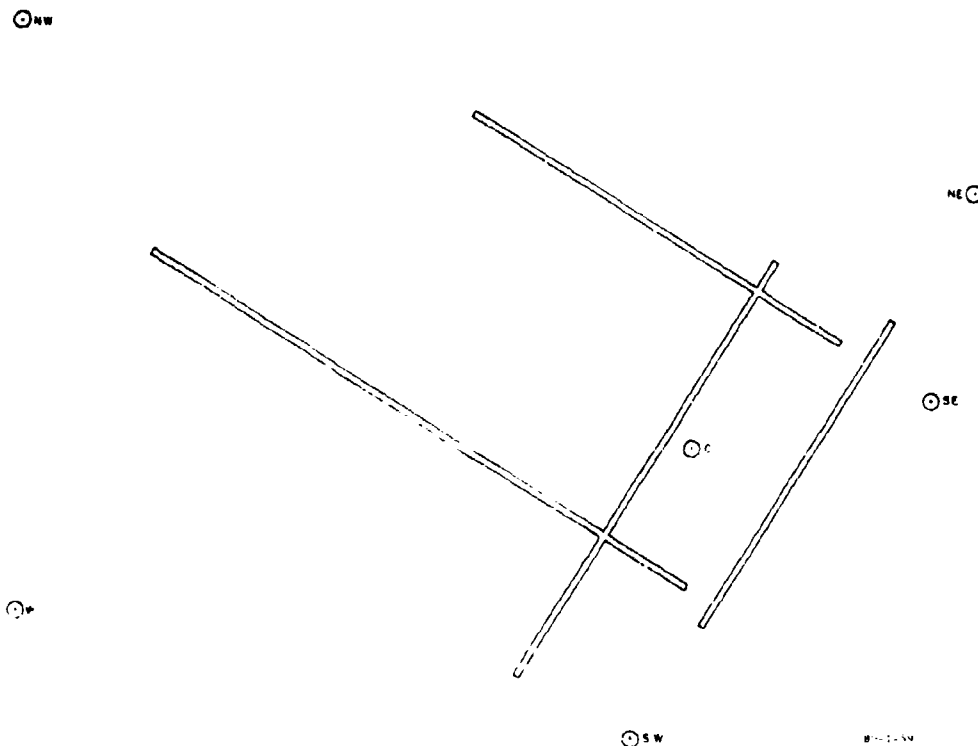


FIGURE 59. AIRPORT RUNWAY MAP WITH ANEMOMETER LOCATIONS, J. F. KENNEDY INTERNATIONAL AIRPORT, NEW YORK

The airport experiences three principal types of weather phenomena: cold fronts, thunderstorms, and seabreeze fronts. Cold fronts in the New York area occur year round, although they are not particularly strong in summer months. Winter cold fronts are sometimes quite strong in terms of wind shear because of New York's northern latitude. They approach the airport from the west, northwest, or north.

Despite the fact that the most disastrous aircraft accident attributed to thunderstorm-produced wind shear occurred at Kennedy, this area does not normally receive much thunderstorm activity compared with Florida or the lee of the Rocky Mountains. In fact, climatological records show that only an average of 19 thunderstorms occur annually; about half that number are severe. Thunderstorm activity is confined to the warm months. Some of this convective activity is of the generally innocuous tropical thunderstorm type, but some is of the squall line type, which tends to form along cold frontal boundaries and which might frequently produce wind shears hazardous to flight.

The third weather feature producing horizontal shear is the seabreeze front. Seabreeze fronts at Kennedy do not appear to pose an aircraft hazard. For example, on several days in May 1978 attended by seabreeze fronts crossing Kennedy in the afternoon, LLWSAS alarms were triggered, and pilots were appropriately warned. When questioned, pilots reported little difficulty in maintaining altitude and no large loss in airspeed while passing through the fronts. The seabreeze appears to be innocuous for large air carrier operations. Its passage over an airport requires a runway change which might be routine at most airports, but is not a simple action at Kennedy because of its effect on heavy air traffic flow over the metropolitan New York area.

The seabreeze is important, though, in one other aspect. Its passage over the Kennedy airport and the subsequent change to use of the 22 runways sets up a scenario like the one on June 24, 1975. On that day, thunderstorms had developed over Northern New Jersey and moved over Manhattan and Queens. The seabreeze front had passed the airport in midafternoon, and the presence of seabreeze frontal shears enhanced by the thunderstorm shears produced a wind flow pattern hazardous to flight. Since the midfield wind was from the southwest, approach corridors of runways 22R and 22L crossed areas affected by thunderstorms. Thunderstorms and the seabreeze front often interact like this at Kennedy and such a scenario will likely be repeated. However, with LLWSAS in operation, remote sensors will detect large horizontal wind shears 1/2 to 1 mile from runway thresholds.

The northwest sensor at Kennedy is located south of the Belt Parkway, west of Leffertz Boulevard, and at the east end of the Aqueduct Race Track overflow parking lot. The sensor is on a 35-foot utility pole. Discounting seabreeze fronts, this anemometer is critical roughly 70 percent of the time. Both cold fronts and thunderstorm gust fronts will pass this anemometer first most of the time. This factor makes this remote facility the most important. The site is free of obstructions for 1,000 feet in all directions. This sensor was moved to its present position in January 1979 from the original location near the 13R middle marker. This relocation was made to provide additional warning time to controllers and pilots of fronts moving toward the airport from the northwest.

The west site is off airport property in the AIRINC compound within Gateway National Park. The park is actually a natural causeway connecting Queens to the beach islands. It is fairly heavily wooded. The Crossbay Boulevard roadbed, elevated above the natural terrain in addition to the nearby tall trees,

requires that this sensor be mounted 65 feet above ground. A utility pole is used. This is the tallest mast in the LLWSAS program. Its position, however, is well above nearby surface obstructions, affording the sensor good exposure to the large roughness-free water surfaces in all directions except along the principal axis of the causeway. When the wind is from directions parallel to the causeway (roughly north or south), there will be some turbulence. This site is critical about 10 to 15 percent of the time with respect to thunderstorm and cold front wind shifts but is critical virtually 90 percent of the time for seabreeze fronts. As such, it frequently gives warning to controllers of incipient runway changes associated with seabreeze passages.

The south anemometer is located on an 8-foot Vega-type mast at the 2,400-foot approach light tower to runway 04R. The sensor and approach lights are on a 2,000-foot pier extending south into Jamaica Bay. The sensor was originally about 400 feet further from the threshold at the pier end, but the last several hundred feet at the pier was crushed by surface ice in Jamaica Bay in the winter of 1977-78 and was eventually abandoned. The sensor position has excellent exposure to winds from all quadrants. This sensor is not a critical sensor.

The east sensor is located near the middle marker for runway 22L. The sensor is critical for only about 10 percent of the thunderstorm gust front and cold front cases. Of course, one of these cases was responsible for the disastrous 1975 crash. Therefore, the sensor has in some aspects more political than meteorological significance (in terms of the critical nature of the sensor, it is ranked third in importance of the five remotes). Such a viewpoint is enhanced by the great difficulty NAFEC has had in keeping this remote site operational. In addition to routine and expected equipment problems during the test period, there have been nine acts of vandalism at this site, each of which has incapacitated the sensor or data transmission. The equipment has had a 10 percent inoperative rate due to this unforeseen factor.

The sensor is located in an area free of major obstructions to wind from all quadrants except the north. To the north, about 1,000 feet away, lies a densely populated area. The houses and trees do not significantly shelter the anemometer, however, because the sensor compound is on a manmade knoll about 15 feet above the surrounding marsh. The sensor is atop a 20-foot utility pole.

It was observed during the course of the LLWSAS test that the seabreeze front, first detected by the west sensor, moves across the airport but often slows or stops before reaching the east sensor. The reason for this is not clear, but probably has to do with the irregularly shaped land-water interface around the airport. The result is that five of the six LLWSAS sensors will be affected by an onshore breeze from the south or southwest, and the east sensor on the other side of the front will be affected by an offshore north or northwest wind. After the front passes the centerfield sensor, the active runways are typically changed from the 31 runways to the 22 runways. This will cause approaching aircraft to pass through the wind shear zone of the seabreeze front in the vicinity of the east sensor. Since seabreeze frontal shears are

usually weak, this penetration may not cause undue problems, but the scenario is deemed worthy of mention.

The centerfield sensor at Kennedy is not at the airport's geographical center (which is cluttered by terminal buildings) but is offset to the southeast side off the airport between the 13-31 runways. The sensor is atop a 20-foot Willard-type tower. This tower has a frangible base and is climbable. This mast was a replacement for a Vega-type tower which blew over in a high wind storm. The centerfield sensor has good exposure to winds from all quadrants.

BOSTON LOGAN, MASSACHUSETTS. The Boston Logan LLWSAS facility was not part of the original operational test program. The system was installed on August 2, 1978. No data were collected at this facility, but results gleaned from the analysis of data at the other six airports were available at the time of the Boston installation and were used to determine the adequacy of siting and other relevant LLWSAS criteria. However, like Atlanta, this facility has a large potential alarm miss rate (table 13) because of restrictions to locating the airport's critical sensors in the optimum position.

The Boston system differs from the systems at the other airports in that it has updated versions of the tower cab displays, diagnostic display, and software to drive this new hardware. In addition, the Boston system utilizes yagi-type antennae at remote sites and a pole-type omnidirectional antenna at the master station. Boston was also the first to be equipped with TRACON room displays (previously discussed under LLWSAS Hardware) which are to be installed at the other six airports in the near future. With these new features, Boston serves as the LLWSAS prototype upon which future LLWSAS facilities will be modeled.

Because Boston was not part of the LLWSAS operational test, there will be no detailed discussion of this facility.

#### SUMMARY

An operational test of the LLWSAS was conducted at six major United States airports (Tampa, Atlanta, Houston, Oklahoma City, Denver, and New York) between June 1977 and March 1979 (a seventh LLWSAS facility was added at Boston in August 1978). The equipment has now been certified for operational use.

LLWSAS is a surface mesonet network of anemometers connected via radio telemetry to a master station controller/computer. Each remote facility contains a sensor on a tall mast, a radio antenna, and an electronics box which houses a battery, power supply, and five printed circuit boards. The master station contains a radio transceiver, antenna, controller, computer, paper tape reader, UPS, CRT diagnostic display, keyboard, and incandescent tower cab displays. During the test, a floppy disk was used to collect data. The system utilizes state-of-the-art, solid-state electronics.

Although other surface mesonetworks are used for meteorological research purposes, this is first operational application of the mesonetwork concept for aviation safety. The network continuously monitors surface wind, and detects large horizontal shears through the data processing and the ultimate calculation of the vector difference between each remote station and reference centerfield station. A 15-knot vector difference is the warning threshold. (The simple vector difference threshold of 15 knots is modified at Atlanta by inclusion of a direction difference relationship.) The information displayed in the tower cab and relayed to pilots, however, is not the vector difference but the actual wind direction and speed from the remote station indicating an alarm as well as the centerfield anemometer readings.

The LLWSAS also determines the centerfield peak wind (gusts) by electronically selecting the maximum analog voltage between interrogations. The information is relayed to the master station and displayed on the cab indicator if the peak wind exceeds the centerfield mean wind speed by 9 knots or more.

#### CONCLUSIONS

The Low-Level Wind Shear Alert System (LLWSAS) was designed to detect large horizontal wind shears associated with thunderstorms and cold fronts. Shears are inferred by measuring the wind and calculating the vector difference. Test results show that the system works as expected in detecting shears in thunderstorms and strong cold fronts. The system will also detect shears associated with the so-called seabreeze front and will respond to the shears associated with small-scale turbulent eddies, especially if the mean airport wind is high. The latter two types of alarms were unexpected. The system is highly sensitive to the location of anemometers with respect to local terrain and obstructions. The failure to recognize the significance of this factor ultimately led to many site relocations. It should be strongly emphasized in future planning. The effect of wind sheltering, if significant, will be to lower the vector difference threshold and induce false alarms. LLWSAS will not detect vertical shears or vertical motions; however, such motions are often associated with the atmospheric events producing horizontal shears.

The system has not been altered drastically since inception, although a number of small changes to the basic design have been made during the course of the test. These changes were necessary to perfect the sensor and electronics package, adjust the system hardware and software to the operating environment, and respond to the needs of the user. To summarize these changes:

1. The electric speed model F-420 anemometer, initially used at centerfield, was found to have output signals uncondusive to digitizing. The sensor was replaced by the type used at remote stations (Belfort Vectorvane).
2. The cathode-ray tube (CRT) used in the tower cab environment was found inadequate, and it was replaced by an incandescent filament display. The CRT was reverted to the equipment room as a diagnostic display with the output reformatted for maintenance purposes.

3. The method of computing a gust factor from digitized data was found inadequate. A peak wind detector was fabricated and installed as a separate printed circuit board at the centerfield station. This board accepts analog signals and selects the peak wind between interrogations. The peak wind signal is then digitized and transmitted to the master station on a separate channel.

4. The anemometer siting criteria used in initial sensor positioning emphasized logistical factors at the expense of meteorological (system performance) factors. System performance was noticeably degraded in many cases, requiring the relocation and/or raising of sensors to:

- a. move the sensor away from or raise it above obstructions to the wind;
- b. move the sensor further away from the centerfield station to obtain the required minimum distance between the pair;
- c. move sensor(s) to obtain better warning coverage in all quadrants of the airport and to achieve network symmetry;
- d. move the sensor off centerline to prevent impingement of wing tip vortices.

5. One of the LLWSAS assigned radio frequencies (162.350 megahertz) was within 0.5 kilohertz of the rapidly expanding National Oceanic and Atmospheric Administration (NOAA) Weather Radio Network. Inexpensive broadband radio receivers, if operated close to LLWSAS airports when monitoring weather information, would receive the LLWSAS data transmissions as background noise. The LLWSAS radio frequency was subsequently changed to 169.375 megahertz at affected airports (Atlanta, Houston, Oklahoma City, and the National Aviation Facilities Experimental Center).

6. Special software modifications were made to the basic program at Denver to provide special handling and display of data in mountain (foehn) wind conditions and at Atlanta to modify the basic vector difference algorithm to reduce incidents of false alarms induced by terrain irregularities.

7. An uninterruptible power supply (UPS) was added as a standard item to the master station hardware when it was determined that the specific model of processor used could not effectively filter alternating current power interruptions of 40 microseconds or less causing the LLWSAS central processing unit (CPU) to fail. The UPS effectively screens noise and regulates the alternating current power input to the CPU (via the memory backup and alternating/direct current converter).

8. Numerous electronics hardware modifications were made by the principal contractor to adapt the LLWSAS equipment to the rather severe demands of continuous operation and high reliability. The most significant modifications were those made to the master station controller, remote modem, and remote power supply.

9. Two small additions were made to the cab displays: (a) data time-out light to indicate to controllers when the CPU had ceased sending data and (b) control to vary the intensity of the audible alarm.

10. Freestanding, hollow-tube, frangible towers were found unsuitable for LLWSAS anemometers. Utility poles are recommended but are not frangible.

11. Vandalism is an important consideration in choosing sites accessible by the public, especially in those areas where there is public hostility to airport operations.

## REFERENCES

1. Bromley, E. Jr., Aeronautical Meteorology: Progress and Challenges—Today and Tomorrow, Bulletin of the American Meteorological Society, Vol. 58, November 1977.
2. Byers, H. R. and Braham, R. R., The Thunderstorm, U.S. Department of Commerce, Washington, D.C., June 1949.
3. Lee, J. T., Thunderstorms Turbulence and Radar Echoes—1964 Data Studies, Proceedings Fifth Annual National Conference on Environmental Effects on Aircraft and Propulsion Systems, U.S. Naval Air Turbine Test Station, Superintendent of Documents, 1965.
4. Charba, J., Application of Gravity Current Model to Analysis of Squall-Line Gust Front, Monthly Weather Review, Vol. 102, February 1974.
5. Goff, R. C., Thunderstorm-Outflow Kinematics and Dynamics, NOAA Technical Memo No. ERL NSSL-75, December, 1975.
6. Caracena, F., Weather Analysis, NTSB Exhibit No. 5E-1 of Stapleton Accident, 1976.
7. Fujita, T. and Caracena, F., An Analysis of Three Weather-Related Aircraft Accidents, Bulletin of the American Meteorological Society, Vol. 58, 1977.
8. Frost, W., Crosby, B., and Camp, D. W., Flight Through Thunderstorm Outflows, Journal of Aircraft, Vol. 16, No. 11, November 1979.
9. McCarthy, J., Blick, E. F., and Bensch, R. R., Jet Transport Performance in Thunderstorm Wind Shear Conditions, NASA Contractor Report 3207, December 1979.
10. Cotton, W. R. and George, R. L., A Summer with PAM, Proceedings Fourth Symposium on Meteorological Observations and Instrumentation, Denver, Colorado, April 10-14, 1978.
11. National Transportation Safety Board, Aircraft Accident Report, NTSB-AAR-76-14, Continental Airlines, Denver, Colorado, August 7, 1975.
12. National Transportation Safety Board, Aircraft Accident Report, NTSB-AAR-78-3, Southern Airlines, New Hope, Georgia, April 4, 1977.
13. National Transportation Safety Board, Aircraft Accident Report, NTSB-AAR-74-14, Iberian Airlines, Boston, Massachusetts, December 17, 1973.
14. International Civil Aviation Organization, Report of the 8th Air Navigation Conference, Doc. 9101, AN-CONF/8, Montreal, 1974.

15. Bowen, A. J. and Lindley, D., A Wind-Tunnel Investigation of the Wind Speed and Turbulence Characteristics Close to the Ground over Various Escarpment Shapes, Boundary-Layer Meteorology, Vol. 12, 1977.
16. Bedard, A. J. Jr., Merrem, F. H., Simms, D., and Cairns, M. M., A Thunderstorm Gust-Front Detection System: Part I. System Operation and Significant Case Studies; Part II. Statistical Results, FAA Report No. FAA-RD-79-55, August 1979.
17. Goff, R. C., Lee, J. T., and Brandes, E. A., Gust Front Analytical Study, FAA Report No. FAA-RD-77-119, December 1977.
18. Garodz, L. J., Abbreviated Full-Scale Flight Test Investigation of the Lockheed L1011 Trailing Vortex System Using Tower Fly-By Technique, FAA Report No. FAA-AFS-1-76-2, May 1976.
19. Barnes, S. L., Mesoscale Objective Map Analysis Using Weighted Time-Series Observations, National Oceanic and Atmospheric Administration Report No. ERL NSSL-62, March 1973.
20. National Transportation Safety Board, Aircraft Accident Report, NTSB-AAR-76-8, Eastern Airlines, New York Kennedy Airport, June 24, 1975.